FRACTIONAL BLACK-SCHOLES EQUATIONS AND THEIR ROBUST NUMERICAL SIMULATIONS

SAMUEL MEGAMENO NUUGULU

A Thesis submitted in fulfilment of the requirements for the degree of Doctor of Philosophy in the Department of Mathematics and Applied Mathematics at the Faculty of Natural Sciences, University of the Western Cape

Supervisor: Prof. Kailash C. Patidar
Co-Supervisor: Prof. Frednard Gideon

February 2020

KEYWORDS

Computational Finance

Option Pricing

Non-random Fractional Stochastic Processes

Fractal Market Hypothesis

Fractional Black-Scholes Partial Differential Equations

American, European and Double Barriers Options

Front-Fixing Transformations

Free Boundary Problems

Finite Difference Methods

Convergence and Stability Analysis.

ABSTRACT

Fractional Black-Scholes Equations and their Robust Numerical Simulations

by

Samuel Megameno Nuugulu

PhD Thesis, Department of Mathematics and Applied Mathematics, Faculty of Natural Sciences, University of the Western Cape

Conventional partial differential equations under the classical Black-Scholes approach have been extensively explored over the past few decades in solving option pricing problems. However, the underlying Efficient Market Hypothesis (EMH) of classical economic theory neglects the effects of memory in asset return series, though memory has long been observed in a number financial data. With advancements in computational methodologies, it has now become possible to model different real life physical phenomenons using complex approaches such as, fractional differential equations (FDEs). Fractional models are generalised models which based on literature have been found appropriate for explaining memory effects observed in a number of financial markets including the stock market. The use of fractional model has thus recently taken over the context of academic literatures and debates on financial modelling. Fractional models are usually of a non-linear and complex nature, which pose a considerable amount of computational and theoretical difficulties in deriving their analytical solutions. To the best of our knowledge, currently, there exist no tractable exact/analytical solution methods for solving fractional Black-Scholes equations, and as such, numerical solution methods become of a vital importance in understanding nature of solutions to such models. This thesis therefore, serves to derive some Generalised (fractional) Black-Scholes Partial Differential Equations (fBS-PDEs), as well as, propose their re-

spective tractable, efficient and robust numerical simulation methods. The proposed models and their respective numerical methods are used to price standard as well as exotic options on continuous dividend paying stocks. The fractional models presented herein, falls within two categories; the time-fractional Black-Scholes Partial Differential Equations(tfBS-PDEs) as well as those which are generalised in both time and space directions, i.e. the time-space-fractional Black-Scholes Partial Differential Equations (tsfBS-PDEs). Though it involves a considerable amount of computational difficulties to construct tractable, efficient solution methods for fractional models, we were able to construct a number of reliable numerical solutions schemes for the considered models. Overall, results herein indicates that, the fractional Black-Scholes framework and the accompanying numerical computations are well suited and appropriate methods for pricing continuous dividend paying stock options. Furthermore, the fractional Black-Scholes approach has outperformed its classical counterpart (classical Black-Scholes model) in calculating the best option premiums under all considered market conditions.

February 2020.

DECLARATION

I declare that *Fractional Black-Scholes Equations and their Robust Numerical Simulations* is my own work, that it has not been submitted before for any degree or examination at any other university, and that all sources I have used or quoted have been indicated and acknowledged by complete references.

Samuel Megameno Nuugulu February 2020

Signed 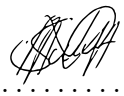 .....

ACKNOWLEDGEMENT

Firstly, thanks to the Almighty God for giving me the strength to complete my studies. Special appreciations goes to my two academic supervisors, Prof. Kailash. C. Patidar and Ass. Prof. Frednard Gideon for their collective supports and ideas which played a very crucial role in shaping my research work. In particular, I want to thank Prof. Patidar for his enthusiasm and invaluable knowledge, and Prof. Gideon for his insightful advices during my visits at the University of Namibia (UNAM). Words cannot express how grateful I am to my parents, Tate. Mateus Nuugulu and Meme. Maria Petrus-Nuugulu, thank you for raising me in a very caring and loving family, to all my siblings, thank you all for the support. Thanks to the many good friends I made in Cape Town, a special mention goes to my colleague and friend Cde. David Elago who has been more like a brother during our stay in Cape Town. I feel indebted to Dr M. Mugochi, Head of Mathematics Department at UNAM, the Dean of the Faculty of Science and the entire UNAM management for making sure that my staff-development leaves were always approved when necessary. My sincere gratitudes goes to the UNAM HR Department, specific mention goes to Ms. Florence Katuuo for always attending to my requests. I was privileged to have benefited from numerous research fundings from the following institutions: German Academic Exchange Service (DAAD), Namibia Students Financial Assistance Fund (NSFAF), National Commission on Research Science and Technology (NCRST) and the Centre of Excellence in Mathematical and Statistical Sciences (CoE-MaSS) through Prof. Patidar and Department of Mathematics at UWC. Their collective fundings afforded me opportunities to showcase my research work to a broader Mathematical community at local and international conferences.

DEDICATION

This thesis work is dedicated to my lovely wife **Annastasia Kakenya Nuugulu**, who has been a constant source of support and encouragement during the challenging moments of my graduate school days and life in general. I am truly thankful for having you in my life. This work is also dedicated to my parents, **Tt. Mateus Thiophilus Nuugulu** and **Mm. Maria Petrus-Nuugulu**, and to all my siblings **Teofilus Kandali Nuugulu**, **Timoteus Nalimanguluke Nuugulu**, **Junias Tengelela Nuugulu**, **Selma Nampa Nuugulu**, **Matheus Simaneka Nuugulu**, and our last born **Klaudia Ndagwedha Nuugulu**, may you all be inspired to do more and continue being the source of inspiration that you are as a family.

Contents

List of Tables

List of Figures

List of Publications

Part of this thesis has been submitted in the form of the following research papers submitted to international journals for publications:

1. S.M. Nuugulu , F. Gideon, K.C. Patidar: On numerical solution of a time-fractional Black-Scholes Equation (submitted).

2. S.M. Nuugulu , F. Gideon, K.C. Patidar: A robust numerical scheme for a stock exchange time fractional Black-Scholes partial differential equation (submitted).

3. S.M. Nuugulu , F. Gideon, K.C. Patidar: An Efficient Finite Difference Approximation for a time-fractional Black-Scholes PDE arising via a Fractal Market Hypothesis(submitted).

4. S.M. Nuugulu , F. Gideon, K.C. Patidar: Derivation and robust simulation of a fractional Black-Scholes equation on pricing American options (submitted).

5. S.M. Nuugulu , F. Gideon, K.C. Patidar: An efficient numerical method for pricing double barrier options on an underlying asset following a fractal stochastic process (submitted).

6. S.M. Nuugulu , F. Gideon, K.C. Patidar: A robust θ difference method for a time-space-fractional Black-Scholes equation (submitted).

Chapter 1

General Introduction

This chapter presents the general introduction of the thesis. The chapter introduces the general ideas and concepts of the theory of fractional calculus and its application to finance. The chapter further highlights the review of numerous literatures related to other subsequent chapters in this thesis. Lastly the chapter conclude with the structure of the remainder of the thesis.

1.1 Literature review

Since the discovery of the celebrated "Black-Scholes-Merton" asset pricing formula in the early 1970s, the application of Black-Scholes (BS) partial differential equations (PDEs) in valuation of derivative instruments became very popular. The popularity of the approach can be mainly attributed to the belief that the approach provided the best and most effective asset valuation tool of the time. Besides the application in derivatives pricing, dynamical behaviours of financial markets, attributed to ill-informed splash trading for example, has led to a formation of a number of speculative bubbles and volatility smiles in market data. Often when these speculative bubbles burst, unfavourable economic recessions and crises become inevitable.

It is worth noting that in derivative markets, once the price evolution process for a particular asset is specified, it is possible to address the question of how to price deriva-

tive contracts on this particular asset. One of the most common classes of derivative instruments in the markets are called options. An option is a financial contract that gives the holder the right, but not obligation, to buy or sell a specified quantity of an underlying asset, e.g., a stock, at a fixed price, called the strike price, before or on the expiration date. Since it is a right and not an obligation, the holder of the contract can decide not to exercise the option and let it to expire worthless.

There are two main types of options: standard and non-standard. Standard options are further categorised as European or American type. The European options can only be exercised on the expiration date, whereas, the American options are more flexible and can be exercised at anytime on or before the expiration date. These options can further be divided into two categories - call options (which give their holders the rights to buy) or put options (which give their holders the rights to sell).

Another rather complex kind of tradable options available in the market today are exotic options. Over the years exotic options have become very popular. Today, a large variety of exotic options are readily available to investors as they are cheaper and many offers specific tailor-made protections to the investors, see for example ([13, 42, 61, 98]) and some references therein.

Several factors can provide an explanation for the wide popularity of exotic options. One is the almost unlimited flexibility in the sense that they can be tailored to address a specific needs which may not be possible with standard options. For example, an investor who would like to hedge against a large drop in the underlying asset price can sell a down-and-in put with the barrier set at a lower level as a cheapest way to purchase the underlying asset.

On the other hand, exotic options play a significant hedging role in meeting investors need in very cost effective ways, see ([13]). Also, according to [13] rational investors are moving away from buying general protections and rather focusing on designing complex strategies which serves to address their specific exposures at any given point in time. Most of these complex strategies are based on exotic options.

The oldest type of exotic options are barrier options. Barrier options in general

come in two forms, knock-out option (disappearing) or knock-in (appearing) when the underlying asset price triggers some pre-set price levels ([14]). Barrier options are thus conditional options, and depends on whether the barrier(s) have been breached during the lifetime of the option. Barrier options are also part of a class of options called path-dependent options. According to Buchen and Konstandatos ([13]) barrier options are usually cheaper than their vanilla counterparts, this is due to the fact that a buyer of a barrier option has a more specific view of the underlying asset price dynamics within the time to maturity of the option as compared to its vanilla counterparty. Another hybrid of barrier options are the so-called partial time barrier options ([13]). Here, the barrier is monitored (or active) for a time period that is shorter than the expiry time. These options are also called window barrier options. Another refinement of these barrier options are those options where barrier(s) are monitored discretely in time, a comprehensive coverage of these kind of options can be found for example in ([14, 33, 36]) to mention but a few.

The concept of option pricing is both a theoretical and a practical problem in computational finance. The derivation of the classical Black - Scholes equation which is at the center of option pricing theory was based on the Efficient Market Hypothesis (EMH) assumption. Of primary concern in the EMH and this derivation in general is that assets price returns are assumed to follow a Gaussian process. Of course, in the earlier days of trading, the Black-Scholes equation in its classical form was a very efficient asset pricing tool and as such it found enormous applications in the general spectrum of derivative pricing. Later, however, it turned out that splash trading presumably informed by classical contemporary theory, and also done with little to no knowledge of evolutions of markets dynamics has led to a formation of a number of speculative market bubbles, which in turn led to a lot of financial troubles. For a comprehensive account on speculative bubbles and their roles in financial crises among other market anomalies see for example,([1, 22, 54]) and some references therein.

Among other factors, the recurrent occurrence of unexpected fluctuations, i.e., sudden unexpected rise/fall in stock prices renders the use of the classical Black Scholes

approach inappropriate. Taleb in [91] refers to such rare occurrences as "black-swan events" from his popular book entitled: "The black-swan: The impact of the highly improbable". According to Taleb [91] a black-swan is "A highly improbable event with three principal characteristics: it is unpredictable; it carries a massive impact; and, after the fact, we concoct an explanation that makes it appear less random, and more predictable, than it was". According to Kleinert [54], the existence of black-swan events in financial markets is a severe obstacle to all hedging attempts. Kleinert in ([54]) further argued that based on the central limit theorem, one would normally consider price changes as a result of random steps of a given finite size and demonstrates that these series of random walks build up to a complete Gaussian process. However, in an event where a black-swan occur, some steps can become very irregular, resulting into a combined process that exhibits power-law properties. It is therefore of vital importance that models beyond the classical Black-Scholes setup, those that have the capacity to explain the effects of "black-swan events", as well as their solutions, both numerical and analytical if possible are developed.

Recall that valuing options under the classical Black-Scholes framework, one assumes that the market consists of a risky asset, e.g., a stock, and a riskless asset such as a bond. Emanating from its assumptions, the classical Black-Scholes approach suffers from a few drawbacks, namely, (i) constant rate of return, (ii) constant volatility, and (iii) no dividend, taxes or transactional costs. Interest rates are bound to market forces and as such, cannot remain constant over a longer period of time. Based on empirical evidence, most traded asset returns exhibit memory structures, regimes of un-even fluctuations, volatility smiles and clustering. Therefore, assuming constant volatility may introduce some model risk. Furthermore, it is worth noting that trading of financial assets may involve transactional costs, taxation as well as dividend payments. It is therefore crucial that in designing asset valuation models, one pays ample attention to the case-by-case practicalities of relaxing some of these assumptions.

Empirical evidence in ([25, 37, 103]) and some references therein suggest that the assumption of log-normality of returns and Gaussian shocks under-represent the actual

dynamics of unanticipated jumps in asset returns. To circumvent this among other issues, a number of suggestions has been made, for example replacing the standard Brownian motion with a Levy processes which according to Zhang et al. [103] exhibits long fat tails while capturing the volatility smiles and skewness which may not be captured using the classical Black-Scholes models.

Weakening some assumptions of the classical Black-Scholes approach, some researchers suggested a few improved-models, such as, stochastic interest rate models [24, 28, 32, 81], jump-diffusion models [3, 24, 31, 55, 71, 85], stochastic volatility models [11, 28, 80, 81, 87], models with transactional costs [30, 43, 88, 100, 101], dividend payments based models [7, 68, 80, 81] as well as regime-switching models [19, 87].

Bielecki et al. [10] also gave an extension of the no-arbitrage pricing theory to pricing dividend-paying securities in discrete-time markets with transaction costs. They showed that when there are no transaction costs on the dividends paid by a securities, the no-arbitrage conditions under the efficient friction assumption market become equivalent to the existence of a consistent pricing system. Recently, [88] solved a space-time fractional European option pricing model in the presence of transaction costs and tested the practicability of their results on market real data. In the general case, when there are transaction costs on the dividends, the no-arbitrage condition is open. This is so because, if a security pays dividends, the security price falls by the amount of dividend payout. Arbitrage opportunities vanishes because investors are compensated with the same amount of price depreciation back in cash through the dividends paid out to them.

Recent models with dividend payments, include but not limited to [68],[81] and [7]. Martin-Vaquero et al. in ([68]) derived a stabilized explicit Runge-Kutta method for solving American option on Multi-assets with dividends. Rana and Ahmad in ([81]) used the Glosten-Jagannathan-Runkle - Generalized Autoregressive Conditional Heteroscedasticity (GJR-GARCH) forecasted volatility in pricing European call options on dividend paying stocks. Ballerster et al. [7] derived a robust numerical method for pricing vanilla options with discrete dividend payments.

Another notable setback of the classical Black Scholes approach as well as many of its revised versions discussed above is that their resultant models involve integer order derivatives and integrals. According to Panas ([77]) integer order derivatives only capture localised information (change) around a point. However, with changing market conditions, which led to an evolvement of some unusual structures in financial markets, such as, repeated patterns and trends, heavy tailedness in the distributions of asset returns, volatility smiles and clustering, presents a considerable amount of practical challenges in using models involving integer (local) derivatives. The need for better and robust approaches has therefore become very imperative.

On the other hand, dynamical trading, always involve some residual risks emanating from the imperfection of the correlations between the underlying process and the risky counterpart and hence choosing an underlying stochastic process under which, the discounting asset price movements at-least asymptotically follows a martingale would best serve to eliminate the associated risk. That is so, because of the fact that the underlying processes are usually correlated with the substitutes (risky counterparts) which creates markets incompleteness. Furthermore, attributed to the principle of no-arbitrage, there can be infinitely many martingale measures in any such portfolio setup, which would allow for the underlying (stock) to be directly correlated to the risk. If one wishes to therefore overcome the associated uncertainty, it is ideal to employ an appropriate underlying stochastic process, one that is able to capture the dynamical behaviours of the underlying (stock) price movements.

The study on pricing stock options via classical Black-Scholes approach is based on the well known efficient market hypothesis (EMH), i.e, martingale property of price movements. The consequence of using these types of models is that it is almost impossible to infer any additional information from historical price movements to predict the future prices. It therefore became imperative that for one to better understand future price movements, there is a need to pay ample attentions to the repeated historical patterns and trends.

Contrary to what the efficient market hypothesis may suggest, unusual structures

and patterns observed in a number of financial markets data can strongly be attributed to the following three factors, (i). markets discount everything (markets will always respond to news and events), (ii). as behavioural finance suggests, asset prices moves in trends and patterns forming structures depicting investors'/traders' psychology, and lastly that (iii). these repeated market structures may persist and are most likely to re-occur more often than expected (history mostly always repeat itself).

In recent years, after the discovery of fractal geometry and fractal dynamics of financial markets, see ([25, 66, 103]) progress has been made in the design of new revolutionary models circumventing some of the unrealistic assumptions of the classical Black-Scholes models. At the centre of the revolution are fractional calculus based models.

Mandelbrot [64] in the late sixties observed that stock price returns exhibits heavy tails features, as a result, they proposed an exponential non-Gaussian Levy type of process for modelling heavy tailed stock returns. Fast forward, in the mid 1990s, emanating from a series of his publications on the theory of fractal geometry, Mandelbrot certainly revolutionised the world of science, finance and applied economics. The fields of finance and applied economics being some of his most subtle areas of interests, led him onto the path of discovering the fractal geometry of financial markets.

Falling under chaos theory is the Fractal Market Hypothesis (FMH) which helps in explaining market behaviours based on the idea of Mandelbrot fractal geometry [67]. As one may recall from elementary fractional calculus, fractals are fragmented geometric structures which when broken down into smaller parts would still maintain the shape and structure of the whole. From financial markets point of view, one may look at stock price movements as fractals, the market structures on bigger time frames are preserved on smaller time frames. Repeated self-similar patterns have long been observed in financial market data, for some accounts with reference to stock markets see for example [37, 54, 77] and some references therein. Mandelbrot and Cioczek-Georges in ([66]) suggested yet another modification of the classical Black-Scholes model using his theory of fractal geometry ([67]) which help capture memory

and heredity features observed in financial data see [6, 37, 77, 97, 101, 103]. The later approach of Mandelbrot and Cioczek-Georges [66] suggest replacing the standard Brownian motion with a generalised/fractional Brownian motion. The generalised Brownian motion is characterised by a hurst parameter H $(0 < H \leq 1/2)$, such that it is equivalent to a standard Brownian motion when $H = 1/2$.

According to Panas [77] local derivative based mathematical models can only capture localized information about change in price at a particular point and time, as such, these models may not be appropriate for modeling dynamics of markets depicting unusual structures such as jumps and repeated patterns. Panas in ([77]) indicated that memory effects in financial data occurs in two forms: memory due to the noise and that due to the trend. He further mentioned that that incorporating a fractional Brownian motion as the governing process of the underlying dynamics can only help to capture the noise memory effects and not the trend memory effects.

To the best of our knowledge, the work by Mandelbrot and Cioczek-Georges [66] put them at the forefront of the pioneering works in the area of application of fractional calculus to financial modeling and literature. They were first to suggest an approach whereby one analogously replace the standard Brownian motion in the classical Black-Scholes model with a fractional Brownian motion (fBM) characterised by a Hurst parameter $H \in (0, 1]$. Unlike in the standard case, the hurst parameter H in the fBM helps in explaining the effects of memory. Some recent literatures on the similar approach are Jumarie ([46]), Wei-Gou ([95]), and Liang ([63]) to mention but a few.

The Hurst parameter and fractional derivative operators involved in models driven by fractal processes are increasingly becoming popular and effective tools for explaining the effects of memory in financial markets. In the contemporary setting, to capture effects of memory under the classical Black-Scholes setup, some researchers, for example, ([46, 63, 66]) suggested replacing the standard Brownian motion in the underlying (stock) dynamics with a fractional Brownian motion.

There has been a widespread applications of fractional Brownian motions based models in finance. Jumarie [46], Liang et al. [63], Mandelbrot and Cioczek-Georges

[66], Wei-Gou et al. [95], to mention but a few, are some of the authors who applied fractional Brownian motion based models to pricing of equities, wallets, options and to general portfolio optimization problems.

Fractional Brownian motion based models have two very important features, namely; self-similarity and long-range dependence (hereditary properties), see [77, 95] and references therein. These features allows for the best capture and representation of extreme behaviours of stock price movements, they also help in explaining the effects of repeated patterns and trends in price movements. Jumarie in ([49]) pointed out that asset price volatility can be well captured by fractional Brownian motion which presents some random-like features suitable in explaining the effects of uneven fluctuations in stock price movements.

Motivated by the ideal that fractional calculus provide a powerful tool for explaining effects of memory observed in a number of physical systems and phenomenons, a growing number of research work on fractional Black-Scholes models has been published. Recall that memory effects come in two forms; the noise memory effects and trend memory effects. Incorporating a fractional Brownian motion as the underlying process for the pricing dynamics only capture the noise memory effects [77]. However, based on collective arguments in ([16, 73, 78]), fractional derivative based models are very good mathematical tools for explaining dynamics of complex processes, irregular increments and trend memory effects which are exhibited by a number of financial instruments time series.

The use of standard fractional Brownian motions in fractional models introduces a considerable amount of mathematical complexity in finding solutions to the models. For this reason, Jumarie [49] suggested an alternative which is to consider a non-random fractional stochastic dynamics subjected to the usual standard Brownian motion instead of analogously replacing governing process with a standard fractional Brownian motion as discussed above.

Models resulting from the Jumarie [49] approach are generically referred to as fractional partial differential equations (fPDEs). In the Black-Scholes setup, there are

three main classes of fractional Black-Scholes partial differential equations (fBS-PDEs), namely; the time-fractional Black-Scholes (tfBS) PDEs, the space-fractional Black-Scholes (sfBS) PDEs and the time-space-fractional Black-Scholes (tsfBS) PDEs. With the tfBS-PDEs, the time derivative is replaced by a corresponding fractional derivative of order α ($0 < \alpha \leq 1$), whereas, in the case of sfBS-PDEs, the space derivatives are replaced by their corresponding fractional derivatives of order α and β ($0 < \alpha \leq 1$) and ($1 < \beta \leq 2$) respectively. In the case of tsfBS-PDEs, one has a combination of the two. The pioneering ideas in the derivation of these fPDEs and other subsequent concepts on fractional calculus herein can strongly be attributed to a series of work by Jumarie in ([46, 47, 48, 49]). A number of authors built on the approach, either by deriving semi-analytic solutions to the models mostly via the fractional Laplace transform method or by suggesting some numerical methods for solving the models.

Among others Chen et al. [25] followed an approach almost similar to that of Jumarie [49], but instead maintained the usual Gaussian dynamics and only analogous replaced the integer derivatives in the Black-Scholes PDE with their corresponding fractional order derivatives α and β ($0 < \alpha \leq 1$ and $1 < \beta \leq 2$).

Since the fractional derivative operators involved in all these fractional approaches are of a non-local nature, full tractable analytical methods for solving fractional Black-Scholes models are seldomly available. As such numerical approaches are the only possibly available avenues to help understand the nature of solutions to these models.

There is empirical evidence suggesting that fractional models, unlike classical ones weighs information on the underlying asset price over a range of parameters instead of only looking at the localised information about the underlying asset price, see for example, [3, 37, 77, 95] and references therein. Therefore, as such, fractional models are deemed more appropriate in capturing unusual dynamics of financial assets series, hence provide a much more reliable approach to pricing of assets and financial derivatives such as American options (which can be exercised anytime before or on maturity).

The valuation of American options has long been a subject of active research in computational and mathematical finance. American option problems are usually of a

non-linear nature. The non-linearity in American option problems is introduced by the early exercise features associated with the contract, as such, it has been widely accepted that there exist no tractable analytical methods for solving American option problems. Apart from the nonlinearity of American option problems, modelling American options using fractional models pose yet another challenge in terms of the involved mathematical complexity as well as in the holistic understanding and development of analytical solutions to such models. For these reasons, tractable analytical methods for solving American option fractional Black-Scholes PDEs are seldom available in literature. The emphasise is therefore mainly focused on the development of numerical techniques. In designing a numerical method for solving American option problems, one ought to take into account the fact that the design of the involved model leads to a free boundary value problem and as such, the location of the boundary is unknown at each point in time. A robust numerical method should therefore be able to determine the location of the free boundary in addition to computing a fair value of the option.

It should also be noted that though the design of numerical methods for pricing American option problems under the classical Black-Scholes approach has been extensively explored and still remain a subject of active research, the same can not be said under the fractional Black-Scholes setup. It is therefore imperative that robust, efficient and accurate numerical techniques for solving fractional Black-Scholes models for American options are developed.

One of the best numerical techniques for pricing American options is a technique based on the front-fixing algorithm. The front-fixing method has long been applied to a wide range of problems arising in population dynamics ([20]) and finance [21, 52, 53, 75, 90, 104]. However, there are numerous other techniques used in solving American option problems, for example singularity separating methods [39, 90] and Penalty methods [28, 75] among others. The basic idea behind the front-fixing technique is to use some change of variables to transform the problem from a moving boundary problem to a fixed boundary problem.

A growing number of researchers have devoted efforts to the study of numerical

methods for fractional models. Zhuang and Liu in ([105]) proposed an unconditional stable implicit difference scheme for solving time fractional diffusion equations. In an approach almost similar to that of Zhuang and Liu [105], Chang-Ming, et al. [23] proposed a finite difference method for solving fractional subdiffusion equations as well as proposed a Fourier analysis method for analysing numerical methods to fractional models. Though authors such as Decreusefond and Ustunel [27] among others, had suggested some analysis methods for fractional models prior to Chang-Ming, et al. [23], the analysis presented in [23] has now become the basis of theoretical analysis of numerical methods to fractional differential equations. Zhang, et al. [103] constructed a second order accurate discrete implicit numerical scheme for a space-fractional Black-Scholes equation. Zhang, et al. [103] concluded that their so-called fast bi-conjugate gradient stabilised method was able to reduce the storage space from $O(k^2)$ to $O(k)$ and simultaneously reduced the computational cost from $O(k^3)$ to $O(k \log k)$ per iteration, where k is the number of grid points in space. Apart from finite difference based methods, other new techniques have been proposed. For example in [40] the authors proposed two techniques for solving time-fractional Black-Scholes models, namely: Residual Power Series method (RPSM) and collocation based mesh-free method.

Currently, there exists no perfect analytic solutions for fractional fractional Black-Scholes equations. Though tractable analytic solutions to fractional differential equations are rare in general, there has been a few recent developments on the design of semi-analytic solutions. Chen, et al. [25] presented an analytic solution to a time-fractional Black-Scholes for pricing double barrier options. Liang, et al. [63] derived an analytic solution for a bi-fractional Black-Scholes-Merton model using the Laplace transform technique. A similar technique was later used in Kumar, et al. [56] in pricing European option problems. Other analytical techniques such as fractional variation iteration method are discussed in Ahmad, et al. [2], those based on Homotopy perturbation under Sumudu transform of the fractional derivatives can be found in Asma, et al. [4].[56] used the Laplace homotopy perturbation method, which is combination of the Laplace transform and the homotopy perturbation method in deriving a solution

to the fractional Black-Scholes equation with boundary condition for a European option pricing problem. This thesis therefore serves to suggest new, robust and tractable numerical techniques for solving fractional Black-Scholes equations applied to different practical market settings.

1.2 Outline of the thesis

The rest of the thesis is organised as follows.

Chapter 1 presented a general introduction of the thesis as well as a thorough review of related literatures. Pertinent gaps were identified and appropriate models as well as their approximation methods identified will be presented in subsequent chapters.

In Chapter 2 a time-fractional Black-Scholes PDE (tfBS-PDE) as well as its implicit numerical scheme are proposed. The derivation of the model and design of an unconditionally stable scheme are presented. Some numerical examples for pricing European put options pricing problems.

Chapter 3 serves to suggest a robust numerical scheme which is based on the generalisation of the Crank Nicholson (CN) difference method to solving the tfBS-PDE. Through rigorous theoretical analysis of the method is presented, and results therein indicates that the method is both convergent and unconditionally stable. Two numerical examples are presented to illustrate the robustness of the method.

Using the concept of Fractional Market Hypothesis (FMH), Chapter 4 suggest a model governed by some non-Gaussian fractional stochastic process. We derived a time-fractional Black-Scholes PDE (tfBS-PDE) and suggest a robust high order numerical method. We further discuss the stability and convergence properties of the numerical method followed by some numerical experiments confirming the theoretical observations.

Chapter 5 presents the design and analysis of one of the most robust numerical technique for pricing American options, under a time-fractional Black-Scholes setting. The proposed method therein is based on a front-fixing finite difference algorithm, one

which allow for the simultaneous computation of the option value as well as the optimal exercise boundary. Subsequent sections therein, presents the procedures involved, from the construction of the involved time fractional Black-Scholes PDE (tfBS-PDE), to the design of the numerical method which is based on the front-fixing transformation, incorporating the early exercise features of American options into the original model derivation.

Chapter 6 incorporates the concept of pricing double barrier options in the time-fractional Black-Scholes framework. The underlying motivation to price double barrier options via the time-fractional Black-Scholes framework is justified by evidence of presence of "long memory" in the time direction observed in many financial assets' time series. A numerical scheme for solving a double barrier option pricing time-fractional Black-Scholes equation is also suggested. The theoretical analysis results for stability and convergence are also presented therein.

Chapter 7 present the construction of a numerical solution method to a time-space fractional Black-Scholes Partial Differential Equation (tfBS-PDE). The existence and uniqueness of the constructed numerical scheme, its computational stability and convergence analysis are discussed therein and lastly, some numerical examples demonstrating the efficiency and robustness of the involved numerical method in solving time-tfBS-PDEs are presented.

Finally, Chapter 8 briefly present a summary of the whole thesis as well as highlight the scope for future research.

Chapter 2

An implicit finite difference scheme for a time-fractional Black-Scholes equation

In this chapter, dividend paying European stock options are modelled via a time-fractional Black-Scholes (tfBS) partial differential equation (PDE). The fractional derivatives used and subsequent results herein, are based on the Caputo and Jumarie (modified-Reimann-Liouville) derivative framework, coupled with some results from the Jumarie-fractional (generalised) Taylor series. The fractional stochastic dynamics is an appropriate framework to capture the market fluctuations in which random fractional white noise has the potential to estimate accurate European put option premiums, while providing a good numerical convergence.

2.1 Introduction

The motive in studying option pricing from a fractional calculus point of view is mainly due to the non-local nature of the involved fractional derivative operators and the underlying fractal processes. Fractional derivatives provide the best tools in explaining the trend and noise memory effects as well as capturing non-localised information about

the stock price movements, something that standard Brownian motions based models may fail to explain.

The aim of this chapter is two fold: firstly, to construct a time-fractional (tfBS) PDE for pricing European options on continuous dividend paying stocks, and, secondly, to propose an implicit finite difference method for solving these type of fractional partial differential equations (FPDEs). Through rigorous mathematical analysis, we establish that, the derived implicit finite difference scheme is unconditionally stable. To support these theoretical deductions, we present some numerical examples in the proposed framework on pricing European put options under different sets of continuous dividend yields.

The rest of the chapter is organised as follow, Section 2.2 presents some useful results regarding fractional derivatives that are very fundamental to the chapter. Specific focus is on three very common definitions of derivatives of fractional orders. Simultaneously, this section provides a brief account of work on the derivation of the tfBS-PDE for pricing options on dividend paying stocks. In Section 2.3, we present the derivation of an implicit finite difference scheme for solving the tfBS-PDE presented in Section 2.2. The theoretical analysis and discussion of the stability and convergence properties of the numerical scheme are discussed in Section 2.4. To substantiate and validate the theoretical claims regarding the proposed numerical method, extensive numerical experiments are presented in Section 2.5. Finally, some concluding remarks and scope for further research directions are presented in Section 2.6.

2.2 Time-fractional Black-Scholes (BS) Equation

In this section, firstly we present some key results about fractional derivatives. As far as the definitions of fractional derivatives are concerned, we only focus on three common derivative definitions, namely, those of the Remann-Liouville, Caputo, and Jumarie definition. We then present the derivation of the time-fractional Black-Scholes PDE for pricing options on stocks that pay continuous dividends.

2.2.1 Some mathematical preliminaries on fractional derivatives

In most recent literature, derivatives of fractional orders are defined in the Caputo, Reimann-Liouville and Jumarie (*modified Reimann-Liouville*) sense. For a detailed treatment for different types of fractional derivatives, merits and de-merits of their usage, see ([5]) and references therein. Some good discussions can be found in ([46, 47, 48, 49]).

In this section, we briefly review some preliminaries on fractional differentiation as well as present a brief derivation of the model under consideration.

Definition 2.2.1. ***Caputo fractional derivative***

Let $u : \mathbb{R} \to \mathbb{R}$ be a continuous, but not necessarily a differentiable function. The Caputo fractional derivative of order α is defined as follow

$$D_C^{\alpha} u(t) = \frac{1}{\Gamma(\eta - \alpha)} \int_0^t \frac{d^{\eta} u(\tau)}{dt^{\eta}} \frac{1}{(t-\tau)^{\alpha-\eta+1}} d\tau, \qquad \eta - 1 < \alpha < \eta. \tag{2.2.1}$$

Definition 2.2.2. ***Reimann-Liouville fractional derivative***

Let $u : \mathbb{R} \to \mathbb{R}$ be a continuous, but not necessarily a differentiable function. Then, the Reimann-Liouville fractional derivative of order α is given by

$$D_{RL}^{\alpha} u(t) = \frac{1}{\Gamma(\eta - \alpha)} \frac{d^{\eta}}{dt^{\eta}} \int_0^t \frac{u(\tau)}{(t-\tau)^{\alpha-\eta+1}} d\tau, \qquad \eta - 1 < \alpha < \eta. \tag{2.2.2}$$

The Riemann-Liouville derivative has certain disadvantages when modelling real-world phenomenons ([47]). For example, the Riemann-Liouville derivative of a constant is not zero. In addition, if an arbitrary function is a constant at the origin, its fractional derivative has a singularity at the origin, for example, the exponential and Mittag-Leffler functions. These disadvantages reduce the field of application of the Riemann-Liouville fractional derivative ([5]). Some of these disadvantages can be circumvented by modifying the Reimann-Liouville definition.

Jumarie in ([47]) modified the Reimann-Liouville derivative using the concept of

fractional differencing coupled with his theory of Jumarie-fractional (generalised) Taylor series. The definition by Jumarie takes into account the existence of a fractional derivative at $t = 0$, which is undefined in the Caputo and Reimann-Liouville derivatives.

Definition 2.2.3. ***Jumarie (modified Reimann-Liouville) derivative***

Let $u : \mathbb{R} \to \mathbb{R}$ be a continuous, but not necessarily a differentiable function, and suppose $u(t)$ is

(i) a constant K, then its Jumarie fractional derivative of order α is defined by

$$D_J^\alpha u(t) = \begin{cases} \frac{K}{\Gamma(\eta-\alpha)} t^{-\alpha+1-\eta}, & \alpha \leq \eta - 1, \\ 0, & \alpha > \eta - 1, \end{cases} \tag{2.2.3}$$

(ii) not a constant, then

$$D_J^\alpha u(t) = \frac{1}{\Gamma(\eta-\alpha)} \frac{d^\eta}{dt^\eta} \int_0^t \frac{\{u(\tau) - u(0)\}}{(t-\tau)^\alpha} d\tau, \quad \eta - 1 < \alpha < \eta. \tag{2.2.4}$$

Definition 2.2.4. ***Generalized (fractional) Taylor series***

Let $u : \mathbb{R} \to \mathbb{R}$ be a continuous function such that $u(t)$ has a fractional derivative of order $k\alpha$, for some positive integer k and $0 < \alpha \leq 1$, then the following equality holds

$$u(t+h) = \sum_{k=0}^{\infty} \frac{h^{k\alpha}}{\Gamma(1+k\alpha)} u^{(k\alpha)}(t), \quad 0 < \alpha \leq 1, \tag{2.2.5}$$

where $u^{(k\alpha)}(t)$ represent the fractional derivative of $k\alpha$-th order of $u(t)$.

Definition 2.2.5 provide a consistent framework for defining fractional derivatives of constant functions, which align fractional calculus to classical integer calculus.

Definition 2.2.5. ***Fractional differencing***

Let $u : \mathbb{R} \to \mathbb{R}$ be a continuous, but not necessarily a differentiable function, and

let $\kappa > 0$ denote the discretization step in t. Define the forward operator $FW(\kappa)$ by

$$FW(\zeta)u(t) = u(t+\kappa), \tag{2.2.6}$$

then, the fractional difference of order $\eta - 1 < \alpha < \eta$, of $u(t)$ is defined by the expression

$$\begin{aligned} \Delta^{\alpha}u(t) &= (FW-1)^{\alpha}u(t), \\ &= \sum_{\zeta=0}^{\infty}(-1)^{\zeta}\begin{pmatrix}\alpha\\ \zeta\end{pmatrix}u(t+(\alpha-\zeta)\kappa), \qquad \eta \in \mathbb{N}. \end{aligned} \tag{2.2.7}$$

2.2.2 Derivation of the time-fractional BS-PDE

In deriving the time-fractional BS-PDE, let us first assume that the stock price dynamics follows the following fractional stochastic equation

$$dS = rSdt + \sigma\omega(t)(dt)^{\alpha/2}, \qquad 0 < \alpha \leq 1, \tag{2.2.8}$$

where S and σ are respectively the price and volatility of the stock, r is the risk-free interest rate, and $\omega(t)$ denotes the standard Wiener process. In the presence of continuous dividends, denoted by δ, the above equation change to

$$dS = (r-\delta)Sdt + \sigma\omega(t)(dt)^{\alpha/2}, \qquad 0 < \alpha \leq 1. \tag{2.2.9}$$

Let us also consider the following important identities, which, according to Jumarie [49] are consistent with the generalised Taylor series defined in Definition 2.2.4:

$$d^{\alpha}t = \frac{1}{\Gamma(2-\alpha)}t^{1-\alpha}(dt)^{\alpha}, \qquad 0 < \alpha \leq 1, \tag{2.2.10}$$

$$d^{\alpha}S = \Gamma(1+\alpha)dS, \qquad 0 < \alpha \leq 1, \tag{2.2.11}$$

and

$$\frac{d^{\alpha}S}{(dS)^{\alpha}} = \frac{1}{\Gamma(2-\alpha)}S^{1-\alpha}, \qquad 0 < \alpha \leq 1. \tag{2.2.12}$$

Combining (2.2.11) and (2.2.12), we obtain a conversion formula which allows us to convert integer derivatives to fractional derivatives and vice versa:

$$dS = \frac{S^{(1-\alpha)}}{\Gamma(1+\alpha)\Gamma(2-\alpha)}(dS)^{\alpha}, \qquad 0 < \alpha \leq 1. \tag{2.2.13}$$

Suppose $V = V(S,t)$ represent the value of a European put option, and suppose that $V(S,t)$ satisfies the assumption 2.2.6

Assumption 2.2.6. *Assume the function $V(S,t)$ is sufficiently smooth with respect to S and its α derivative with respect to time exists for some α $(0 < \alpha \leq 1)$.*

Consider the risk-free investment interest rate dynamic equation

$$dV = rVdt. \tag{2.2.14}$$

Multiplying both sides of (2.2.14) with $\Gamma(1-\alpha)$, we obtain

$$\Gamma(1-\alpha)dV = \Gamma(1-\alpha)rVdt. \tag{2.2.15}$$

Now, combining (2.2.15) with (2.2.11) yields the variational fractional increment process

$$d^{\alpha}V = \Gamma(1+\alpha)rVdt. \tag{2.2.16}$$

Equation (2.2.16) along with (2.2.13) yield the following fractional interest rate dy-

namic equation

$$d^{\alpha}V = \frac{rV}{\Gamma(2-\alpha)}t^{1-\alpha}(dt)^{\alpha}. \tag{2.2.17}$$

Since $V(S,t)$ is sufficiently smooth with respect to S and its α-derivative $(0 < \alpha \leq 1)$ with respect to t exists, applying the fractional Taylor series (2.2.5) of order α on $V(S,t)$ up to remaining error term yields

$$dV = \frac{1}{\Gamma(1+\alpha)}\frac{\partial^{\alpha}V}{\partial t^{\alpha}}(dt)^{\alpha} + \frac{\partial V}{\partial S}dS + \frac{1}{2}\frac{\partial^2 V}{\partial S^2}(dS)^2. \tag{2.2.18}$$

Combining this with Itô's lemma on equation (2.2.9), we obtain

$$dV = \frac{1}{\Gamma(1+\alpha)}\frac{\partial^{\alpha}V}{\partial t^{\alpha}}(dt)^{\alpha} + (r-\delta)S\frac{\partial V}{\partial S}dt + \frac{1}{2}\sigma^2 S^2\frac{\partial^2 V}{\partial S^2}(dt)^{\alpha}. \tag{2.2.19}$$

Using the conversion formula (2.2.13) but in terms of t, we can replace dt in (2.2.19) with

$$dt = \frac{t^{1-\alpha}(dt)^{\alpha}}{\Gamma(1+\alpha)\Gamma(2-\alpha)}, \tag{2.2.20}$$

to obtain

$$dV = \frac{1}{\Gamma(1+\alpha)}\frac{\partial^{\alpha}V}{\partial t^{\alpha}}(dt)^{\alpha} + \frac{(r-\delta)}{\Gamma(1+\alpha)\Gamma(2-\alpha)}St^{1-\alpha}\frac{\partial V}{\partial S}(dt)^{\alpha} + \frac{1}{2}\sigma^2 S^2\frac{\partial^2 V}{\partial S^2}(dt)^{\alpha}. \tag{2.2.21}$$

Multiplying both sides of (2.2.21) with $\Gamma(1+\alpha)$, we obtain

$$\Gamma(1+\alpha)dV = \left(\frac{\partial^{\alpha}V}{\partial t^{\alpha}} + \frac{(r-\delta)}{\Gamma(2-\alpha)}St^{1-\alpha}\frac{\partial V}{\partial S} + \frac{\Gamma(1+\alpha)}{2}\sigma^2 S^2\frac{\partial^2 V}{\partial S^2}\right)(dt)^{\alpha}. \tag{2.2.22}$$

Using (2.2.17), the left-hand side of (2.2.22) can be re-written as

$$\begin{aligned} \Gamma(1+\alpha)dV &= d^{\alpha}V, \\ &= \frac{rV}{\Gamma(2-\alpha)}t^{1-\alpha}(dt)^{\alpha}. \end{aligned} \tag{2.2.23}$$

Using (2.2.23) along with (2.2.22), we obtain

$$\frac{rV}{\Gamma(2-\alpha)}t^{1-\alpha} = \frac{\partial^{\alpha}V}{\partial t^{\alpha}} + \frac{(r-\delta)}{\Gamma(2-\alpha)}St^{1-\alpha}\frac{\partial V}{\partial S} + \frac{\Gamma(1+\alpha)}{2}\sigma^2S^2\frac{\partial^2V}{\partial S^2}. \tag{2.2.24}$$

Equation (2.2.24) can further be simplified into the following tfBS-PDE

$$\frac{\partial^{\alpha}V}{\partial t^{\alpha}} = \left(rV - qS\frac{\partial V}{\partial S}\right)\frac{t^{1-\alpha}}{\Gamma(2-\alpha)} - \frac{\Gamma(1+\alpha)}{2}\sigma^2S^2\frac{\partial^2V}{\partial S^2},\ q = r-\delta;\ 0<\alpha\leq 1 \tag{2.2.25}$$

We can now proceed with developing a robust numerical scheme to solve the tfBS-PDE (2.2.25) coupled with the following boundary and terminal conditions

$$\left.\begin{aligned} V(S,0) &= \max(K-S,0), \\ V(0,t) &= Ke^{-r(T-t)}, \\ \lim_{S\to\infty} V(S,t) &= 0, \end{aligned}\right\} \tag{2.2.26}$$

where K is the strike price of the European put option and T is the maturity time.

2.3 Numerical method

In this section, we present the construction of an implicit numerical method for solving (2.2.25) along with (2.2.26). To begin with, let L and N be positive integers and define $h = 1/L$ and $k = 1/N$ as the space and time step-sizes, respectively. Define

$S_l = lh; \quad l = 0, 1, 2, ..., L$ and $t_n = nk; \quad n = 0, 1, 2, ..., N$, such that $S_l \in [S_{min}, S_{max}]$ and $t_n \in [0, T]$. Furthermore, define $V_l^n = V(S_l, t_n)$ as the solution at the grid point $(S_l, t_n) = (lh, nk)$.

Using the definition of Caputo fractional derivative given in (2.2.1) for $\eta = 1$, the time-derivative in (2.2.25) can be approximated by

$$\begin{aligned}
\frac{\partial^\alpha V(S_l,t_n)}{\partial t^\alpha} &= \frac{1}{\Gamma(1-\alpha)}\int_0^{t_n}\frac{\partial V(S_l,\tau)}{\partial t}(t_n-\tau)^{-\alpha}d\tau,\\
&= \frac{1}{\Gamma(1-\alpha)}\sum_{j=1}^{n}\int_{(j-1)k}^{jk}\left(\frac{V_l^j-V_l^{j-1}}{k}+O(k)\right)(nk-\tau)^{-\alpha}d\tau,\\
&= \frac{1}{\Gamma(1-\alpha)}\sum_{j=1}^{n}\left(\frac{V_l^j-V_l^{j-1}}{k}+O(k)\right)\left(\frac{(nk-(j-1)k)^{1-\alpha}-(nk-jk)^{1-\alpha}}{1-\alpha}\right),\\
&= \frac{1}{\Gamma(1-\alpha)}\frac{1}{1-\alpha}\sum_{j=1}^{n}\left(\frac{V_l^j-V_l^{j-1}}{k}+O(k)\right)\left[(n-j+1)^{1-\alpha}-(n-j)^{1-\alpha}\right]k^{1-\alpha},\\
&= \frac{1}{\Gamma(2-\alpha)}\frac{1}{k^\alpha}\sum_{j=1}^{n}\left[V_l^j-V_l^{j-1}\right]\left[(n-j+1)^{1-\alpha}-(n-j)^{1-\alpha}\right]\\
&\quad+\frac{1}{\Gamma(2-\alpha)}\sum_{j=1}^{n}\left[(n-j+1)^{1-\alpha}-(n-j)^{1-\alpha}\right]O(k)k^{1-\alpha},\\
&= \frac{1}{\Gamma(2-\alpha)}\frac{1}{k^\alpha}\sum_{j=1}^{n}(V_l^j-V_l^{j-1})\left[(n-j+1)^{1-\alpha}-(n-j)^{1-\alpha}\right]\\
&\quad+\frac{1}{\Gamma(2-\alpha)}\sum_{j=1}^{n}\left[(n-j+1)^{1-\alpha}-(n-j)^{1-\alpha}\right]O(k^{2-\alpha}). \qquad (2.3.1)
\end{aligned}$$

Shifting the indices in (2.3.1) we obtain

$$\begin{aligned}
\frac{\partial^\alpha V(S_l,t_n)}{\partial t^\alpha} &= \frac{1}{\Gamma(2-\alpha)}\frac{1}{k^\alpha}\sum_{j=1}^{n}\left(V_l^{n-j+1}-V_l^{n-j}\right)\left[j^{1-\alpha}-(j-1)^{1-\alpha}\right]\\
&\quad+\frac{1}{\Gamma(2-\alpha)}\sum_{j=1}^{n}\left[j^{1-\alpha}-(j-1)^{1-\alpha}\right]O(k^{2-\alpha}). \qquad (2.3.2)
\end{aligned}$$

Let

$$\rho_\alpha := \frac{1}{\Gamma(2-\alpha)}\frac{1}{k^\alpha}, \tag{2.3.3}$$

and

$$\beta_j := j^{1-\alpha} - (j-1)^{1-\alpha}; \quad j = 1, 2, \cdots, n, \tag{2.3.4}$$

such that $1 = \beta_1 > \beta_2 > \cdots > \beta_n \to 0$. Substituting ρ_α and β_j into (2.3.2) yield

$$\begin{aligned}
\frac{\partial^\alpha V(S_l, t_n)}{\partial t^\alpha} &= \rho_\alpha \sum_{j=1}^{n} \beta_j \left(V_l^{n-j+1} - V_l^{n-j}\right) + \frac{1}{\Gamma(2-\alpha)} \sum_{j=1}^{n} \beta_j O(k^{2-\alpha}), \\
&= \rho_\alpha \sum_{j=1}^{n} \beta_j \left(V_l^{n-j+1} - V_l^{n-j}\right) + \frac{1}{\Gamma(2-\alpha)} n^{1-\alpha} O(k^{2-\alpha}), \\
&= \rho_\alpha \sum_{j=1}^{n} \beta_j \left(V_l^{n-j+1} - V_l^{n-j}\right) + \frac{1}{\Gamma(2-\alpha)} \left(\frac{t_n}{k}\right)^{1-\alpha} O(k^{2-\alpha}), \\
&= \rho_\alpha \sum_{j=1}^{n} \beta_j \left(V_l^{n-j+1} - V_l^{n-j}\right) + \frac{t_n^{1-\alpha}}{\Gamma(2-\alpha)} k.
\end{aligned} \tag{2.3.5}$$

The time derivative in (2.2.25) is therefore approximated by

$$\frac{\partial^\alpha V(S_l, t_n)}{\partial t^\alpha} = \rho_\alpha \sum_{j=1}^{n} \beta_j (V_l^{n-j+1} - V_l^{n-j}) + O(k). \tag{2.3.6}$$

One can clearly see that for $j = 1$ and $\alpha = 1$ the fractional difference formula (2.3.6) reduces to the classical finite difference formula

$$\frac{\partial V(S_l, t_n)}{\partial t} = \frac{V_l^n - V_l^{n-1}}{k} + O(k).$$

Now, the first and second spatial derivatives in (2.2.25) are discretised using the

usual forward and central finite difference approximations, respectively, i.e.,

$$\frac{\partial V(S_l,t_n)}{\partial S}=\frac{V_{l+1}^n-V_l^n}{h}+O(h) \tag{2.3.7}$$

and

$$\frac{\partial^2 V(S_l,t_n)}{\partial S^2}=\frac{V_{l+1}^n-2V_l^n+V_{l-1}^n}{h^2}+O(h^2). \tag{2.3.8}$$

Using (2.3.6), (2.3.7) and (2.3.8) into (2.2.25), we obtain the full scheme

$$\begin{aligned}\rho_\alpha\sum_{j=1}^{n}\beta_j(V_l^{n-j+1}-V_l^{n-j}) &= \left(rV_l^n-(r-\delta)l(V_{l+1}^n-V_l^n)\right)\frac{(nk)^{1-\alpha}}{\Gamma(2-\alpha)}\\ &\quad-\frac{\Gamma(1+\alpha)\sigma^2l^2}{2}\left(V_{l+1}^n-2V_l^n+V_{l-1}^n\right).\end{aligned} \tag{2.3.9}$$

Now (2.3.9) can be further simplified to have the form

$$a_{nl}V_{l-1}^n+b_{nl}V_l^n+c_{nl}V_{l+1}^n=(1-\beta_2)V_l^{n-1}+\sum_{j=2}^{n-1}\varphi_jV_l^{n-j}+\beta_nV_l^0, \tag{2.3.10}$$

where

$$\varphi_j:=\beta_j-\beta_{j+1};\quad j=1,2,\cdots,n, \tag{2.3.11}$$

and

$$\begin{aligned}a_{nl} &= \rho_\alpha^{-1}\left(\frac{\Gamma(1+\alpha)\sigma^2l^2}{2}\right),\\ b_{nl} &= 1-\rho_\alpha^{-1}\left(\Gamma(1+\alpha)\sigma^2l^2+\frac{(r+(r-\delta)l)\,(nk)^{1-\alpha}}{\Gamma(2-\alpha)}\right),\\ c_{nl} &= \rho_\alpha^{-1}\left(\frac{\Gamma(1+\alpha)\sigma^2l^2}{2}+\frac{(r-\delta)l(nk)^{1-\alpha}}{\Gamma(2-\alpha)}\right);\quad l=1,2,\cdots,L.\end{aligned}$$

The matrix representation of the above is given by

$$\mathbf{A}_n\mathbf{U}_n = \varphi_1\mathbf{U}_{n-1} + \varphi_2\mathbf{U}_{n-2} + \cdots + \varphi_{n-1}\mathbf{U}_1 + \beta_n\mathbf{U}_0, \tag{2.3.12}$$

which can further be written as

$$\mathbf{A}_n\mathbf{U}_n = \mathbf{b}_n, \tag{2.3.13}$$

where

$$\mathbf{A}_n = \begin{pmatrix} a_{1n} & b_{1n} & c_{1n} & 0 & \cdots & \cdots & 0 \\ 0 & a_{2n} & b_{2n} & c_{2n} & & & \vdots \\ \vdots & & \ddots & \ddots & \ddots & & \vdots \\ \vdots & & & a_{l-1n} & b_{l-1n} & c_{l-1n} & 0 \\ 0 & \cdots & \cdots & 0 & a_{Ln} & b_{Ln} & c_{Ln} \end{pmatrix}, \quad \mathbf{U}_n = \begin{pmatrix} V_0^n \\ V_1^n \\ \vdots \\ V_{L-1}^n \\ V_L^n \end{pmatrix},$$

$$\mathbf{b}_n = \sum_{j=1}^{n-1} \varphi_j \mathbf{U}_{n-j} + \beta_n \mathbf{U}_0.$$

Remark 2.3.1. The following observations can easily be verified

$$\left.\begin{array}{l} 1 = \beta_1 > \beta_2 > \cdots \beta_n \to 0, \\ \varphi_1 = 1 - \beta_2, \\ \sum_{j=1}^{n-1} \varphi_j = 1 - \beta_n, \\ \sum_{j=1}^{\infty} \varphi_j = 1 > 1 - (2^{1-\alpha} - (2-1)^{1-\alpha}) = 2 - 2^{1-\alpha} = \varphi_1 > \varphi_2 > \cdots \to 0. \end{array}\right\} \tag{2.3.14}$$

Now, before we proceed further, we analyze the numerical method presented above.

2.4 Analysis of the numerical method

In this section we present the stability and convergence analysis of our implicit finite difference scheme (2.3.9).

2.4.1 Stability Analysis

Let $\tilde{V}_l^n; l = 0, 1, 2, \cdots L; n = 0, 1, 2, \cdots N;$ be an approximate solution obtained by using (2.3.9). Define $\varepsilon_l^n = V_l^n - \tilde{V}_l^n$ as the truncation error, such that $\varepsilon_0^n = \varepsilon_L^n = 0$ for all n.

Now setting $n = 1$ in (2.3.9) and simplifying further, we have

$$\rho_\alpha^{-1}\left(\frac{\Gamma(1+\alpha)\sigma^2 l^2}{2}\right)V_{l-1}^1 + \left(1 - \rho_\alpha^{-1}\left(\Gamma(1+\alpha)\sigma^2 l^2 + \frac{(r+(r-\delta)l)\,(nk)^{1-\alpha}}{\Gamma(2-\alpha)}\right)\right)V_l^1$$
$$+\rho_\alpha^{-1}\left(\frac{\Gamma(1+\alpha)\sigma^2 l^2}{2} + \frac{(r-\delta)l(nk)^{1-\alpha}}{\Gamma(2-\alpha)}\right)V_{l+1}^1 = V_l^0, \tag{2.4.1}$$

which can be represented as

$$a_{1l}V_{l-1}^1 + b_{1l}V_l^1 + c_{1l}V_{l+1}^1 = V_l^0, \tag{2.4.2}$$

where

$$\begin{aligned}
a_{1l} &= \rho_\alpha^{-1}\left(\frac{\Gamma(1+\alpha)\sigma^2 l^2}{2}\right), \\
b_{1l} &= 1 - \rho_\alpha^{-1}\left(\Gamma(1+\alpha)\sigma^2 l^2 + \frac{(r+(r-\delta)l)\,(nk)^{1-\alpha}}{\Gamma(2-\alpha)}\right), \\
c_{1l} &= \rho_\alpha^{-1}\left(\frac{\Gamma(1+\alpha)\sigma^2 l^2}{2} + \frac{(r-\delta)l(nk)^{1-\alpha}}{\Gamma(2-\alpha)}\right), \quad l = 1, 2, \cdots, L.
\end{aligned}$$

Using the error equation along with (2.4.2), we obtain

$$a_{1l}\varepsilon_{l-1}^1 + b_{1l}\varepsilon_l^1 + c_{1l}\varepsilon_{l+1}^1 = \varepsilon_l^0, \quad n = 1, \tag{2.4.3}$$

and with (2.3.10), we obtain

$$a_{nl}\varepsilon_{l-1}^{n} + b_{nl}\varepsilon_{l}^{n} + c_{nl}\varepsilon_{l+1}^{n} = \sum_{j=1}^{n-1} \varphi_j \varepsilon_{l}^{n-j} + \beta_n \varepsilon_{l}^{0}, \quad n \geq 2. \tag{2.4.4}$$

In matrix notations, (2.4.3) and (2.4.4) can be written as

$$\left.\begin{aligned} &\mathbf{A}_1\mathbf{E}_n = \mathbf{E}_0, && n = 1 \\ &\mathbf{A}_n\mathbf{E}_n = \varphi_1\mathbf{E}_{n-1} + \varphi_2\mathbf{E}_{n-2} + \cdots + \varphi_{n-1}\mathbf{E}_1 + \beta_n\mathbf{E}_0, && n \geq 2 \end{aligned}\right\} \tag{2.4.5}$$

where

$$\mathbf{E}_n = \begin{pmatrix} \varepsilon_1^n \\ \varepsilon_2^n \\ \vdots \\ \varepsilon_{L-1}^n \end{pmatrix}. \tag{2.4.6}$$

With above notations, we now prove the following theorem.

Theorem 2.4.1. *The implicit finite difference scheme (2.3.9) is unconditionally stable and its global error satisfies*

$$\|\mathbf{E}_n\|_\infty \leq \|\mathbf{E}_0\|_\infty, \quad \textit{for } n = 1, 2, 3, \cdots, N.$$

Proof. Suppose $n = 1$ and let

$$| \varepsilon_m^1 | = \max_{1 \leq l \leq L-1} | \varepsilon_l^1 | . \tag{2.4.7}$$

Then using (2.4.3), we see that

$$\begin{aligned} \|E_1\|_\infty &= |\ \varepsilon_m^1\ |, \\ &\leq |\ a_{1m}\varepsilon_{m-1}^1 + b_{ml}\varepsilon_m^1 + c_{1m}\varepsilon_{m+1}^1\ |, \\ &= |\ \varepsilon_l^0\ |, \\ &\leq \|\mathbf{E}_0\|_\infty, \end{aligned} \tag{2.4.8}$$

which implies that

$$\|\mathbf{E}_1\|_\infty \leq \|\mathbf{E}_0\|_\infty.$$

Now suppose for $n \geq 2$, we have

$$\|\mathbf{E}_{n-1}\|_\infty \leq \|\mathbf{E}_0\|_\infty.$$

Define

$$|\ \varepsilon_m^n\ | = \max_{1\leq l\leq L-1} |\ \varepsilon_l^n\ |\ . \tag{2.4.9}$$

Hence

$$\begin{aligned}
\|\mathbf{E}_n\|_\infty &= |\ \varepsilon_m^n\ |, \\
&\leq |\ a_{nm}\varepsilon_{m-1}^n + b_{nm}\varepsilon_m^n + c_{nm}\varepsilon_{m+1}^n\ |, \\
&= |\ \varphi_1\mathbf{E}_{n-1} + \varphi_2\mathbf{E}_{n-2} + \cdots + \varphi_{n-1}\mathbf{E}_1 + \beta_n\mathbf{E}_0\ |, \\
&\leq \varphi_1\ |\ \mathbf{E}_{n-1}\ | + \varphi_2\ |\ \mathbf{E}_{n-2}\ | + \cdots + \varphi_{n-1}\ |\ \mathbf{E}_1\ | + \beta_n\ |\ \mathbf{E}_0\ |, \\
&\leq \varphi_1\|\mathbf{E}_{n-1}\|_\infty + \varphi_2\|\mathbf{E}_{n-2}\|_\infty + \cdots + \varphi_{n-1}\|\mathbf{E}_1\|_\infty + \beta_n\|\mathbf{E}_0\|_\infty, \\
&\leq \varphi_1\|\mathbf{E}_0\|_\infty + \varphi_2\|\mathbf{E}_0\|_\infty + \cdots + \varphi_{n-1}\|\mathbf{E}_0\|_\infty + \beta_n\|\mathbf{E}_0\|_\infty, \\
&= (\varphi_1 + \varphi_2 + \cdots + \varphi_{n-1} + \beta_n)\ \|\mathbf{E}_0\|_\infty, \\
&= \left(\sum_{j=1}^{n-1}\varphi_j + \beta_n\right)\|\mathbf{E}_0\|_\infty, \\
&= (1 - \beta_n + \beta_n)\ \|\mathbf{E}_0\|_\infty, \\
&= \|\mathbf{E}_0\|_\infty. \qquad (2.4.10)
\end{aligned}$$

Therefore

$$\|\mathbf{E}_n\|_\infty \leq \|\mathbf{E}_0\|_\infty \ \text{ for all } \ n = 1, 2, \cdots, N,$$

which completes the proof of the theorem.

2.4.2 Convergence Analysis

Let U_l^n be the exact solution of (2.2.25) with condition (2.2.26) at the grid point (S_l, t_n). Define $e_l^n = U_l^n - V_l^n$, with $\mathbf{e}^n = (e_1^n, e_2^n, \cdots, e_{L-1}^n)^T$ and $\mathbf{e}^0 = 0$. Now since the errors e_l^n satisfy (2.3.10) and (2.4.2), we have for $n \geq 2$

$$a_{nl}e_{l-1}^n + b_{nl}e_l^n + c_{nl}e_{l+1}^n = \sum_{j=1}^{n-1}\varphi_j e_l^{n-j} + R_l^n, \qquad (2.4.11)$$

and for $n = 1$

$$a_{1l}e_{l-1}^1 + b_{1l}e_l^1 + c_{1l}e_{l+1}^1 = R_l^1. \qquad (2.4.12)$$

In the above, the remainder term R_l^n is obtained from (2.3.9) by multiplying both sides of the equation by $k^\alpha\Gamma(2-\alpha)$. This gives

$$\begin{aligned} R_l^n &= \sum_{j=1}^{n}\beta_j\left[V(S_l,t_{n+1-j})-V(S_l,t_{n-j})\right]-\mu k^\alpha V(S_l,t_n)-\omega k^\alpha\left[V(S_{l+1},t_n)-V(S_l,t_n\right] \\ &\quad +\beta k^\alpha\Gamma(2-\alpha)\left[V(S_{l+1},t_n)-2V(S_l,t_n)+V(S_{l-1},t_n)\right], \end{aligned} \tag{2.4.13}$$

where

$$\mu = rt^{1-\alpha},\ \ \omega=(r-\delta)lt^{1-\alpha}\ \text{ and }\ \beta=\frac{l^2\sigma^2\Gamma(1+\alpha)}{2}.$$

Define

$$L_k^\alpha V(S_l,t_n) := \frac{k^{-\alpha}}{\Gamma(2-\alpha)}\sum_{j=1}^{n}\beta_j\left[V(S_l,t_{n+1-j})-V(S_l,t_{n-j})\right], \tag{2.4.14}$$

then

$$\begin{aligned} &\left|\frac{\partial^\alpha V(S_l,t_n)}{\partial t^\alpha}-L_k^\alpha V(S_l,t_n)\right| \\ &\le \frac{1}{\Gamma(1-\alpha)}\sum_{j=1}^{n}\int_{(j-1)k}^{jk}\left|\frac{\partial V(S_l,\tau)}{\partial\tau}-\frac{(V(S_l,t_{n+1-j})-V(S_l,t_{n-j}))}{k}\right|\frac{d\tau}{(t_n-\tau)^\alpha}, \\ &\le \frac{1}{\Gamma(1-\alpha)}k\sum_{j=1}^{n}\int_{(j-1)k}^{jk}\frac{d\tau}{(t_n-\tau)^\alpha}, \\ &\le \frac{C}{\Gamma(1-\alpha)}k\int_0^{jk}\frac{d\tau}{(t_n-\tau)^\alpha}, \\ &\le C_1k, \end{aligned} \tag{2.4.15}$$

where C and C_1 are constants independent of h and k. Therefore

$$\begin{aligned} L_k^\alpha V(S_l,t_n) &= \frac{k^{-\alpha}}{\Gamma(2-\alpha)}\sum_{j=1}^{n}\beta_j\left[V(S_l,t_{n+1-j})-V(S_l,t_{n-j})\right] \\ &= \frac{\partial^\alpha V(S_l,t_n)}{\partial t^\alpha}+C_1k. \end{aligned} \tag{2.4.16}$$

We further note that

$$\frac{V(S_{l+1},t_n)-V(S_l,t_n)}{h}=\frac{\partial V(S_l,t_n)}{\partial S}+C_2h, \tag{2.4.17}$$

and

$$\frac{V(S_{l+1},t_n)-2V(S_l,t_n)+V(S_{l-1},t_n)}{h^2}=\frac{\partial^2 V(S_l,t_n)}{\partial S^2}+C_3h^2. \tag{2.4.18}$$

Substituting (2.4.16) - (2.4.18) into (2.4.13) and simplifying, we obtain

$$\begin{aligned} R_l^n &= k^\alpha\Gamma(2-\alpha)\left[\frac{\partial^\alpha V(S_l,t_n)}{\partial t^\alpha}-\frac{\mu}{\Gamma(2-\alpha)}V(S_l,t_n)-\frac{\omega}{\Gamma(2-\alpha)}\frac{\partial V(S_l,t_n)}{\partial S}+\beta\frac{\partial^2 V(S_l,t_n)}{\partial S^2}\right] \\ &\quad +C_1k^{1+\alpha}+C_2k^\alpha h+C_3k^\alpha h^2, \end{aligned} \tag{2.4.19}$$

where C_2 and C_3 are constants independent of h and k.

From (2.4.19), we have

$$\begin{aligned} \mid R_l^n \mid &\leq \hat{C}(k^{1+\alpha}+k^\alpha(h+h^2)), \\ &\leq \hat{C}(k^{1+\alpha}+k^\alpha h), \qquad (h^2\leq h), \end{aligned} \tag{2.4.20}$$

where $\hat{C}$ is a generic constant.

We can now prove the following main result.

Theorem 2.4.2. *Let V_l^n be the approximation of the exact solution U_l^n obtained via the implicit scheme (2.3.9). Then, there exist a constant $\widetilde{C}$, such that*

$$\max_{n,l}\|V_l^n-U_l^n\|\leq\widetilde{C}(k+h),\ \ \textit{for}\ \ l=1,2,\cdots,L-1\ \ \textit{and}\ \ n=1,2,\cdots,N.$$

Proof. To proceed, let

$$\|\mathbf{e}^n\|_\infty=\mid e_m^n\mid=\max_{1\leq l\leq L-1}\mid e_l^n\mid.$$

For $n = 1$, we have

$$\begin{aligned} \|\mathbf{e}^1\|_\infty &= \mid e_m^1 \mid, \\ &\leq \mid a_{1m}e_{m-1}^1 + b_{1m}e_l^1 + c_{1m}e_{m+1}^1 \mid, \\ &= \mid R_l^1 \mid, \\ &\leq \hat{C}\beta_1^{-1}(k^{1+\alpha} + k^\alpha h) \ \text{(using (2.4.20))}. \end{aligned} \tag{2.4.21}$$

Now, for $n \geq 2$, we have

$$\begin{aligned} \|\mathbf{e}^n\|_\infty &= \mid e_m^n \mid, \\ &\leq \mid a_{nm}e_{m-1}^n + b_{nm}e_m^n + c_{nm}e_{m+1}^1 \mid, \\ &= \mid \varphi_1\mathbf{e}^{n-1} + \varphi_2\mathbf{e}^{n-2} + \cdots + \varphi_1\mathbf{e}^1 + R_m^n \mid, \\ &\leq \varphi_1 \mid \mathbf{e}^{n-1} \mid + \varphi_2 \mid \mathbf{e}^{n-2} \mid + \cdots + \varphi_{n-1} \mid \mathbf{e}^1 \mid + \mid R_m^n \mid, \\ &\leq \varphi_1 \mid \mathbf{e}^{n-1} \mid + \varphi_2 \mid \mathbf{e}^{n-2} \mid + \cdots + \varphi_{n-1} \mid \mathbf{e}^1 \mid + \hat{C}(k^{1+\alpha} + k^\alpha h), \\ &\leq \varphi_1\|\mathbf{e}^{n-1}\|_\infty + \varphi_2\|\mathbf{e}^{n-2}\|_\infty + \cdots + \varphi_{n-1}\|\mathbf{e}^1\|_\infty + \hat{C}(k^{1+\alpha} + k^\alpha h), \\ &\leq (\varphi_1 + \varphi_2 + \cdots + \varphi_{n-1} + \beta_n)\beta_n^{-1}\hat{C}(k^{1+\alpha} + k^\alpha h), \\ &= \left(\sum_{j=1}^{n-1}\varphi_j + \beta_n\right)\beta_n^{-1}\hat{C}(k^{1+\alpha} + k^\alpha h), \\ &= (1 - \beta_n + \beta_n)\,\beta_n^{-1}\hat{C}(k^{1+\alpha} + k^\alpha h), \\ &= \hat{C}\beta_n^{-1}(k^{1+\alpha} + k^\alpha h). \end{aligned} \tag{2.4.22}$$

We further notice that

$$\begin{aligned}
\lim_{n\to\infty}\frac{\beta_n^{-1}}{n^\alpha} &= \lim_{n\to\infty}\frac{n^{-\alpha}}{n^{1-\alpha}-(n-1)^{1-\alpha}},\\
&= \lim_{n\to\infty}\frac{n^{-\alpha}}{n^{1-\alpha}}\left(\frac{1}{1-(1-\frac{1}{n})^{1-\alpha}}\right),\\
&= \lim_{n\to\infty}\frac{n^{-1}}{1-(1-\frac{1}{n})^{1-\alpha}},\\
&= \lim_{n\to\infty}\frac{n^{-1}}{(1-\alpha)n^{-1}},\\
&= \frac{1}{1-\alpha}. \qquad (2.4.23)
\end{aligned}$$

Therefore, from (2.4.21) and (2.4.22), we have

$$\begin{aligned}
\|\mathbf{e}^n\|_\infty &\leq \hat{C}n^\alpha(k^{1+\alpha}+k^\alpha h),\\
&= \hat{C}n^\alpha k^\alpha(k+h),\\
&= \hat{C}t_n^\alpha(k+h) \ \text{ since } \ t_n = nk \leq T,\\
&= \widetilde{C}(k+h) \ \text{ where } \ \widetilde{C} = \hat{C}t_n^\alpha. \qquad (2.4.24)
\end{aligned}$$

This completes the proof of the theorem.

In the next section, we present a set of numerical results confirming theoretical results presented above.

2.5 Numerical results

In this section the pricing of standard European put options using the time-fractional BS-PDE (2.2.25) is implemented via the implicit finite difference scheme (2.3.9) along with conditions (2.2.26). We consider two examples with varying dividend yields, and the order of the time derivative (α) ranging from 0.1 to 0.9. We further present results for error and convergence rates.

Example 2.5.1. Consider equation (2.2.25) subject to conditions (2.2.26) for pricing a European put option with the following parameters: $K = 150,\ r = 0.055,\ \sigma = 0.1,\ T = 1,\ S_{\max} = 450,\ L = 30,\ N = 50, \delta = 0.025,\ 0.045$ and 0.065.

Example 2.5.2. Consider equation (2.2.25) subject to conditions (2.2.26) for pricing a European put option with the following parameters: $K = 200,\ r = 0.065,\ \sigma = 0.025,\ T = 1,\ S_{\max} = 600,\ L = 33,\ N = 100, \delta = 0.045$ and 0.085.

In order to show that the proposed scheme is unconditionally stable and converge with order one in both time and asset price, the results are presented in tables 2.5.1 and 2.5.2 for Example 2.5.1 and in tables 2.5.3 and 2.5.4 for Example 2.5.2.

Table 2.5.1: Maximum absolute errors for Example 2.5.1 with $r = 0.055$ and $\delta = 0.065$.

α	$N = 40$	$N = 80$	$N = 160$	$N = 320$	$N = 640$
0.1	6.1152e-02	3.1069e-02	1.5659e-02	7.8606e-03	3.9381e-03
0.2	5.9707e-02	3.0276e-02	1.5245e-02	7.6491e-03	3.8312e-03
0.3	5.7925e-02	2.9330e-02	1.4758e-02	7.4021e-03	3.7069e-03
0.4	5.5896e-02	2.8272e-02	1.4218e-02	7.1294e-03	3.5698e-03
0.5	5.3692e-02	2.7136e-02	1.3641e-02	6.8388e-03	3.4240e-03
0.6	5.1370e-02	2.5948e-02	1.3040e-02	6.5369e-03	3.2726e-03
0.7	4.8978e-02	2.4731e-02	1.2427e-02	6.2289e-03	3.1183e-03
0.8	4.6552e-02	2.3503e-02	1.1809e-02	5.9190e-03	2.9631e-03
0.9	4.4121e-02	2.2277e-02	1.1194e-02	5.6107e-03	2.8088e-03
1.0	4.1705e-02	2.1064e-02	1.0586e-02	5.3066e-03	2.6567e-03

Table 2.5.2: Convergence rates for Example 2.5.1 with $r = 0.055$ and $\delta = 0.065$.

α	$N = 80$	$N = 160$	$N = 320$	$N = 640$
0.1	0.98	0.99	0.99	1.00
0.2	0.98	0.99	0.99	1.00
0.3	0.98	0.99	1.00	1.00
0.4	0.98	0.99	1.00	1.00
0.5	0.98	0.99	1.00	1.00
0.6	0.99	0.99	1.00	1.00
0.7	0.99	0.99	1.00	1.00
0.8	0.99	0.99	1.00	1.00
0.9	0.99	0.99	1.00	1.00
1.0	0.99	0.99	1.00	1.00

Table 2.5.3: Maximum absolute errors for Example 2.5.2 with $r = 0.065$ and $\delta = 0.045$.

α	$N = 40$	$N = 80$	$N = 160$	$N = 320$	$N = 640$
0.1	1.5661e-01	8.1330e-02	4.1509e-02	2.0978e-02	1.0547e-02
0.2	1.3930e-01	7.2084e-02	3.6713e-02	1.8533e-02	9.3120e-03
0.3	1.2548e-01	6.4751e-02	3.2926e-02	1.6607e-02	8.3404e-03
0.4	1.1445e-01	5.8938e-02	2.9934e-02	1.5088e-02	7.5750e-03
0.5	1.0574e-01	5.4365e-02	2.7586e-02	1.3898e-02	6.9759e-03
0.6	9.8970e-02	5.0832e-02	2.5777e-02	1.2983e-02	6.5152e-03
0.7	9.3914e-02	4.8203e-02	2.4435e-02	1.2304e-02	6.1741e-03
0.8	9.0418e-02	4.6397e-02	2.3516e-02	1.1840e-02	5.9410e-03
0.9	8.8420e-02	4.5378e-02	2.3001e-02	1.1581e-02	5.8109e-03
1.0	8.7951e-02	4.5161e-02	2.2896e-02	1.1530e-02	5.7857e-03

Table 2.5.4: Convergence rates for Example 2.5.2 with $r = 0.065$ and $\delta = 0.045$.

α	$N = 80$	$N = 160$	$N = 320$	$N = 640$
0.1	0.95	0.97	0.98	0.99
0.2	0.95	0.97	0.99	0.99
0.3	0.95	0.98	0.99	0.99
0.4	0.96	0.98	0.99	0.99
0.5	0.96	0.98	0.99	0.99
0.6	0.96	0.98	0.99	0.99
0.7	0.96	0.98	0.99	0.99
0.8	0.96	0.98	0.99	0.99
0.9	0.96	0.98	0.99	0.99
1.0	0.96	0.98	0.99	0.99

In Figures 2.5.1 to 2.5.3 and Figures 2.5.7 and 2.5.8, we plot the European put payoffs at maturity using the parameters as indicated in examples 2.5.1 and 2.5.2, respectively. The solid line indicates the intrinsic payoffs whereas the line with asterics indicates the approximated payoffs. For the second Example 2.5.2 the same set of parameter values for α were used and almost similar observations were obtained. Due to space limitations, only two cases, i.e., $\delta = 0.045$ and 0.085 are presented in the results below. In Figures 2.5.4 to 2.5.6 and Figures 2.5.9 and 2.5.10, we plot payoffs throughout the life span of the options for examples 2.5.1 and 2.5.2, respectively.

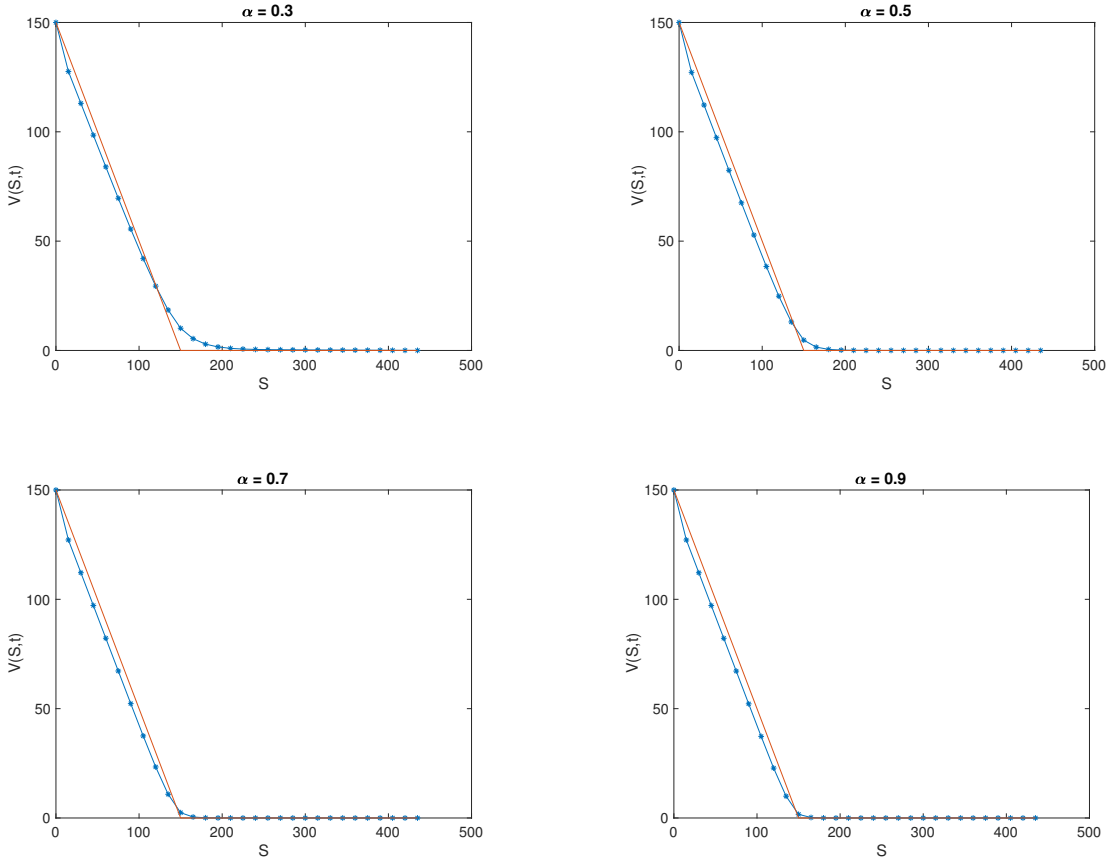

Figure 2.5.1: Payoffs for $\alpha = 0.3,\ 0.5,\ 0.7,\ 0.9,\ \delta = 0.025$ and $t = T$.

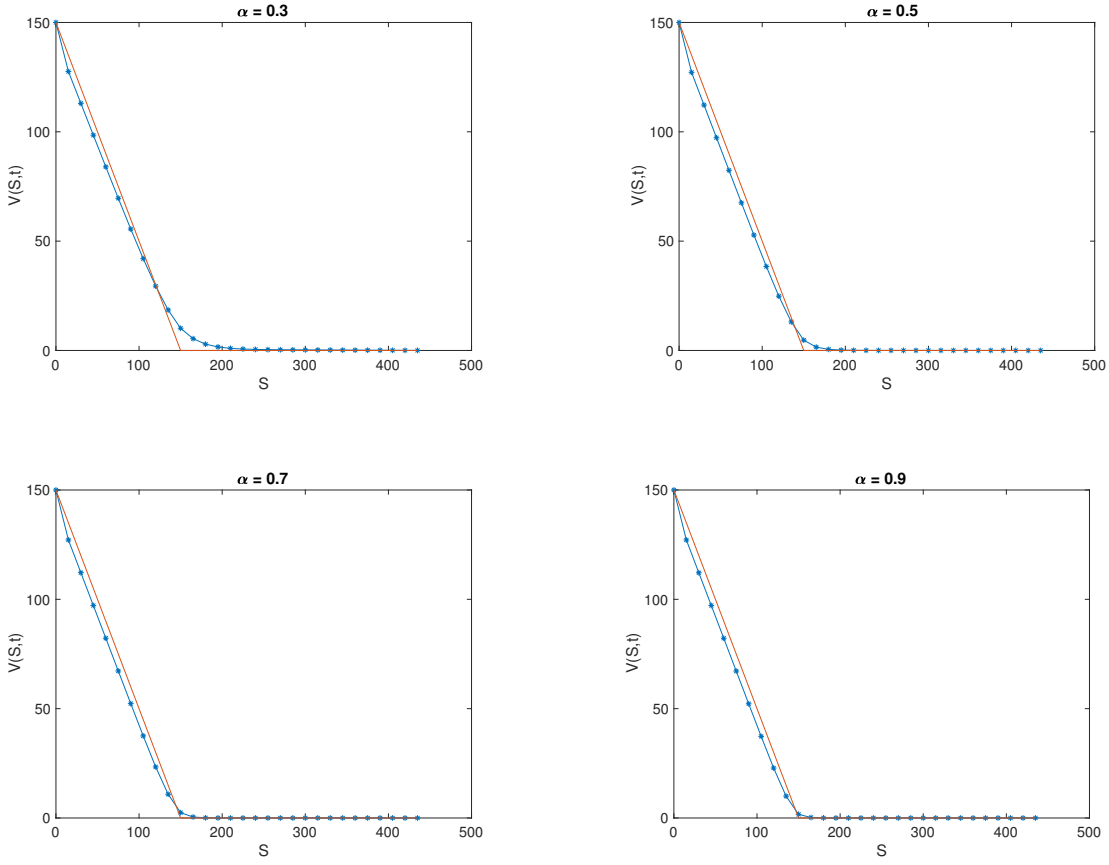

Figure 2.5.2: Payoffs for $\alpha = 0.3,\ 0.5,\ 0.7,\ 0.9,\ \delta = 0.045$ and $t = T$.

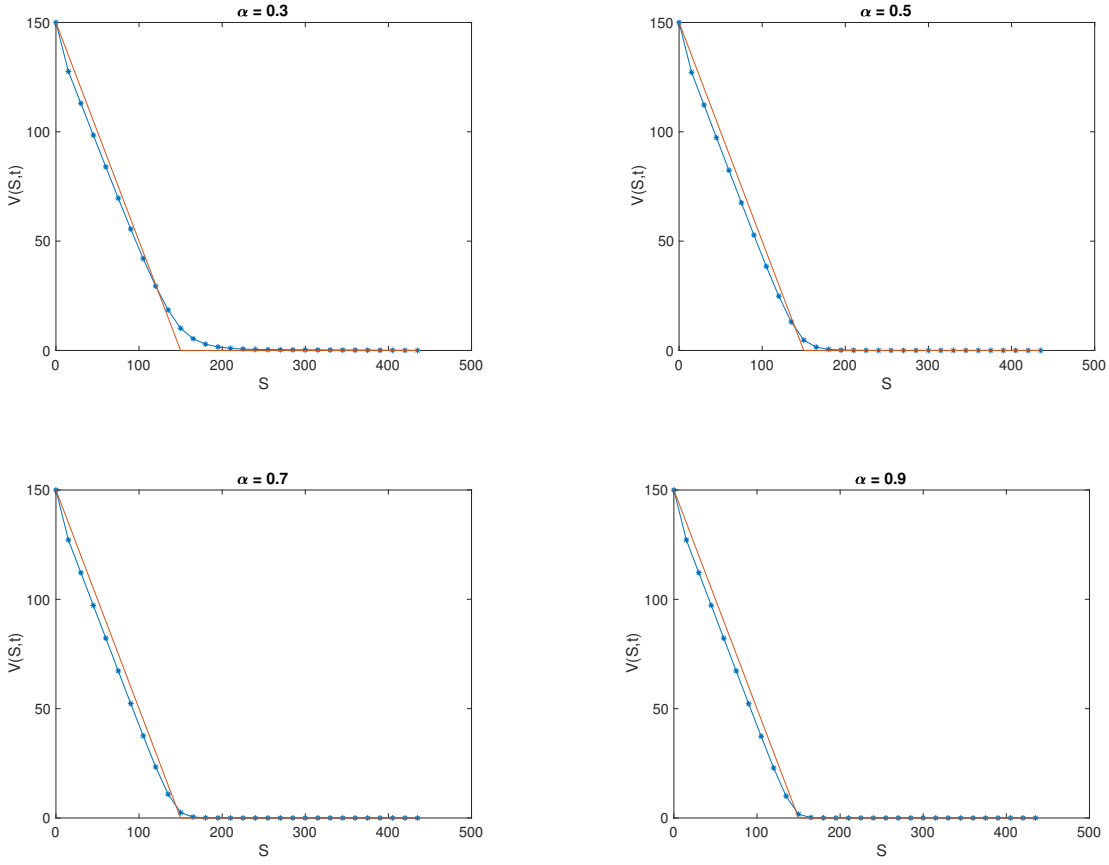

Figure 2.5.3: Payoffs for $\alpha = 0.3,\ 0.5,\ 0.7,\ 0.9,\ \delta = 0.065$ and $t = T$.

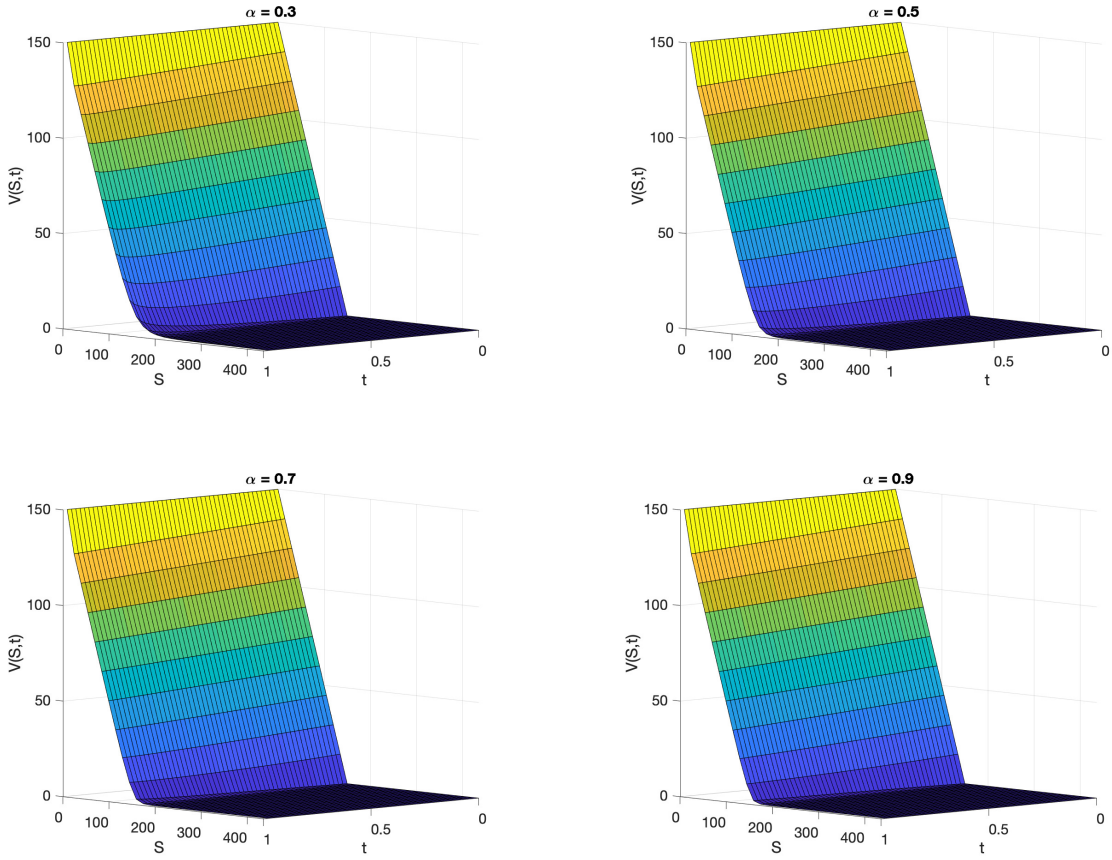

Figure 2.5.4: Payoffs for $\alpha = 0.3,\ 0.5,\ 0.7,\ 0.9,\ \delta = 0.025$, for all $0 \leq t \leq T$.

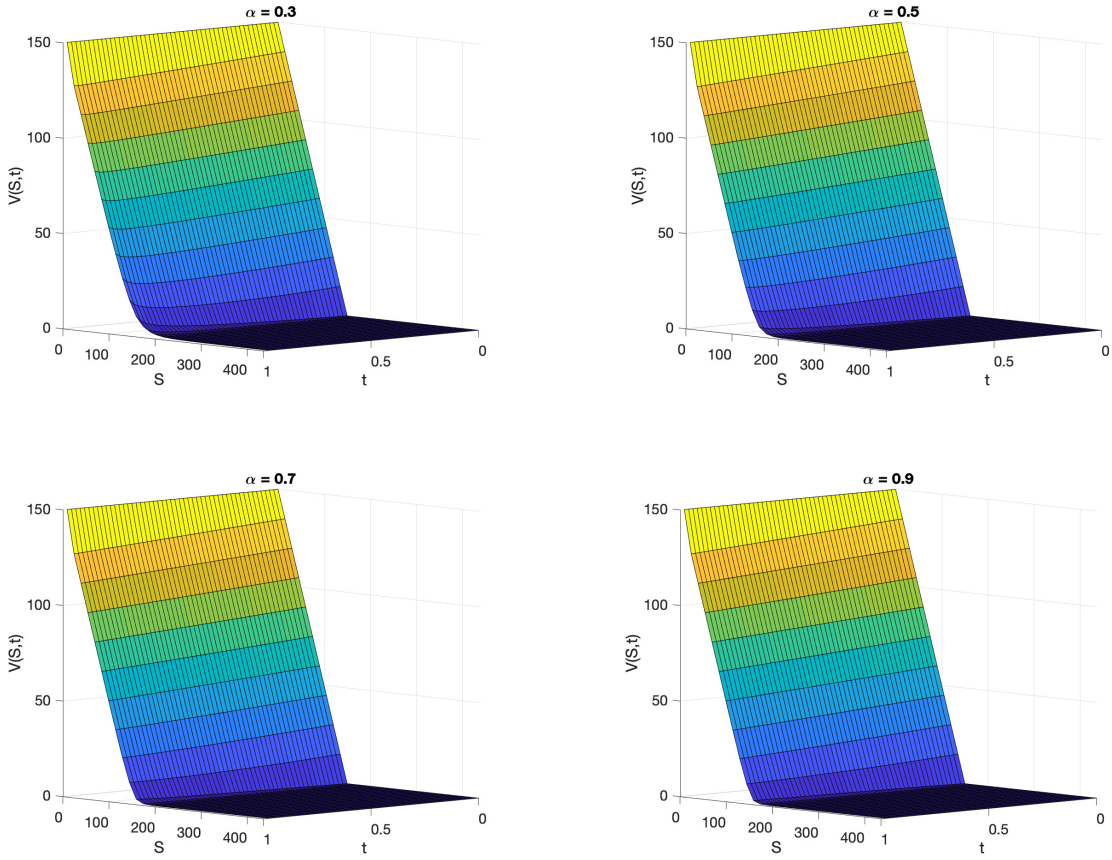

Figure 2.5.5: Payoffs for $\alpha = 0.3,\ 0.5,\ 0.7,\ 0.9,\ \delta = 0.045$, for all $0 \leq t \leq T$.

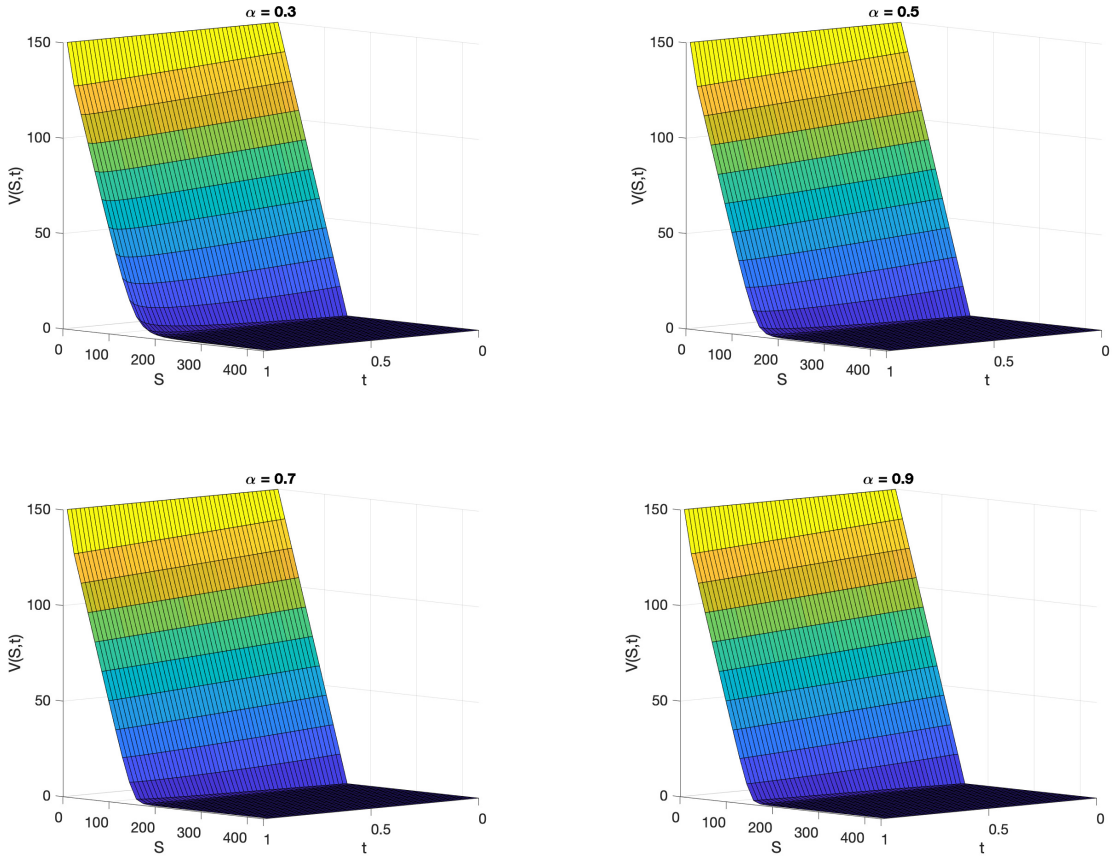

Figure 2.5.6: Payoffs for $\alpha = 0.3,\ 0.5,\ 0.7,\ 0.9,\ \delta = 0.065$, for all $0 \leq t \leq T$.

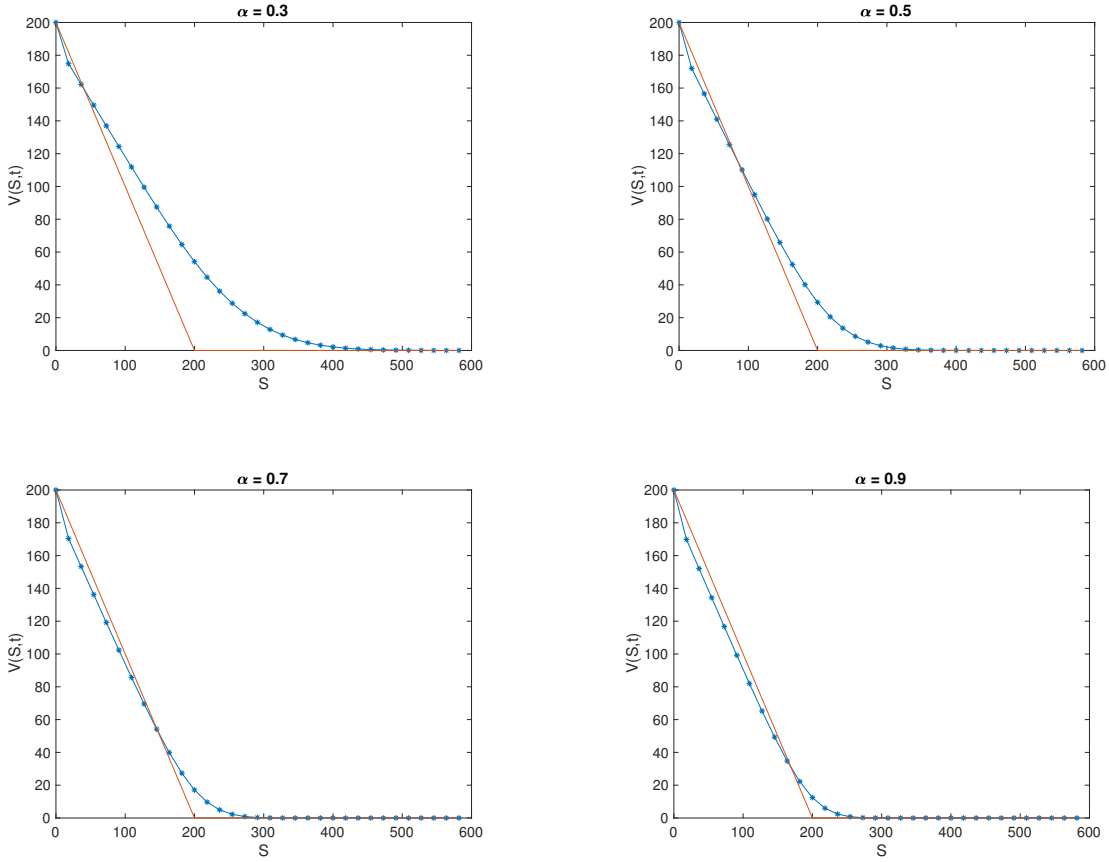

Figure 2.5.7: Payoffs for $\alpha = 0.3,\ 0.5,\ 0.7,\ 0.9,\ \delta = 0.045$ and $t = T$.

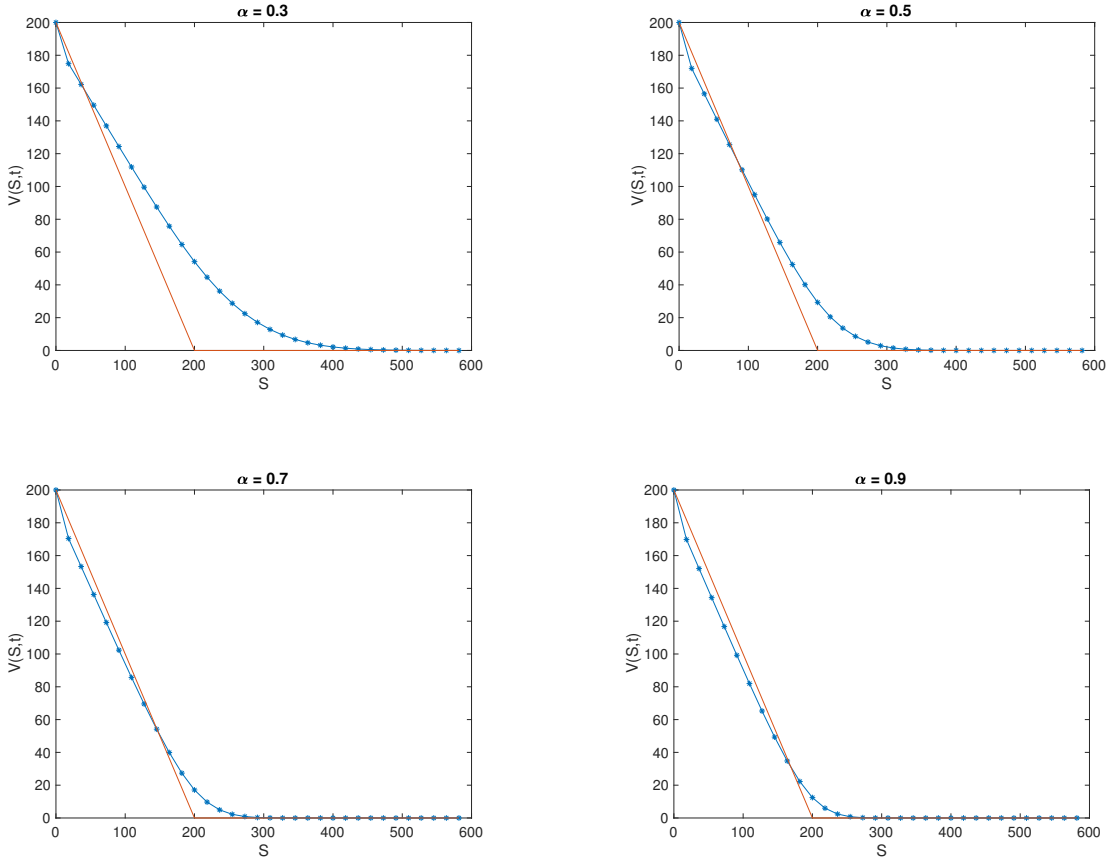

Figure 2.5.8: Payoffs for $\alpha = 0.3,\ 0.5,\ 0.7,\ 0.9,\ \delta = 0.085$ and $t = T$.

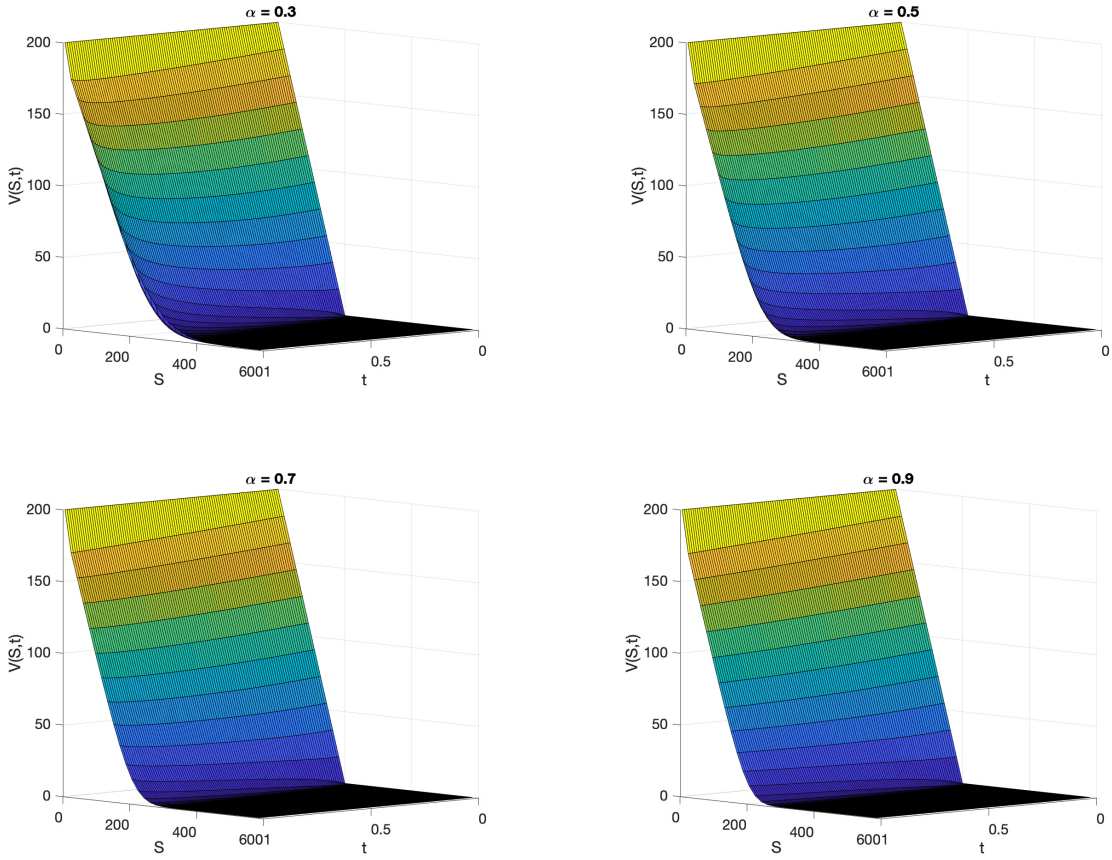

Figure 2.5.9: Payoffs for $\alpha = 0.3,\ 0.5,\ 0.7,\ 0.9,\ \delta = 0.045$ for all $0 \leq t \leq T$.

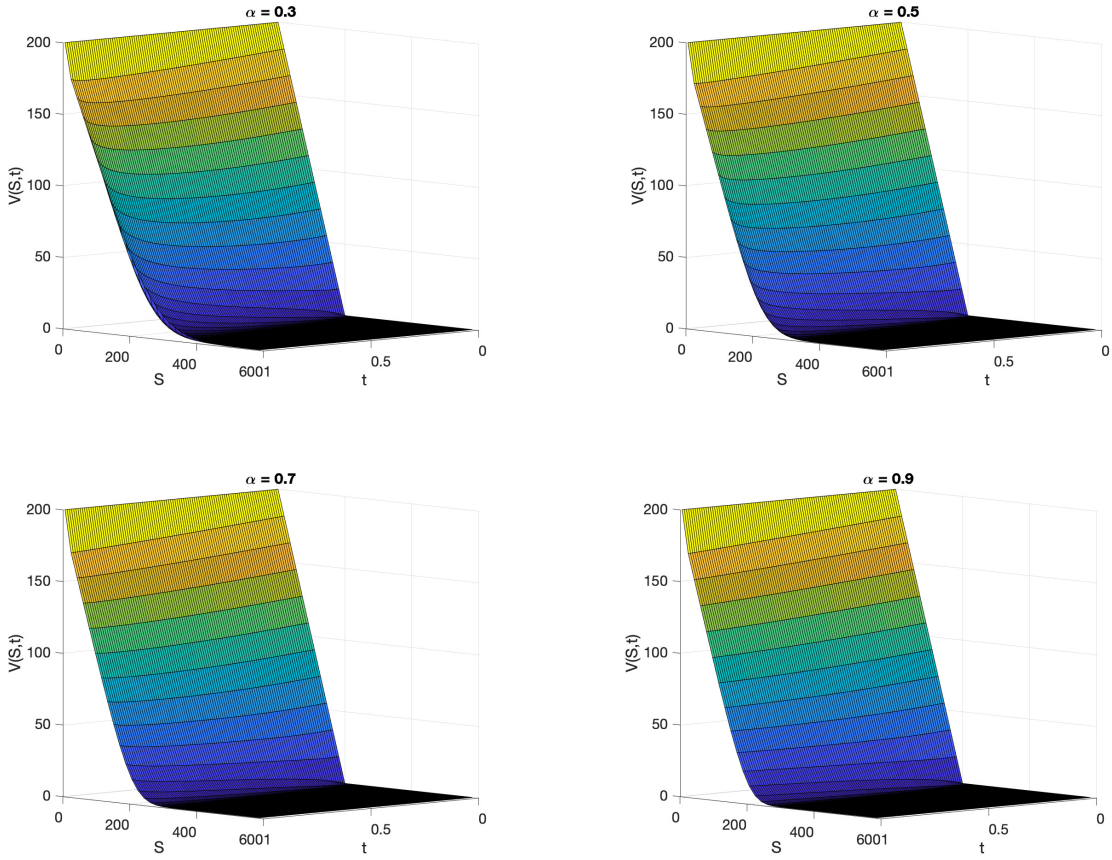

Figure 2.5.10: Payoffs for $\alpha = 0.3,\ 0.5,\ 0.7,\ 0.9,\ \delta = 0.085$ for all $0 \leq t \leq T$.

As one can see from the results presented above, the accuracy of the results is better in the case when $1/2 \leq \alpha \leq 1$ as compared to when $0 < \alpha < 1/2$. However, from the numerical point of view, α can be chosen to be small or large. And also, the fact that the proposed method is unconditionally stable, the choice of α does not affect the overall convergence of the method, see tables eg. 2.5.2 and 2.5.4. One may further note that, the restriction on α to be between 0.5 and 1 is not too large a hindrance, as regular markets's conditions would not require extreme lower values of α, since under such extremely lower α values, the underlying stock price S_t returns become

negatively correlated, which signal anti-persistent features which in-turn violates some key fundamental asset pricing assumptions. Similar observations are made under all considered dividend yields. To this end, it is worth noting that, changing the dividend yield does have a significant effect on the put premium results, if one carefully contrast the premium profiles obtained at different dividend yields, regardless of the value of α, one can observe that, high dividends yields are associated with high put premiums. This is true because, the underlying stock price is expected to drop by the amount of the dividend payout and hence a higher dividend yield would imply a higher put premium.

2.6 Summary and discussions

In this chapter, we formulated a time-fractional Black-Scholes PDE for pricing standard European put options written on a dividend paying stock. Then we designed and analyzed an implicit finite difference scheme for solving tfBS-PDEs. We proved that the proposed method is unconditionally stable and converges with order one in both time and asset direction. Two numerical examples supporting the theoretical claims were presented. As we can see from all the results presented, the proposed method is quite efficient for all values of the order of the fractional derivative considered in the simulations. Our results suggest that, the fractional framework is a very effective and robust approach for calculating European put premiums.

As can be seen from our results, the tfBS-PDE model produces option premiums curves which are very different from what classical theory may suggest. Another important feature to note is that the BS models proposed in the classical framework are known to produce option premium curves which are similar in shape and hence may not fully capture the effects of unanticipated market movements, whereas the fractional Black-Scholes models have the ability to produce premium curves which are quite sensitive to changes in associated parameters, such as, volatility, dividend, interest rate, news events etc. In summary, if sufficient market data is available, the fractional BS

models can be calibrated to produce option price curves that take into account a variety of different market conditions.

Currently, we are investigating other higher order methods for solving the tfBS-PDE presented in this chapter. Therefore in the Chapter 3 we present a much high order numerical scheme for solving time-fractional Black-Scholes PDEs.

Chapter 3

A Robust Crank Nicholson Scheme for a Stock Exchange Time Fractional Black-Scholes Equation

This chapter presents a robust numerical scheme based on the extension of the Crank Nicholson difference method in solving the tfBS-PDE obtained under the assumption that the stock market does exhibit some unexplained hereditary/memory features. Through rigorous theoretical analysis, our results indicate that the method is both convergent and unconditionally stable. Some numerical results are also presented to illustrate the robustness of the method.

3.1 Introduction

There is empirical evidence in support of the assertion that fractional stochastic models are well suited for modelling systems and phenomenons exhibiting hereditary characters. The use of fractional models to explain memory observed in a number of financial markets including the stock market has recently taken over the context of academic literatures and debates within the financial mathematic and behavioural finance disciplines. The efficient market hypothesis used in contemporary financial modelling liter-

atures often neglects the effects of memory, though memory has long been observed in a number financial data. In assuming the stock market exhibits some unexplained memory structures, depicted by some non-random fractional stochastic dynamics which are governed by the usual standard Brownian motion, we obtain a time fractional Black-Scholes (tfBS) partial differential equation PDE for pricing stock options.

Though the chapter presents a robust numerical scheme for solving tfBS-PDEs for pricing European stock options, ideas and techniques presented herein can be extended to solving tsfBS-PDEs. The method under consideration is an extension of the Crank-Nicholson method to solving tfBS-PDEs. To the best of our knowledge, this approach has not yet been experimented in solving time-fractional Black-Scholes PDEs.

The method herein does not only prove to have an advantage over unconditional stability, but it also attain high accuracy compared to it's implicit and explicit methods. In the implicit and explicit cases, the order of accuracy in time maybe lower than the one in the asset direction. For example, if one wish to reduce the approximation error by four, one has to increase the temporal gird size by four and the spatial one (asset direction) by two, which results in eight times longer computational time. Our method therefore considerably reduces the computational time involved in computing the solution while attaining overall convergent and unconditional stable results.

The rest of this chapter is organized as follow, Section 3.2 present a brief derivation of the tfBS-PDE for pricing European options on continuous dividend paying stocks. In Section 3.3, we present the detailed construction of the numerical scheme. A comprehensive theoretical analysis of the method in terms of convergence and stability is presented in Section 3.4. Two practical examples on the use of the approach for pricing European put stock options can be found in Section 3.5. Lastly, Section 3.6 present some concluding remarks and set the scope for future research.

3.2 The time fractional Black-Scholes PDE

3.2.1 Model specification

Suppose the stock price S follows the following non-random fractional stochastic process presented in a fractional Maruyama representation $dB_\alpha(t) = \omega(t)(dt)^{\alpha/2}$

$$dS = (r-\delta)Sdt + \sigma S\omega(t)(dt)^{\alpha/2},\ 0 < \alpha \leq 1, \tag{3.2.1}$$

where $B_\alpha(t)$ is a fractal process governed by a Gaussian white noise $\omega(t)$, with σ^2 representing the volatility while r and δ represent the risk-free interest rate and the continuous dividend yield respectively.

The fractional dynamic equation (3.2.1) generalize the standard Brownian motion $B(t)$ given by $dB(t) = \omega(t)dt^{1/2}$ with $dB_\alpha(t) = \omega(t)(dt)^{\alpha/2}$ where $0 < \alpha \leq 1$.

Note that, when $\alpha = 1$, equation (3.2.1) is equivalent to a geometric Brownian motion.

It is further worth noting that, unlike in the standard Brownian motion, the non-Gaussian fractional process (3.2.1) does not make any prior assumption about the underlying distribution of the stock price (S). However, it does make inferences on how the market is scaling with respect to time. This feature is very important in modelling market cycles in forms of repeated patterns.

From equation (3.2.1) one can derive two families of fractional Black-Scholes PDEs, namely; tfBS-PDEs as well as tsfBS PDEs. Fundamental to the derivation of the tfBS-PDE are three key conversion formulae useful in converting between integer and fractional derivatives. According to ([49]) the following identities are well consistent with the fractional (Generalized) Taylor series expansion.

$$d^\alpha t = \frac{1}{\Gamma(2-\alpha)} t^{1-\alpha}(dt)^\alpha,\ 0 < \alpha \leq 1, \tag{3.2.2}$$

$$d^{\alpha}S = \Gamma(1+\alpha)dS, \quad 0 < \alpha \leq 1, \tag{3.2.3}$$

and

$$\frac{d^{\alpha}S}{(dS)^{\alpha}} = \frac{1}{\Gamma(2-\alpha)}S^{1-\alpha}, \ 0 < \alpha \leq 1. \tag{3.2.4}$$

Combination of the two indentities (3.2.3) and (3.2.4) results in the following derivative conversion formula

$$dS = \frac{S^{(1-\alpha)}}{\Gamma(1+\alpha)\Gamma(2-\alpha)}(dS)^{\alpha}, \ 0 < \alpha \leq 1. \tag{3.2.5}$$

If we let $V = V(S,t)$ represent the option value such that it is sufficiently smooth in the asset direction and that atleast its fractional time derivative of order α $(0 < \alpha \leq 1)$ exists, then, combining the evolution equation of a safe investment

$$dV = rVdt, \tag{3.2.6}$$

with the conversion formula (3.2.5) results in the following fractional interest rate (safe investment evolution) equation

$$d^{\alpha}V = \frac{rV}{\Gamma(2-\alpha)}t^{1-\alpha}(dt)^{\alpha}. \tag{3.2.7}$$

Since $V(S,t)$ is sufficiently smooth in the asset direction and fractionally differentiable in time up to order α $(0 < \alpha \leq 1)$, the fractional Taylor series expansion of $V(S,t)$ upto some remaining error terms yields

$$dV = \frac{1}{\Gamma(1+\alpha)}\frac{\partial^{\alpha}V}{\partial t^{\alpha}}(dt)^{\alpha} + \frac{\partial V}{\partial S}dS + \frac{1}{2}\frac{\partial^2 V}{\partial S^2}(dS)^2. \tag{3.2.8}$$

Combining (3.2.7) with the fractional Itô's lemma applied to equation (3.2.1), cou-

pled with some algebraic manipulations, we obtain the tfBS-PDE

$$\frac{\partial^\alpha V}{\partial t^\alpha} = \left(rV - qS\frac{\partial V}{\partial S}\right)\frac{t^{1-\alpha}}{\Gamma(2-\alpha)} - \frac{\Gamma(1+\alpha)}{2}\sigma^2 S^2\frac{\partial^2 V}{\partial S^2}, \tag{3.2.9}$$

where $q = r - \delta;\ 0 < \alpha \leq 1$, subject to the following initial and boundary conditions for a European put option

$$\left.\begin{aligned} &V(S,0) = \max(K-S,0),\\ &V(0,t) = Ke^{-r(T-t)},\\ &\lim_{S\to\infty} V(S,t) = 0, \end{aligned}\right\} \tag{3.2.10}$$

with K the strike price and T the maturity time. In the next section we present the details and construction of the numerical method.

3.3 Model discretization and numerical scheme

This section present the discretization of derivative terms in the tfBS-PDE (3.2.9) as well as it's full final scheme subject to initial and boundary conditions in (3.2.10).

3.3.1 Model discretization

Let L and N be positive integers and define $h = S_{max}/L$ and $k = T/N$ as the space and time step-sizes respectively. Define $S_l = lh;\ l = 0,1,2,...,L$ and $t_n = nk;\ n = 0,1,2,...,N$, such that $S_l \in [S_{min}, S_{max}]$ and $t_n \in [0,T]$. Furthermore, define $V_l^{n+1} = V(S_l, t_{n+1})$ as the solution at the grid point $(S_l, t_{n+1}) = (lh, (n+1)k)$.

Temporal discretization

Since the Caputo definition allows for incorporation of traditional initial and boundary conditions in the problem formulation, and also due to the fact that, the value of a European option $V(S,t)$ is a time differentiable function, we define the time fractional

derivative in (3.2.9) using Definition 2.2.1. If we let $\eta = 1$, from the time-fractional derivative in (3.2.9) we have

$$\begin{aligned}
\frac{\partial^\alpha V(S_l,t_{n+1})}{\partial t^\alpha} &= \frac{1}{\Gamma(1-\alpha)}\int_0^{t_{n+1}} \frac{\partial V(S_l,\tau)}{\partial t}(t_{n+1}-\tau)^{-\alpha}d\tau,\\
&\leq \frac{1}{\Gamma(1-\alpha)}\sum_{j=1}^{n+1}\int_{jk}^{(j+1)k}\left(\frac{V_l^{j+1}-V_l^{j-1}}{2k}+\mathcal{O}(k^2)\right)((n+1)k-\tau)^{-\alpha}d\tau,\\
&= \frac{1}{\Gamma(1-\alpha)}\frac{1}{1-\alpha}\sum_{j=1}^{n+1}\left(\frac{V_l^{j+1}-V_l^{j-1}}{2k}+\mathcal{O}(k^2)\right)\\
&\quad \left[(n-j)^{1-\alpha}-(n-j+1)^{1-\alpha}\right]k^{1-\alpha},\\
&= \frac{1}{2\Gamma(2-\alpha)}\frac{1}{k^\alpha}\sum_{j=1}^{n+1}\left[V_l^{j+1}-V_l^{j-1}\right]\left[(n-j)^{1-\alpha}-(n-j+1)^{1-\alpha}\right]\\
&\quad +\frac{1}{\Gamma(2-\alpha)}\sum_{j=1}^{n+1}\left[(n-j)^{1-\alpha}-(n-j+1)^{1-\alpha}\right]\mathcal{O}(k^2)k^{1-\alpha},\\
&= \frac{1}{2\Gamma(2-\alpha)}\frac{1}{k^\alpha}\sum_{j=1}^{n+1}(V_l^{j+1}-V_l^{j-1})\left[(n-j)^{1-\alpha}-(n-j+1)^{1-\alpha}\right]\\
&\quad +\frac{1}{\Gamma(2-\alpha)}\sum_{j=1}^{n+1}\left[(n-j)^{1-\alpha}-(n-j+1)^{1-\alpha}\right]\mathcal{O}(k^{3-\alpha}). \qquad (3.3.1)
\end{aligned}$$

Shifting the indices in (3.3.1) by $j = n - j$, we obtain

$$\begin{aligned}
\frac{\partial^\alpha V(S_l,t_n)}{\partial t^\alpha} &= \frac{1}{2\Gamma(2-\alpha)}\frac{1}{k^\alpha}\sum_{j=0}^{n}\left(V_l^{n-j+1}-V_l^{n-j-1}\right)\left[j^{1-\alpha}-(j+1)^{1-\alpha}\right]\\
&\quad +\frac{1}{2\Gamma(2-\alpha)}\sum_{j=0}^{n}\left[j^{1-\alpha}-(j+1)^{1-\alpha}\right]\mathcal{O}(k^{3-\alpha}). \qquad (3.3.2)
\end{aligned}$$

Define

$$\rho_\alpha := -\frac{1}{2\Gamma(2-\alpha)}\frac{1}{k^\alpha}, \qquad (3.3.3)$$

and

$$\beta_j := (j+1)^{1-\alpha} - j^{1-\alpha},\ j = 0, \cdots, n, \tag{3.3.4}$$

where, $1 = \beta_0 > \beta_1 > \beta_2 > \cdots > \to 0$ and $\lim_{n\to\infty} \sum_{j=0}^{n} \beta_j = n^{1-\alpha}$. Substituting ρ_α and β_j into (3.3.2) we obtain

$$\begin{aligned}
\frac{\partial^\alpha V(S_l, t_{n+1})}{\partial t^\alpha} &= \rho_\alpha \sum_{j=0}^{n} \beta_j \left(V_l^{n-j+1} - V_l^{n-j-1}\right) - \frac{1}{\Gamma(2-\alpha)} \sum_{j=0}^{n} \beta_j \mathcal{O}(k^{3-\alpha}), \\
&\leq \rho_\alpha \sum_{j=0}^{n} \beta_j \left(V_l^{n-j+1} - V_l^{n-j-1}\right) - \frac{1}{\Gamma(2-\alpha)} n^{1-\alpha} \mathcal{O}(k^{3-\alpha}), \\
&= \rho_\alpha \sum_{j=0}^{n} \beta_j (V_l^{n-j+1} - V_l^{n-j-1}) - \frac{1}{\Gamma(2-\alpha)} \left(\frac{t_n}{k}\right)^{1-\alpha} \mathcal{O}(k^{3-\alpha}), \\
&= \rho_\alpha \sum_{j=0}^{n} \beta_j (V_l^{n-j+1} - V_l^{n-j-1}) - \frac{t_n^{1-\alpha}}{2\Gamma(2-\alpha)} k^2.
\end{aligned} \tag{3.3.5}$$

The time derivative in (3.2.9) is therefore approximated by

$$\frac{\partial^\alpha V(S_l, t_{n+1})}{\partial t^\alpha} = \rho_\alpha \sum_{j=0}^{n} \beta_j (V_l^{n-j+1} - V_l^{n-j-1}) + \mathcal{O}(k^2). \tag{3.3.6}$$

Spatial discretization

The first and second spatial derivatives in (3.2.9) are approximated respectively by

$$\frac{\partial V(S_l, t_{n+1})}{\partial S} = \frac{V_{l+1}^{n+1} - V_{l-1}^{n+1}}{2h} + \mathcal{O}(h^2), \tag{3.3.7}$$

and

$$\frac{\partial^2 V(S_l, t_{n+1})}{\partial S^2} = \frac{V_{l+1}^{n+1} - 2V_l^{n+1} + V_{l-1}^{n+1} + V_{l+1}^{n} - 2V_l^{n} + V_{l-1}^{n}}{2h^2} + \mathcal{O}(h^2). \tag{3.3.8}$$

3.3.2 The full scheme

Substituting (3.3.6), (3.3.7) and (3.3.8) into (3.2.9), we obtain

$$\rho_\alpha \sum_{j=0}^{n} \beta_j (V_l^{n-j+1} - V_l^{n-j-1}) = \frac{t^{1-\alpha}}{\Gamma(2-\alpha)} \left(r V_l^{n+1} - ql(V_{l+1}^{n+1} - V_{l-1}^{n+1}) \right) - Q_l^n, \quad (3.3.9)$$

where

$$Q_l^n = \frac{\Gamma(1+\alpha)\sigma^2 l^2 \left(V_{l+1}^{n+1} - 2V_l^{n+1} + V_{l-1}^{n+1} + V_{l+1}^n - 2V_l^n + V_{l-1}^n \right)}{4}$$

The above scheme is of the Crank-Nicholson type, which can be broken down into two separate distinct cases, i.e. for when $n = 0$ and when $n \geq 1$.

Setting $n = 0$, and equating the non fictitious point to zero we obtain the following system of equations

$$a_1 V_{l-1}^1 + b_1 V_l^1 + c_1 V_{l+1}^1 = a_0 V_{l-1}^0 + b_0 V_l^0 + c_0 V_{l+1}^0, \quad (3.3.10)$$

where

$$\begin{aligned} a_1 &= \sigma^2 l^2 \frac{\Gamma(1+\alpha)}{4} - ql \frac{t^{1-\alpha}}{\Gamma(2-\alpha)}, \\ b_1 &= \rho_\alpha \beta_0 - r \frac{t^{1-\alpha}}{\Gamma(2-\alpha)} - \sigma^2 l^2 \frac{\Gamma(1+\alpha)}{2}, \\ c_1 &= \sigma^2 l^2 \frac{\Gamma(1+\alpha)}{4} + ql \frac{t^{1-\alpha}}{\Gamma(2-\alpha)}, \end{aligned}$$

and

$$\begin{aligned} a_0 &= -\sigma^2 l^2 \frac{\Gamma(1+\alpha)}{4}, \\ b_0 &= \rho_\alpha \beta_0 + \sigma^2 l^2 \frac{\Gamma(1+\alpha)}{2}, \\ c_0 &= -\sigma^2 l^2 \frac{\Gamma(1+\alpha)}{4}. \end{aligned}$$

For $n \geq 1$:

$$\begin{aligned} a_{n+1}V_{l-1}^{n+1} + b_{n+1}V_l^{n+1} + c_{n+1}V_{l+1}^{n+1} &= a_nV_{l-1}^n + b_nV_l^n + c_nV_{l+1}^n \\ &\quad +\rho_\alpha \sum_{j=1}^{n} \varphi_j V_l^{n-j+1} + \rho_\alpha\beta_{n+1}V_l^0 \quad (3.3.11) \end{aligned}$$

where

$$\begin{aligned} a_{n+1} &= \sigma^2 l^2 \frac{\Gamma(1+\alpha)}{4} - ql\frac{t^{1-\alpha}}{\Gamma(2-\alpha)}, \\ b_{n+1} &= \rho_\alpha\beta_1 - r\frac{t^{1-\alpha}}{\Gamma(2-\alpha)} - \sigma^2 l^2 \frac{\Gamma(1+\alpha)}{2}, \\ c_{n+1} &= \sigma^2 l^2 \frac{\Gamma(1+\alpha)}{4} + ql\frac{t^{1-\alpha}}{\Gamma(2-\alpha)}, \end{aligned}$$

and

$$\begin{aligned} a_n &= -\sigma^2 l^2 \frac{\Gamma(1+\alpha)}{4}, \\ b_n &= \rho_\alpha\beta_1 + \sigma^2 l^2 \frac{\Gamma(1+\alpha)}{2}, \\ c_n &= -\sigma^2 l^2 \frac{\Gamma(1+\alpha)}{4} \\ \varphi_j &= \beta_j - \beta_{j+1};\ j = 0, 1, 2, \cdots, n, \end{aligned} \quad (3.3.12)$$

which leads to the following general matrix representation

$$\mathbf{A}\mathbf{U}^{n+1} = \mathbf{B}\mathbf{U}^n + \sum_{j=1}^{n} \varphi_j \mathbf{U}^{n-j+1} + \mathbf{C}^n, \text{ for all } n \geq 1, \quad (3.3.13)$$

where

$$\mathbf{A} = \begin{pmatrix} a_{n+1} & b_{n+1} & c_{n+1} & 0 & \cdots & \cdots & 0 \\ 0 & a_{n+1} & b_{n+1} & c_{n+1} & & & \vdots \\ \vdots & & \ddots & \ddots & \ddots & & \vdots \\ \vdots & & & a_{n+1} & b_{n+1} & c_{n+1} & 0 \\ 0 & \cdots & \cdots & 0 & a_{n+1} & b_{n+1} & c_{n+1} \end{pmatrix},$$

$$\mathbf{B} = \begin{pmatrix} a_n & b_n & c_n & 0 & \cdots & \cdots & 0 \\ 0 & a_n & b_n & c_n & & & \vdots \\ \vdots & & \ddots & \ddots & \ddots & & \vdots \\ \vdots & & & a_n & b_n & c_n & 0 \\ 0 & \cdots & \cdots & 0 & a_n & b_n & c_n \end{pmatrix}, \tag{3.3.14}$$

$$\mathbf{U}^n = \begin{pmatrix} V_0^n \\ V_1^n \\ \vdots \\ V_{L-1}^n \\ V_L^n \end{pmatrix},$$

and

$$\mathbf{C}^n = \rho_\alpha \beta_n \mathbf{U}_l^0, \text{ for all } n \geq 1.$$

Remark 3.3.1. The following observations are trivial to show

$$\left.\begin{array}{l} 1 = \beta_0 > \beta_1 > \cdots \to 0, \\ \varphi_0 = 1 - \beta_1, \\ \sum_{j=0}^{n} \varphi_j = 1 - \beta_{n+1}, \\ \sum_{j=0}^{\infty} \varphi_j = 1 > 2^{1-\alpha} - (2^{1-\alpha} - 1^{1-\alpha}) = 1 = \varphi_0 > \varphi_1 > \cdots \to 0. \end{array}\right\} \tag{3.3.15}$$

3.4 Analysis of the numerical method

In this section we present the stability and convergence analysis of the scheme presented in (3.3.10)-(3.3.11). The analysis is based on the Fourier series analysis for fractional PDEs.

3.4.1 Stability analysis

Theorem 3.4.1. *The scheme* (3.3.10)-(3.3.11) *along with* (3.2.10) *is unconditionally stable.*

Proof. Let $v_l^n; l = 0, 1, 2, \cdots L; n = 0, 1, 2, \cdots N;$ be an approximate solution to the difference equations (3.3.10)-(3.3.11), and define $\epsilon_l^n = V_l^n - v_l^n$ as the truncation error, such that $\epsilon_0^n = \epsilon_L^n = 0$ for all n. Since the approximate solution satisfy the two equations (3.3.10)-(3.3.11), then, substituting ϵ_l^n into (3.3.10)-(3.3.11) yield

$$a_{1l}\epsilon_{l-1}^1 + b_{1l}\epsilon_l^1 + c_{1l}\epsilon_{l+1}^1 = a_{0l}\epsilon_{l-1}^0 + b_{0l}\epsilon_l^0 + c_{0l}\epsilon_{l+1}^0;\ n = 0, \tag{3.4.1}$$

and for $n \geq 1$ we have

$$\begin{aligned} a_{n+1l}\epsilon_{l-1}^{n+1} + b_{n+1l}\epsilon_l^{n+1} + c_{n+1l}\epsilon_{l+1}^{n+1} \quad &= \quad a_{nl}\epsilon_{l-1}^n + b_{nl}\epsilon_l^n + c_{nl}\epsilon_{l+1}^n + \sum_{j=0}^{n} \varphi_j \epsilon_l^{n-j+1} \\ &\quad +\beta_{n+1}\epsilon_l^0. \end{aligned} \tag{3.4.2}$$

Consider the grids function

$$\epsilon^n(S) = \begin{cases} \epsilon_l^n, & \text{when } S_l - \frac{h}{2} < S \leq S_l + \frac{h}{2},\ l = 1, 2, ..., L-1, \\ \\ 0, & \text{when } 0 \leq S < \frac{h}{2} \text{ or } S_{max} - \frac{h}{2} < S \leq S_{max} + \frac{h}{2}. \end{cases} \tag{3.4.3}$$

The grids $\epsilon^n(S)$ can be represented by the Fourier series

$$\epsilon^n(S) = \sum_{j=1}^{\infty} \varrho_n(j) e^{i2\pi jS/S_{max}};\ n = 0, 1, 2, ..., N, \tag{3.4.4}$$

for

$$\varrho_n(j) = \frac{1}{S_{max}} \int_0^{Smax} \epsilon^n(S) e^{-i2\pi jS/S_{max}} dS;\ n = 0, 1, 2, ..., N. \tag{3.4.5}$$

Let $\epsilon^n = (\epsilon_1^n, \epsilon_2^n, \cdots, \epsilon_{L-1}^n)^T$ and define the norm by

$$\|\epsilon^n\|_2 = \left(\sum_{l=1}^{L-1} h| \ \epsilon_l^n \ |^2 \right)^{1/2} = \left(\int_0^{S_{max}} | \ \epsilon^n(S) \ |^2 dS \right)^{1/2}. \tag{3.4.6}$$

Then, using the Parseval equality

$$\int_0^{S_{max}} | \ \epsilon^n(S)^2 \ | \ dS = \sum_{j=-\infty}^{\infty} | \ \varrho_n(j) \ |^2, \tag{3.4.7}$$

we obtain

$$\|\epsilon^n\|_2^2 = \int_0^{S_{max}} | \ \epsilon^n(S) \ |^2 dS = \sum_{j=-\infty}^{\infty} | \ \varrho_n(j) \ |^2 . \tag{3.4.8}$$

Therefore, the solution to (3.4.1) and (3.4.2) takes the following form

$$\epsilon^n = \varrho_n e^{i\beta lh}, \tag{3.4.9}$$

where $\beta = 2\pi j/S_{max}$ and $i = \sqrt{-1}$. Substituting ϵ^n into (3.4.1) and (3.4.2), we obtain

$$(a_1 e^{-\beta h} + c_1 e^{\beta h} + b_1)\varrho_1 = (a_0 e^{-\beta h} + c_0 e^{\beta h} + b_0)\varrho_0; \ \text{ for } n = 0, \tag{3.4.10}$$

whereas for $n \geq 1$,

$$\begin{aligned}(a_{n+1}e^{-\beta h} + c_{n+1}e^{\beta h} + b_{n+1})\varrho_{n+1} &= (a_n e^{-\beta h} + c_n e^{\beta h} + b_n)\varrho_n + \sum_{j=1}^{n} \varphi_j \varrho_{n+1-j} \\ &\quad +\beta_{n+1}\varrho_0, \end{aligned} \tag{3.4.11}$$

which can further be simplified into

$$\vartheta_1 \varrho_1 = \vartheta_0 \varrho_0; \text{ for } n = 0, \tag{3.4.12}$$

and

$$\vartheta_{n+1}\varrho_{n+1} = \vartheta_n \varrho_n + \sum_{j=1}^{n} \varphi_j \varrho_{n+1-j} + \beta_{n+1}\varrho_0; \text{ for } n \geq 1, \tag{3.4.13}$$

where

$$\vartheta_n = 4a_n \cos \beta h + b_n, \tag{3.4.14}$$

and

$$\begin{aligned}\vartheta_{n+1} &= (a_{n+1} + c_{n+1})(\cos \beta h - i \sin \beta h) + b_{n+1} \\ &= 4a_{n+1} \cos \beta h + b_{n+1}, \text{ (since } a_n = c_n), \end{aligned} \tag{3.4.15}$$

for all $n = 0, 1, 2, \cdots, N-1$.

Now (3.4.12) and (3.4.13) separately yields

$$\varrho_1 = \frac{\vartheta_0}{\vartheta_1}\varrho_0; \text{ for } n = 0, \tag{3.4.16}$$

$$\varrho_{n+1} = \frac{\vartheta_n}{\vartheta_{n+1}}\varrho_n + \frac{1}{\vartheta_{n+1}} \sum_{j=1}^{n} \varphi_j \varrho_{n+1-j} + \frac{\beta_{n+1}}{\vartheta_{n+1}}\varrho_0; \text{ for } n \geq 1. \tag{3.4.17}$$

We note

Remark 3.4.2. The ratio $\left|\frac{\vartheta_n}{\vartheta_{n+1}}\right|$ is monotonically decreasing for all $n = 0, 1, 2, \cdots, N-1$, *i.e.,*

$$\begin{aligned}\left|\frac{\vartheta_n}{\vartheta_{n+1}}\right| &= \left|\frac{4a_n\cos\beta h + b_n}{4a_{n+1}\cos\beta h + b_{n+1}}\right| \\ &\leq \left|\frac{4a_n\cos\beta h + b_n}{4a_n\cos\beta h + b_n}\right| = 1. \end{aligned} \tag{3.4.18}$$

We can also establish,

Proposition 3.4.3. *Suppose* ϱ_{n+1} *is a solution to* (3.4.16) *and* (3.4.17)*, then* $|\varrho_{n+1}| \leq |\varrho_0|$ *; for all* $n = 0, 1, 2, \cdots, N-1$.

Proof. Suppose $n = 0$, then in view of Remark 3.4.2 we have

$$|\varrho_1| = \left|\frac{\vartheta_0}{\vartheta_1}\varrho_0\right| \leq |\varrho_0|\,. \tag{3.4.19}$$

Now let $n \geq 1$ and suppose that $|\ \varrho_n\ | \leq |\ \varrho_0\ |$ for all n, then from (3.4.17), we have

$$\begin{aligned}
|\varrho_{n+1}| &= \left|\frac{\vartheta_n}{\vartheta_{n+1}}\varrho_n + \frac{1}{\vartheta_{n+1}}\sum_{j=1}^{n}\varphi_j\varrho_{n+1-j} + \frac{\beta_{n+1}}{\vartheta_{n+1}}\varrho_0\right| \\
&\leq \left|\frac{\vartheta_n}{\vartheta_{n+1}}\varrho_n\right| + \left|\frac{1}{\vartheta_{n+1}}\sum_{j=1}^{n}\varphi_j\varrho_{n+1-j}\right| + \left|\frac{\beta_{n+1}}{\vartheta_{n+1}}\varrho_0\right|, \\
&\leq \left|\frac{\vartheta_n}{\vartheta_{n+1}}\right||\varrho_n| + \left|\frac{1}{\vartheta_{n+1}}\right|\left|\sum_{j=1}^{n}\varphi_j\varrho_{n+1-j}\right| + \left|\frac{\beta_{n+1}}{\vartheta_{n+1}}\right||\varrho_0|\,, \\
&\leq |\varrho_n| + \left|\sum_{j=1}^{n}\varphi_j\varrho_{n+1-j}\right| + |\beta_{n+1}\varrho_0|\,, \\
&= |\varrho_n| + \varphi_1|\varrho_n| + \varphi_2|\varrho_{n-1}| + \cdots + \varphi_n|\varrho_1| + \beta_{n+1}|\varrho_0|\,, \\
&\leq |\varrho_0| + \varphi_1|\varrho_0| + \varphi_2|\varrho_0| + \cdots + \varphi_n|\varrho_0| + \beta_{n+1}|\varrho_0|\,, \\
&= \left(\sum_{j=0}^{n}\varphi_j + \beta_{n+1}\right)|\varrho_0| = (1 - \beta_{n+1} + \beta_{n+1})|\varrho_0|\,, \text{ (see remark 3.3.1)}, \\
&= |\varrho_0|\,.
\end{aligned} \tag{3.4.20}$$

The above alongside (3.4.7) yields, $\|\epsilon^n\|_2 \leq \|\epsilon^0\|_2$ for all $n = 1, 2, \cdots, N-1$ which completes the proof of theorem 3.4.1.

3.4.2 Convergence analysis

Theorem 3.4.4. *The difference scheme (3.3.10)-(3.3.11) alongside (3.2.10) is convergent and converges with the order $\mathcal{O}(k^2 + h^2)$.*

Proof. Let U_l^n be the exact solution to (3.3.1) and (3.2.10) at the grid point (S_l, t_n). Define $e_l^n = U_l^n - V_l^n$, such that $e_0^n = e_L^n = 0$ for all $n = 0, 1, 2, \cdots, N-1$.

Define the truncation error by

$$\begin{aligned} R_l^n \quad := \quad & \sum_{j=0}^{n} \beta_j \left[V(S_l, t_{n+1-j}) - V(S_l, t_{n-j})\right] - \mu V(S_l, t_{n+1}) - \omega \left[V(S_{l+1}, t_{n+1}) - V(S_l, t_{n+1}\right] \\ & + P_\alpha [V(S_{l+1}, t_{n+1}) - 2V(S_l, t_{n+1}) + V(S_{l-1}, t_{n+1}) + V(S_{l+1}, t_n) \\ & - 2V(S_l, t_n) + V(S_{l-1}, t_n)], \end{aligned} \tag{3.4.21}$$

where

$$\mu = k^\alpha r t^{1-\alpha}, \ \omega = k^\alpha (r - D) l t^{1-\alpha},$$

and

$$P_\alpha = \frac{k^\alpha \Gamma(2-\alpha) \left(l^2 \sigma^2 \Gamma(1+\alpha)\right)}{2}.$$

Note that R_l^n in (3.4.21) is obtained from (3.3.9) by multiplying both sides by the term $k^\alpha \Gamma(2-\alpha)$.

To proceed further, we need the following two properties.

Proposition 3.4.5. *There exist a constant $\tilde{C}$ such that $\mid R_l^n \mid \leq \tilde{C}(k^2 + h^2)$ for all $l = 0, 1, 2, \cdots, L-1$ and $n = 0, 1, 2, \cdots, N$.*

Proof. Define

$$L_k^\alpha V(S_l, t_{n+1}) := \frac{k^{-2\alpha}}{2\Gamma(2-\alpha)} \sum_{j=0}^{n+1} \beta_j \left[V(S_l, t_{n+1-j}) - V(S_l, t_{n-j}) \right],$$

then

$$\begin{aligned}
&\left| \frac{\partial^\alpha V(S_l, t_{n+1})}{\partial t^\alpha} - L_k^\alpha V(S_l, t_{n+1}) \right| \\
&\leq \frac{1}{2\Gamma(1-\alpha)} \sum_{j=0}^{n+1} \int_{jk}^{(j+1)k} \left| \frac{\partial V(S_l, \tau)}{\partial \tau} - \frac{(V(S_l, t_{n+1-j}) - V(S_l, t_{n-j}))}{k^2} \right| \frac{d\tau}{(t_{n+1}-\tau)^\alpha}, \\
&\leq \frac{1}{2\Gamma(1-\alpha)} k^2 \sum_{j=0}^{n+1} \int_{jk}^{(j+1)k} \frac{d\tau}{(t_{n+1}-\tau)^\alpha}, \\
&\leq \frac{C}{2\Gamma(1-\alpha)} k^2 \int_{jk}^{(j+1)k} \frac{d\tau}{(t_{n+1}-\tau)^\alpha}, \\
&\leq C_1 k^2, \qquad (3.4.22)
\end{aligned}$$

where C and C_1 are constants independent of h and k. Therefore

$$\frac{k^{-\alpha}}{2\Gamma(2-\alpha)} \sum_{j=0}^{n+1} \beta_j \left[V(S_l, t_{n-j+2}) - V(S_l, t_{n-j+1}) \right] = \frac{\partial^\alpha V(S_l, t_{n+1})}{\partial t^\alpha} + C_1 k^2. \quad (3.4.23)$$

In a similar way, we can show that

$$\frac{V(S_{l+1}, t_{n+1}) - V(S_{l-1}, t_{n+1})}{2h} = \frac{\partial V(S_l, t_{n+1})}{\partial S} + C_2 h^2, \quad (3.4.24)$$

and

$$\frac{V_{l+1}^{n+1} - 2V_l^{n+1} + V_{l-1}^{n+1} + V_{l+1}^n - 2V_l^n + V_{l-1}^n}{2h^2} = \frac{\partial^2 V(S_l, t_{n+1})}{\partial S^2} + C_3 h^2. \quad (3.4.25)$$

Substituting (3.4.23) - (3.4.25) into (3.4.21) and simplifying, we obtain

$$\begin{aligned} R_l^n &= k^\alpha\Gamma(2-\alpha)\left[\frac{\partial^\alpha V(S_l,t_n)}{\partial t^\alpha} - \frac{\mu}{k^\alpha\Gamma(2-\alpha)}V(S_l,t_n) - \frac{\omega}{k^\alpha\Gamma(2-\alpha)}\frac{\partial V(S_l,t_n)}{\partial S}\right. \\ &\quad \left. + P_\alpha\frac{\partial^2 V(S_l,t_n)}{\partial S^2}\right] + C_1k^{2+\alpha} + C_2k^\alpha h^2 + C_3k^\alpha h^2. \end{aligned} \tag{3.4.26}$$

This implies that

$$\begin{aligned} \mid R_l^n \mid &\leq C_4\left(k^{2+\alpha} + k^\alpha\left(h^2+h^2\right)\right), \\ &\leq \hat{C}\left(k^{2+\alpha} + k^\alpha h^2\right), \\ &= \hat{C}k^\alpha\left(k^2+h^2\right), \\ &\leq \tilde{C}\left(k^2+h^2\right), \qquad (\text{since } 0 < k^\alpha < 1). \end{aligned} \tag{3.4.27}$$

Since the errors e_l^n satisfy equation (3.3.10)-(3.3.11), substituting e_l^n into (3.3.10)-(3.3.11) we obtain

$$a_1e_{l-1}^1 + b_1e_l^1 + c_1e_{l+1}^1 = R_l^1, \tag{3.4.28}$$

and

$$\begin{aligned} a_{n+1}e_{l-1}^{n+1} + b_{n+1}e_l^{n+1} + c_{n+1}e_{l+1}^{n+1} &= a_ne_{l-1}^n + b_ne_l^n + c_ne_{l+1}^n + \sum_{j=1}^{n}\varphi_je_l^{n+1-j} \\ &\quad + R_l^{n+1}. \end{aligned} \tag{3.4.29}$$

Let us define the following grid functions

$$e^n(S) = \begin{cases} e_l^n, & \text{when } S_l - \frac{h}{2} < S \leq S_l + \frac{h}{2},\ l = 1,2,...,L-1, \\ \\ 0, & \text{when } 0 \leq S < \frac{h}{2} \text{ or } S_{max} - \frac{h}{2} < S \leq S_{max} + \frac{h}{2}, \end{cases} \tag{3.4.30}$$

and

$$R^n(S) = \begin{cases} R_l^n, & \text{when } S_l - \frac{h}{2} < S \leq S_l + \frac{h}{2},\ l = 1, 2, ..., L-1, \\ \\ 0, & \text{when } 0 \leq S < \frac{h}{2} \text{ or } S_{max} - \frac{h}{2} < S \leq S_{max} + \frac{h}{2}, \end{cases} \tag{3.4.31}$$

respectively, where $e^n(S)$ and R_l^n can be expanded into the following Fourier series representations

$$e^n(S) = \sum_{j=1}^{\infty} \lambda_n(j) e^{i2\pi jS/S_{max}};\ n = 0, 1, 2, ..., N, \tag{3.4.32}$$

$$R^n(S) = \sum_{j=1}^{\infty} \eta_n(j) e^{i2\pi jS/S_{max}};\ n = 0, 1, 2, ..., N, \tag{3.4.33}$$

for

$$\lambda_n(j) = \frac{1}{S_{max}} \int_0^{Smax} e^n(S) e^{-i2\pi jS/S_{max}} dS;\ n = 0, 1, 2, ..., N, \tag{3.4.34}$$

and

$$\eta_n(j) = \frac{1}{S_{max}} \int_0^{Smax} R^n(S) e^{-i2\pi jS/S_{max}} dS;\ n = 0, 1, 2, ..., N. \tag{3.4.35}$$

Let $e^n = \left(e_1^n, e_2^n, \cdots, e_{L-1}^n\right)^T$ and $R^n = \left(R_1^n, R_2^n, \cdots, R_{L-1}^n\right)^T$ with their second norms as

$$\|e^n\|_2 = \left(\sum_{l=1}^{L-1} h|e_l^n|^2\right)^{1/2} = \left(\int_0^{S_{max}} |e^n(S)|^2 dS\right)^{1/2};\ n = 0, 1, 2, \cdots, N \tag{3.4.36}$$

and

$$\|R^n\|_2 = \left(\sum_{l=1}^{L-1} h|R_l^n|^2\right)^{1/2} = \left(\int_0^{S_{max}} |R^n(S)|^2 dS\right)^{1/2};\ n = 1, 2, 3, \cdots, N. \quad (3.4.37)$$

Now, the Parseval equality imply

$$\int_0^{S_{max}} \left|e^n(S)^2\right| dS = \sum_{j=-\infty}^{\infty} |\lambda_n(j)|^2, \quad (3.4.38)$$

and

$$\int_0^{S_{max}} \left|R^n(S)^2\right| dS = \sum_{j=-\infty}^{\infty} |\eta_n(j)|^2, \quad (3.4.39)$$

which leads to

$$\|e^n\|_2^2 = \int_0^{S_{max}} |e^n(S)|^2 dS = \sum_{j=-\infty}^{\infty} |\lambda_n(j)|^2;\ n = 0, 1, 2, \cdots, N, \quad (3.4.40)$$

and

$$\|R^n\|_2^2 = \int_0^{S_{max}} |R^n(S)|^2 dS = \sum_{j=-\infty}^{\infty} |\eta_n(j)|^2;\ n = 1, 2, 3, \cdots, N. \quad (3.4.41)$$

Suppose that

$$e^n = \lambda_n e^{i\beta lh}, \quad (3.4.42)$$

and

$$R^n = \eta_n e^{i\beta lh}, \quad (3.4.43)$$

for $\beta = 2\pi j/S_{max}$ and $i = \sqrt{-1}$. Substituting e^n and R^n into (3.4.28) and (3.4.29) and

further simplifying we obtain

$$\lambda_1 \vartheta_1 = \eta_1, \text{ when } n = 0, \tag{3.4.44}$$

and

$$\lambda_{n+1}\vartheta_{n+1} = \vartheta_n \lambda_n + \sum_{j=1}^{n} \varphi_j \lambda_{n-j+1} + \eta_{n+1}, \tag{3.4.45}$$

where $\vartheta_{n+1} = 4c_{n+1}\cos\beta h + b_{n+1}$, for $n = 1, 2, \cdots, N$

Proposition 3.4.6. *If λ_n is a solution to (3.4.44) and (3.4.45) for all $n = 0, 1, 2, \cdots, N$, then $\mid \lambda_n \mid \leq C \mid \eta_1 \mid$.*

Proof. From (3.4.27) coupled with (3.4.37), we get

$$\left\| R^{n+1} \right\|_2 \leq \tilde{C}\left(k^2 + h^2\right);\ n = 0, 1, 2, \cdots, N.$$

Therefore, from (3.4.41) we have

$$\mid \eta_{n+1} \mid = \mid \eta_{n+1}(j) \mid \leq C \mid \eta_1 \mid = C \mid \eta_1(j) \mid;\ n = 0, 1, 2, \cdots, N, \tag{3.4.46}$$

for some constant C, independent of h and k.

Let $n = 0$, then, from (3.4.44) we have

$$\mid \lambda_1 \mid = \left| \frac{1}{\vartheta_1} \eta_1 \right| \leq C \left| \eta_1 \right|. \tag{3.4.47}$$

Now suppose $\mid \lambda_n \mid \leq C \mid \eta_1 \mid$ for $n \geq 1$. We show that it is also true for $n + 1$. To

see this, from (3.4.45) we have

$$\begin{aligned}
\mid \lambda_{n+1} \mid &= \left| \frac{1}{\vartheta_{n+1}} \left(\vartheta_n \lambda_n + \sum_{j=1}^{n} \varphi_j \lambda_{n-j+1} + \eta_{n+1} \right) \right|, \\
&\leq \frac{1}{\mid \vartheta_{n+1} \mid} \left(\mid \vartheta_n \mid\mid \lambda_n \mid + \sum_{j=1}^{n} \varphi_j \mid \lambda_{n-j+1} \mid + \mid \eta_{n+1} \mid \right), \\
&\leq \frac{1}{\mid \vartheta_{n+1} \mid} \left(C_0 \mid \eta_1 \mid + \sum_{j=1}^{n} \varphi_j C_j \mid \eta_1 \mid + C_{n+1} \mid \eta_1 \mid \right), \\
&\leq \frac{1}{\mid \vartheta_{n+1} \mid} \left(\bar{C} \mid \eta_1 \mid + \sum_{j=1}^{n} \varphi_j \bar{C} \mid \eta_1 \mid + \bar{C} \mid \eta_1 \mid \right), \ \left(\bar{C} = \max_{0 \leq j \leq n+1} \{C_j\} \right), \\
&\leq \hat{C} \mid \eta_1 \mid + \sum_{j=1}^{n} \varphi_j \hat{C} \mid \eta_1 \mid + \hat{C} \mid \eta_1 \mid, \ \left(\hat{C} = \frac{\bar{C}}{\mid \vartheta_{n+1} \mid} \right), \\
&= \hat{C} \left\{ \mid \eta_1 \mid + \sum_{j=1}^{n} \varphi_j \mid \eta_1 \mid + \mid \eta_1 \mid \right\}, \\
&= \hat{C} \left(3 - \beta_{n+1}\right) \mid \eta_1 \mid, \\
&= C \left| \eta_1 \right|. \qquad (3.4.48)
\end{aligned}$$

Combining the results obtained above, we see that the scheme (3.3.10)-(3.3.11) is convergent, which completes the proof to theorem 3.4.4.

3.5 Numerical experiments

Example 3.5.1. Consider the tfBS equation (3.2.9) subject to initial and boundary conditions (3.2.10) for pricing a standard European put option with the following parameters: $K = 150,\ r = 0.055,\ \sigma = 0.01,\ T = 1,\ S_{\max} = 450,\ L = 100,\ N = 100, \delta = 0.025,\ 0.055$ and 0.065.

Example 3.5.2. Consider the tfBS equation (3.2.9) subject to initial and boundary conditions (3.2.10) for pricing a standard European put option with the following parameters: $K = 200,\ r = 0.065,\ \sigma = 0.025,\ T = 1,\ S_{\max} = 600,\ L = 100,\ N = 100, \delta = 0.045$ and 0.085.

The tabular results for the two examples starting with $N = 50$ for example 3.5.1 and $N = 100$ for example 3.5.2 are presented in tables 3.5.1 to 3.5.4 below. Numerical results confirm our theoretical results and observations presented as theorem 3.4.1 and theorem 3.4.4.

Table 3.5.1: Maximum absolute errors for example 3.5.1 with $r = 0.055$ and $\delta = 0.025$.

α	$N = 100$	$N = 200$	$N = 400$	$N = 800$	$N = 1600$
0.1	1.3714e-02	3.4691e-03	8.7754e-04	2.2198e-04	5.5953e-05
0.2	1.2394e-02	3.1352e-03	7.9308e-04	2.0062e-04	5.0548e-05
0.3	1.0162e-02	2.5506e-03	6.5025e-04	1.6449e-04	4.1409e-05
0.4	9.5623e-03	2.4089e-03	6.1188e-04	1.5478e-04	3.7153e-05
0.5	8.5515e-03	2.0632e-03	5.4720e-04	1.3842e-04	3.4915e-05
0.6	8.0315e-03	2.0216e-03	5.1393e-04	1.3000e-04	3.2785e-05
0.7	7.5609e-03	1.9126e-03	4.8381e-04	1.2239e-04	3.0759e-05
0.8	7.3065e-03	1.8183e-03	4.6753e-04	1.1827e-04	2.9717e-05
0.9	7.1436e-03	1.8170e-03	4.5711e-04	1.1563e-04	2.9250e-05
1.0	7.1202e-03	1.7911e-03	4.5561e-04	1.1525e-04	2.9154e-05

Table 3.5.2: Convergence rates for example 3.5.1 with $r = 0.055$ and $\delta = 0.025$.

α	$N = 200$	$N = 400$	$N = 800$	$N = 1600$
0.1	1.91	1.95	1.98	1.99
0.2	1.92	1.96	1.98	1.99
0.3	1.93	1.96	1.98	1.99
0.4	1.93	1.96	1.98	1.99
0.5	1.93	1.97	1.98	1.99
0.6	1.94	1.97	1.98	1.99
0.7	1.94	1.97	1.98	1.99
0.8	1.94	1.97	1.98	1.99
0.9	1.94	1.97	1.98	1.99
1.0	1.94	1.97	1.98	1.99

Table 3.5.3: Maximum absolute errors for example 3.5.2 with $r = 0.065$ and $\delta = 0.085$.

α	$N = 100$	$N = 200$	$N = 400$	$N = 800$	$N = 1600$
0.1	6.5592e-02	1.6592e-02	4.1972e-03	1.0617e-03	2.6857e-04
0.2	5.8088e-03	1.4694e-02	3.7170e-03	9.4025e-04	2.3784e-04
0.3	5.2147e-02	1.3191e-02	3.3368e-03	8.4408e-04	2.1352e-04
0.4	4.7443e-02	1.2001e-02	3.0358e-03	7.6794e-04	1.9426e-04
0.5	4.3746e-02	1.1066e-02	2.7993e-03	7.0810e-04	1.7912e-04
0.6	4.0893e-02	1.0344e-02	2.6167e-03	6.6192e-04	1.6544e-04
0.7	3.8773e-02	9.8080e-03	2.4810e-03	6.2760e-04	1.5676e-04
0.8	3.7318e-02	9.4400e-03	2.3879e-03	6.0405e-04	1.5080e-04
0.9	3.6499e-02	9.2328e-03	2.3355e-03	5.9079e-04	1.4745e-04
1.0	3.6328e-02	9.1895e-03	2.3246e-03	5.8803e-04	1.4670e-04

Table 3.5.4: Convergence rates for example 3.5.2 with $r = 0.065$ and $\delta = 0.085$.

α	$N = 200$	$N = 400$	$N = 800$	$N = 1600$
0.1	1.95	1.98	1.99	1.99
0.2	1.96	1.98	1.99	1.99
0.3	1.96	1.98	1.99	1.99
0.4	1.96	1.98	1.99	2.00
0.5	1.97	1.98	1.99	2.00
0.6	1.97	1.98	1.99	2.00
0.7	1.97	1.98	1.99	2.00
0.8	1.97	1.98	1.99	2.00
0.9	1.97	1.98	1.99	2.01
1.0	1.97	1.98	1.99	2.01

Maturity payoff curves for the three dividend yields $\delta = 0.025$, 0.055 and 0.065 at $\alpha = 0.1,\ 0.3,\ 0.5,\ 0.7$, and $\alpha = 0.9$ under example 3.5.1 are presented in fig. 3.5.1 below

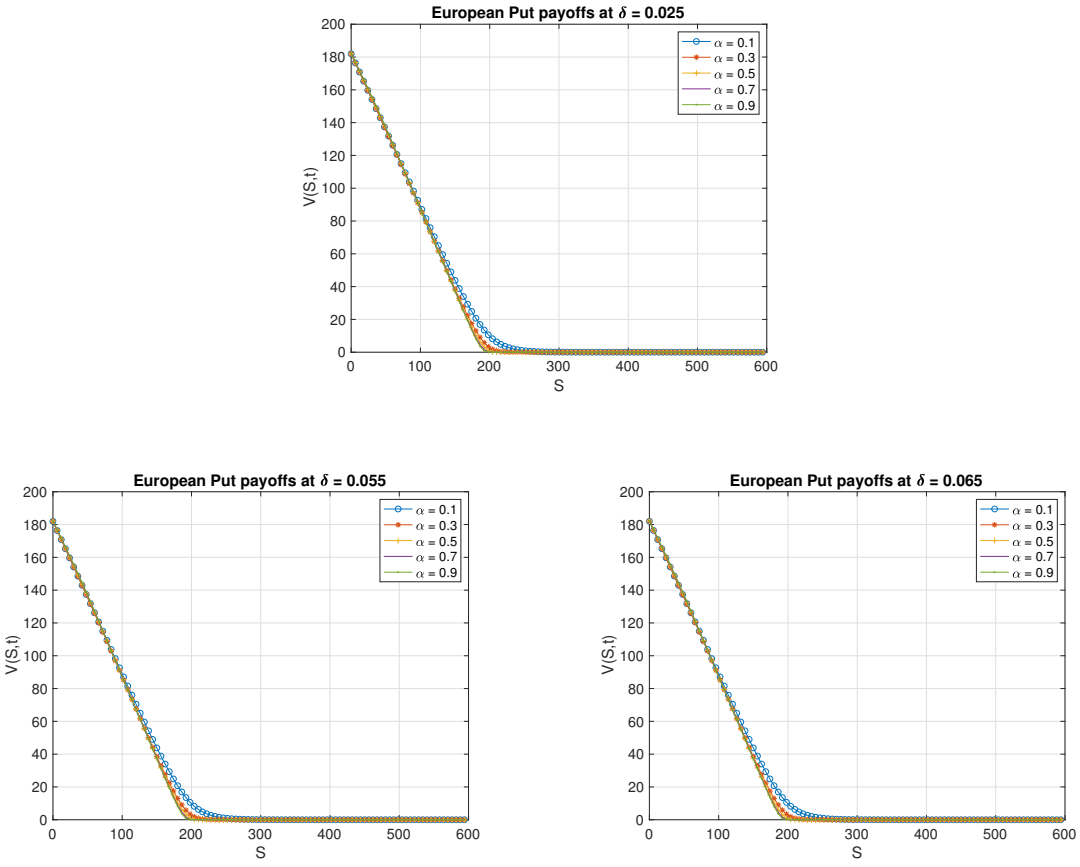

Figure 3.5.1: Payoffs for $\alpha = 0.1,\ 0.3,\ 0.5,\ 0.7,\ 0.9$, and $t = T$.

The general payoff curves throughout the life-time of the option at the five fractional derivative orders (α) for the three considered yield rates under example 3.5.1 are given in figs. 3.5.2 to 3.5.4 below

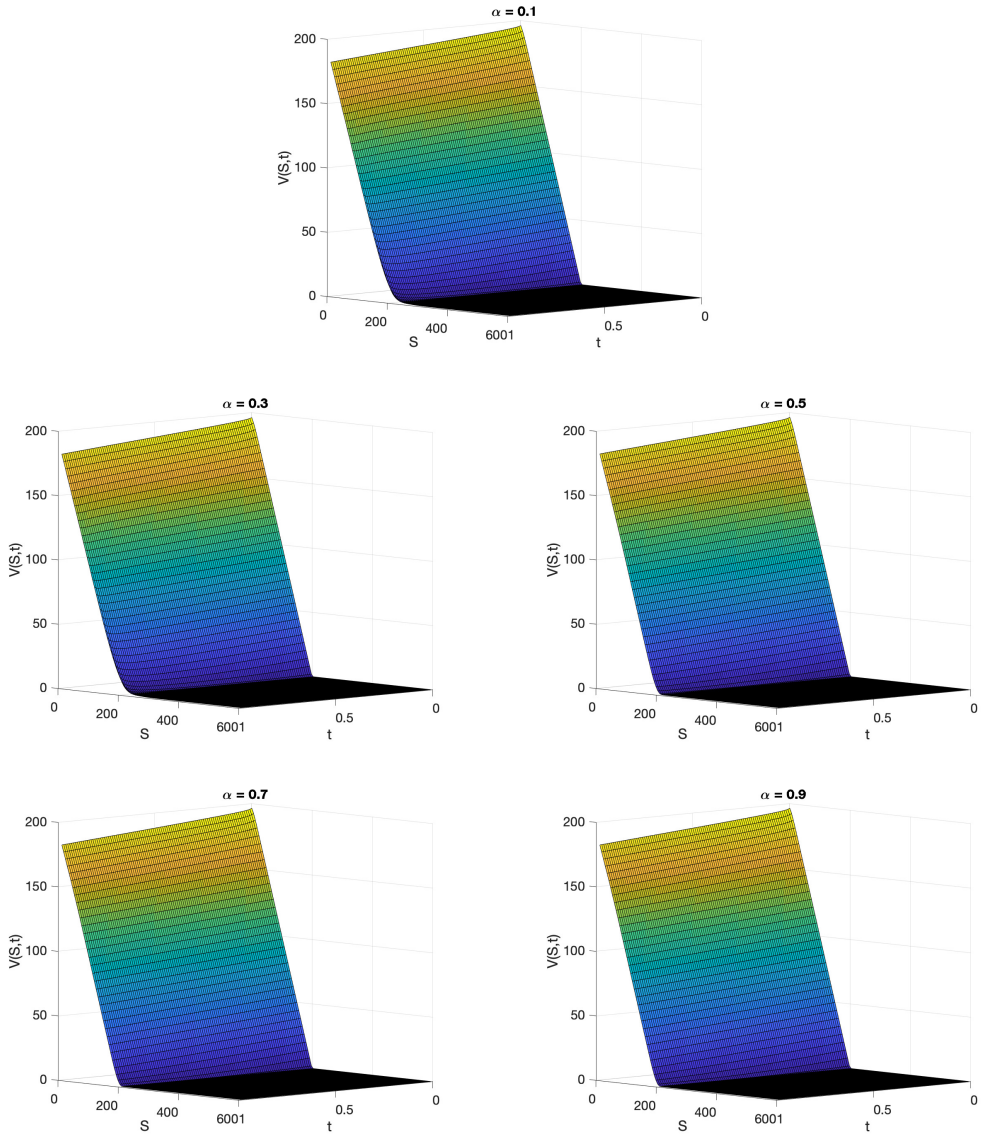

Figure 3.5.2: Payoffs for $\alpha = 0.1,\ 0.3,\ 0.5,\ 0.7,\ 0.9,\ \delta = 0.025$ for all $0 \leq t \leq T$.

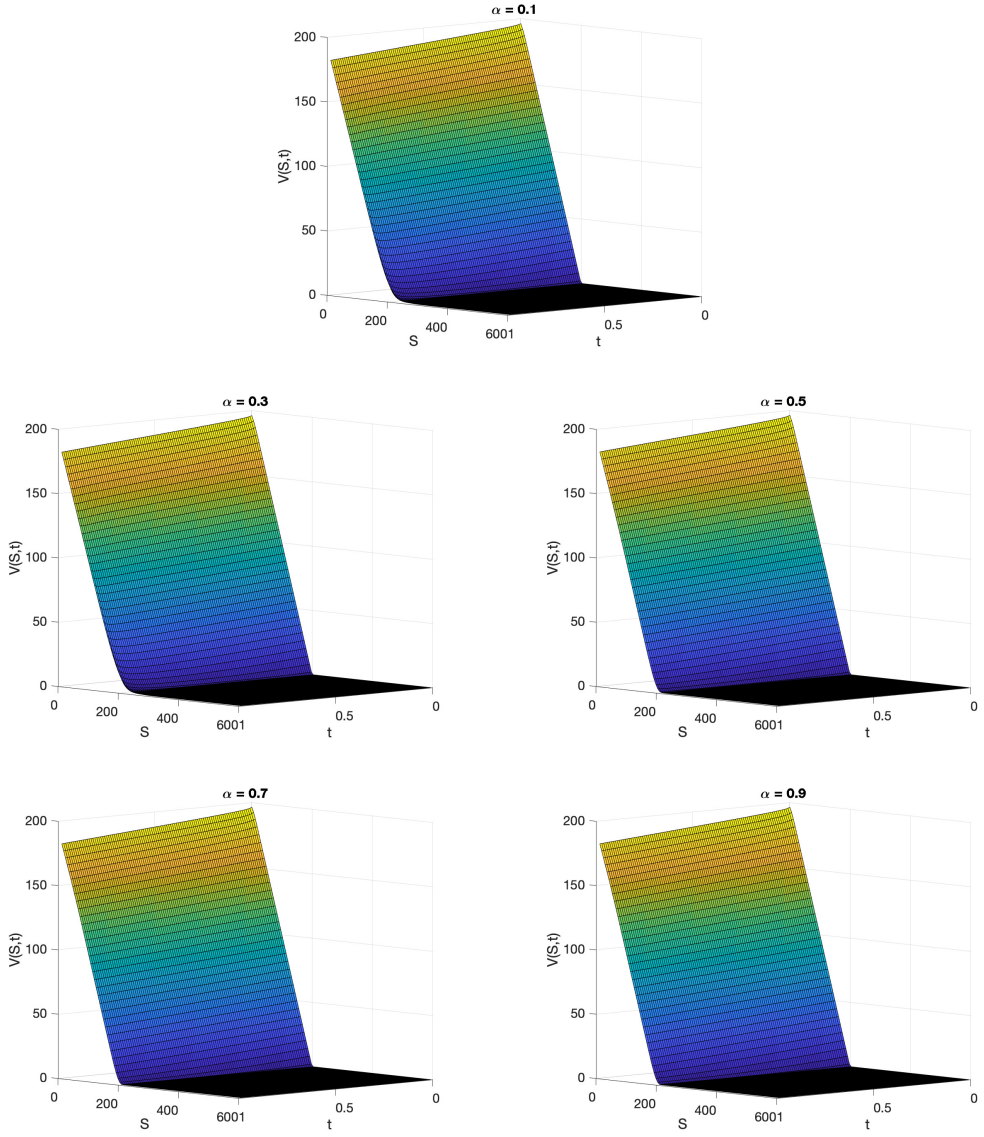

Figure 3.5.3: Payoffs for $\alpha = 0.1,\ 0.3,\ 0.5,\ 0.7,\ 0.9,\ \delta = 0.055$ for all $0 \leq t \leq T$.

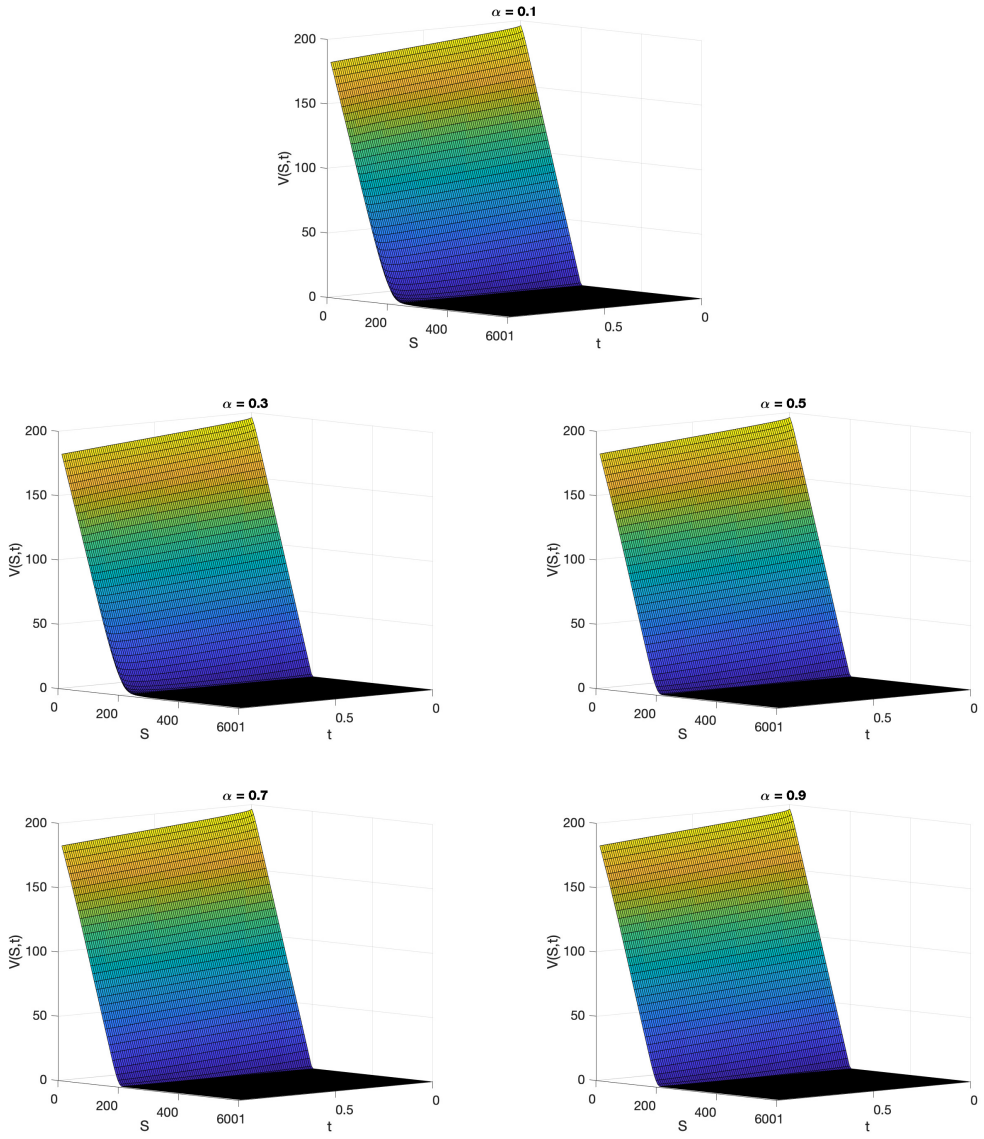

Figure 3.5.4: Payoffs for $\alpha = 0.1,\ 0.3,\ 0.5,\ 0.7,\ 0.9,\ \delta = 0.065$ for all $0 \leq t \leq T$.

To check for the effects of change in option parameters, we considered a second example (example 3.5.2) with a different interest rate r, two different set of dividend yields δ under the same set of five values of α.

The option maturity payoff curves for the two sets of dividend yields considered in example 3.5.2, $\delta = 0.045$ and $\delta = 0.085$ at $\alpha = 0.1,\ 0.3,\ 0.5,\ 0.7,\ 0.9$ are given in

fig. 3.5.5 below.

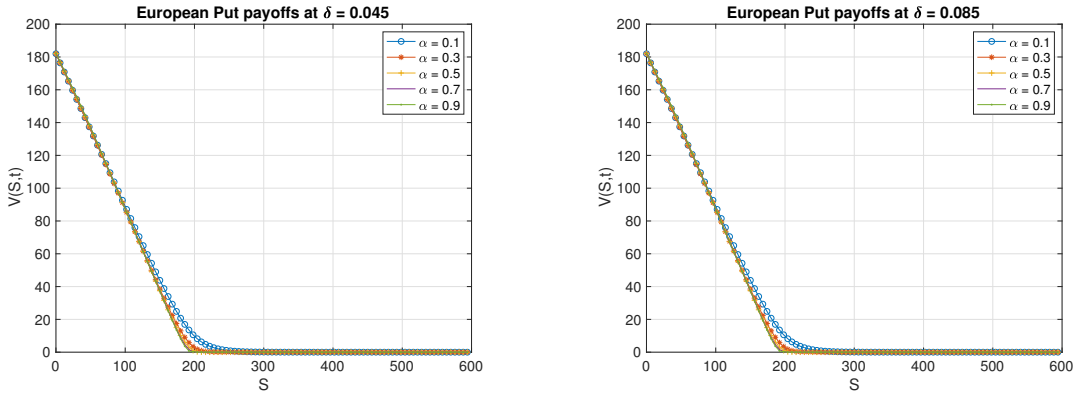

Figure 3.5.5: Payoffs for $\alpha = 0.1,\ 0.3,\ 0.5,\ 0.7,\ 0.9,$ and $t = T$.

The general payoff curves throughout the life-time of the option for $\alpha = 0.1,\ 0.3,\ 0.5,\ 0.7,$ and 0.9 and the two considered dividend yields are given in figs. 3.5.6 and 3.5.7 below

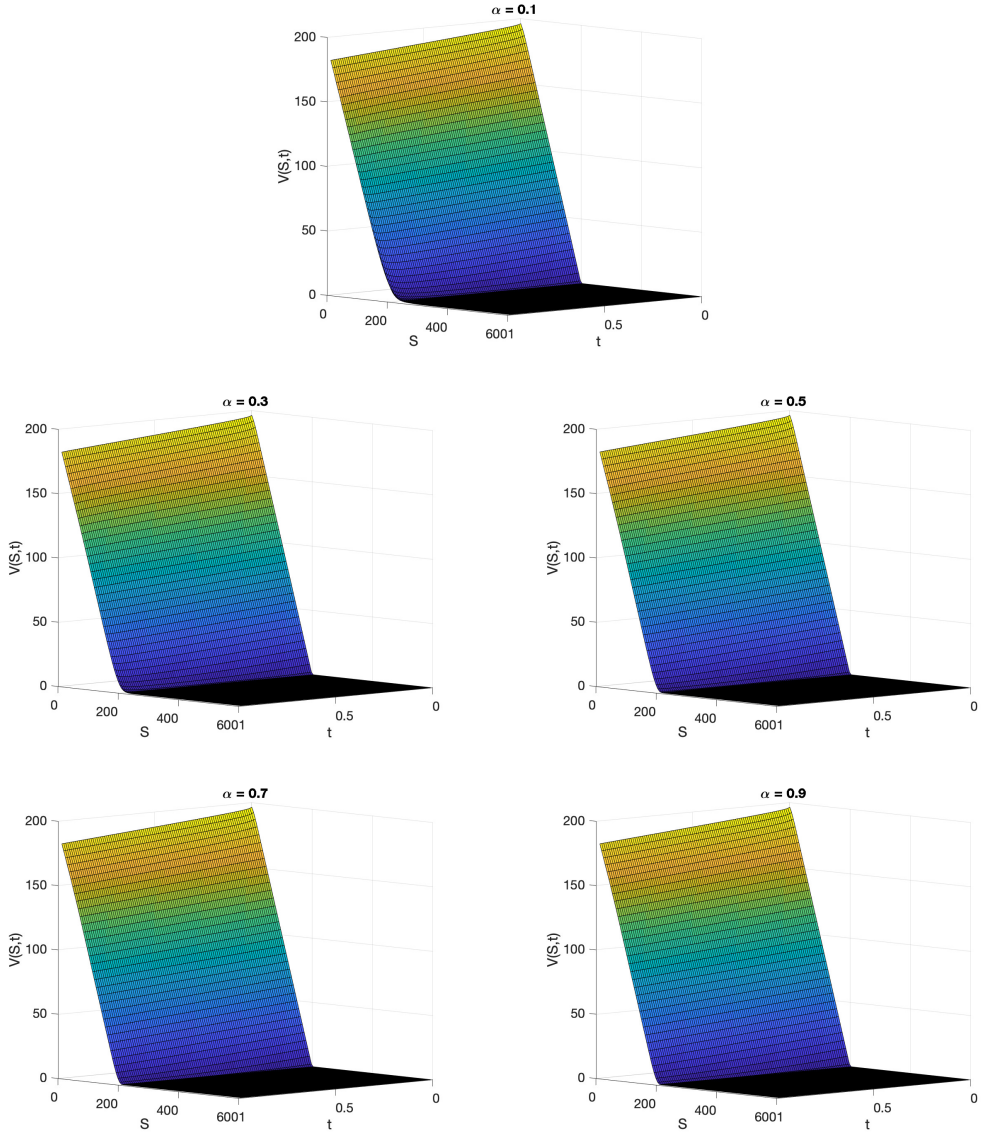

Figure 3.5.6: Payoffs for $\alpha = 0.1,\ 0.3,\ 0.5,\ 0.7,\ 0.9,\ \delta = 0.045$ for all $0 \leq t \leq T$.

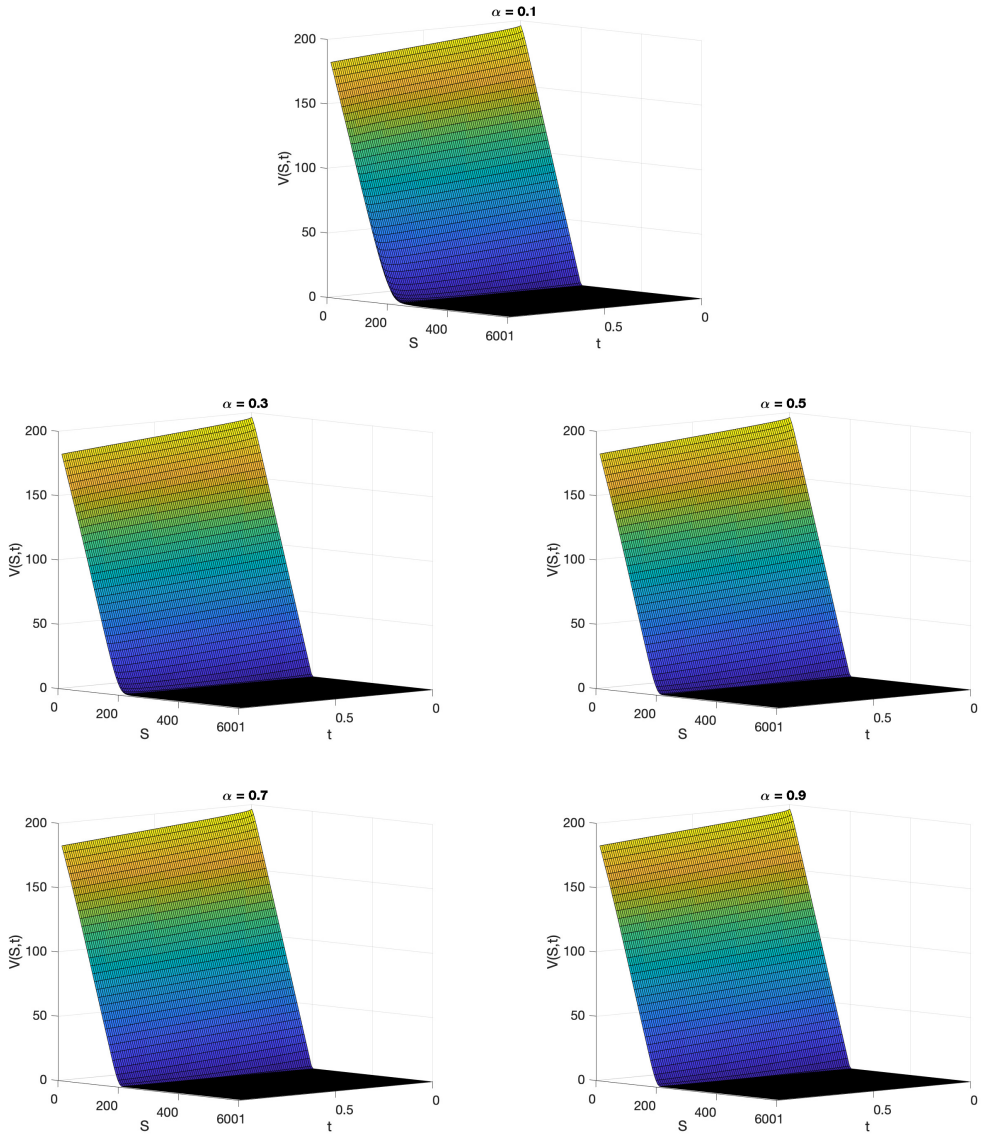

Figure 3.5.7: Payoffs for $\alpha = 0.1,\ 0.3,\ 0.5,\ 0.7,\ 0.9,\ \delta = 0.085$ for all $0 \leq t \leq T$.

3.6 Summary and discussions

In this chapter we proposed a Crank Nicholson type scheme for solving a tfBS-PDE for pricing standard European options written on continuous dividend paying stocks. Two numerical examples were presented. Theoretical and numerical results suggest that the fractional approach is a very efficient option valuing tool compared to its classical

counterpart. In addition, the numerical method and results indicates that our scheme is very robust and efficient in solving tfBS-PDEs. The method does not only reduce computational time but, also attain high order unconditional stable results, in any states of the world and market conditions. One key observation is that, the general payoff curves and profiles are more smoothier when $1/2 \leq \alpha < 1$, and otherwise when $0 < \alpha < 1/2$. With the latter signalling asymmetric performance of the approach and method. These however, implies that, the approach is more robust when $1/2 \leq \alpha < 1$. These observations are not strange or of a contradictory nature. It is expected that $1/2 \leq \alpha < 1$ the involved fractional stochastic process be more persistent and as it is characterised by positive correlations between asset returns' increments, hence, attaining better performance compared to the case when $0 < \alpha < 1/2$ which represent the anti-persistent regime under which the underlying stock price process is characterised by negative correlation between increments. The practical interpretation of these is that, the approach confirms our theoretical observations and general consensus in literature that stock market dynamics are of a power law nature, and that the underlying distributions of stock returns decays slower than the exponential distribution and have no independent increments. It is therefore expected that the method perform better in the region $(1/2 \leq \alpha < 1)$ which is characterised by high persistence and positive correlation as compared to $(0 < \alpha < 1/2)$ when the process covers less and less grounds than the ordinary random process.

Currently we are exploring other higher order methods for solving tfBS and tsfBS-PDEs. We are also interested in the calibration of the models to real-time data. In Chapter 4 we suggest an alternative Fractal Market Hypothesis based time-fractional Black- Scholes Partial Differential Equation (tfBS-PDE), as well as present an efficient numerical scheme for solving it.

Chapter 4

An Efficient Finite Difference Approximation for a Time-Fractional Black-Scholes PDE Arising via a Fractal Market Hypothesis

This chapter presents a Fractal Market Hypothesis based time-fractional Black-Scholes partial differential equation (tfBS-PDE). Herein, we also present a robust high order numerical method for solving the derived tfBS-PDE. Further discussion on the stability and convergence properties of the numerical method and some numerical experiments are presented.

4.1 Introduction

Since the early 70s the study of Black-Scholes (BS) partial differential equations (PDEs) under the Efficient Market Hypothesis (EMH) has been a subject of active research in the derivative pricing area of financial engineering. One of the most common classes of highly traded derivative instruments are options. Pricing of options and many other

derivatives under the Efficient Market Hypothesis (EMH) has some serious setbacks. Hence it has now become obvious, to those familiar with the concept, that the BS models derived under the EMH framework fails to account for a number of realistic price evolutions in real-time markets' data. An alternative approach to the EMH framework is the Fractal Market Hypothesis (FMH) which proposes better and clear explanations of market behaviours during unfavourable market conditions. The FMH approaches are very attractive to asset pricing as they provide for a somewhat unique framework, one that has a potential to transform conventional thinking in asset pricing literature. The involved non-local derivatives and integral operators as well as the accompanying fractional stochastic dynamics in the FMH based models provide the best tools for explaining the dynamics of market anomalies, something that the classical models may fail to explain.

The rest of this chapter is organised as follow, Section 4.2 presents a brief discussion on the development of the involved model. Section 4.3 presents the construction and analysis of the involved difference scheme. To validate our theoretical observations, Section 4.4 presents some practical experiments on pricing European option on continuous dividend paying stocks. The conclusions and recommendations drawn from the study as well as the prospect for future research are presented in Section 4.5.

4.2 Model specification

4.2.1 The fractional Black-Scholes equation

To begin, we assume the stock price (S) dynamics follows a non-random fractional stochastic process given by

$$dS = (r-\delta)Sdt + \sigma S\omega(t)(dt)^{\alpha/2}, \quad 0 < \alpha \leq 1, \tag{4.2.1}$$

where $\omega(t)$ is the Gaussian white noise with mean zero and standard deviation of one. Whereas r and δ represent risk-free interest rate and continuous dividend

respectively. Suppose $B(t)$ denote a standard Brownian motion, then, equation (4.2.1) is a generalization of $B(t)$ by replacing $dB(t) = \omega(t)dt^{1/2}$ with $dB(t) = \omega(t)(dt)^{\alpha/2}$ for some $0 < \alpha \leq 1$.

The fractional process (4.2.1) is more appropriate compared to the standard one because it does not make any prior distributional assumptions about the asset price/returns. The model free assumption provides a better approach to model the power law properties of markets with greater flexibility.

Consider the relation

$$dS = \frac{S^{(1-\alpha)}}{\Gamma(1+\alpha)(\alpha-1)!}(dS)^{\alpha}, \qquad 0 < \alpha < 1. \tag{4.2.2}$$

Suppose $V(S,t)$ is sufficiently smooth with respect to S and its α-derivative exists with respect to time, then theory of interest suggest,

$$dV = rVdt. \tag{4.2.3}$$

The above leads to the variational fractional increment formula

$$d^{\alpha}V = \Gamma(1+\alpha)rVdt. \tag{4.2.4}$$

Using (4.2.4) and (4.2.2), we obtain the following fractional interest dynamic equation

$$d^{\alpha}V = \frac{rV}{(\alpha-1)!}t^{1-\alpha}(dt)^{\alpha}. \tag{4.2.5}$$

The assumption on differentiability and continuity of $V(S,t)$ imply that (4.2.5) satisfy the Generalized Taylor series of order α upto some remaining error terms follows,

$$dV = \frac{1}{\Gamma(1+\alpha)}\frac{\partial^{\alpha}V}{\partial t^{\alpha}}(dt)^{\alpha} + \frac{\partial V}{\partial S}dS + \frac{1}{2}\frac{\partial^2 V}{\partial S^2}(dS)^2. \tag{4.2.6}$$

The Itô's lemma applied on (4.2.1) alongside (4.2.6), yield

$$dV = \frac{1}{\Gamma(1+\alpha)}\frac{\partial^\alpha V}{\partial t^\alpha}(dt)^\alpha + (r-\delta)S\frac{\partial V}{\partial S}dt + \frac{1}{2}\sigma^2 S^2\frac{\partial^2 V}{\partial S^2}(dt)^\alpha. \tag{4.2.7}$$

After some algebraic manipulations and change of derivatives, we obtain the following

$$\begin{aligned} d^\alpha V &= \frac{rV}{(\alpha-1)!}t^{1-\alpha}(dt)^\alpha, \\ &= \left(\frac{\partial^\alpha V}{\partial t^\alpha} + \frac{(r-\delta)}{(\alpha-1)!}St^{1-\alpha}\frac{\partial V}{\partial S} + \frac{\Gamma(1+\alpha)}{2}\sigma^2 S^2\frac{\partial^2 V}{\partial S^2}\right)(dt)^\alpha, \end{aligned} \tag{4.2.8}$$

which implies

$$\frac{rV}{(\alpha-1)!}t^{1-\alpha} = \frac{\partial^\alpha V}{\partial t^\alpha} + \frac{(r-\delta)}{(\alpha-1)!}St^{1-\alpha}\frac{\partial V}{\partial S} + \frac{\Gamma(1+\alpha)}{2}\sigma^2 S^2\frac{\partial^2 V}{\partial S^2}. \tag{4.2.9}$$

Equation (4.2.9) can further be simplified into the following tfBS-PDE

$$\frac{\partial^\alpha V}{\partial t^\alpha} = \left(rV - qS\frac{\partial V}{\partial S}\right)\frac{t^{1-\alpha}}{(\alpha-1)!} - \frac{\Gamma(1+\alpha)}{2}\sigma^2 S^2\frac{\partial^2 V}{\partial S^2}, \tag{4.2.10}$$
$$q = r-\delta; \quad 0 < \alpha \leq 1$$

To ease the computational difficulties involved in computing the solution to the tfBS-PDE in (4.2.10), we transform (4.2.10) into a heat equation by change of variables and then to use the known solution of the heat equation to represent the solution, thereafter change variables back to the original variable $V(S,t)$

First we want to eliminate the term rV in (4.2.10). To do so we assume $V(S,t)$ is differentiable with respect to t. Then, considering the following change of variables

$$V(S,t) = e^{-r(T-t)}v(S,t), \tag{4.2.11}$$

and applying the Caputo derivative on (4.2.11),would yield,

$$V_t^\alpha = D_t^\alpha \left(e^{-r(T-t)}\right) v(S,t) + e^{-r(T-t)} v_t^\alpha,\ 0 < \alpha \leq 1, \tag{4.2.12}$$

where D_t^α is the Caputo derivative with respect to t of order α.

From the generalized Taylor series expansion (2.2.5), we have

$$D_t^\alpha \left(e^{-r(T-t)}\right) = re^{-r(T-t)} \frac{t^{1-\alpha}}{(\alpha-1)!}. \tag{4.2.13}$$

By using (4.2.13) in (4.2.12), we obtain

$$V_t^\alpha(S,t) = re^{-r(T-t)} \frac{t^{1-\alpha}}{(\alpha-1)!} v(S,t) + e^{-r(T-t)} v_t^\alpha(S,t),\ 0 < \alpha \leq 1. \tag{4.2.14}$$

The above equation along with (4.2.10), yields

$$\begin{aligned} re^{-r(T-t)} \frac{t^{1-\alpha}}{(\alpha-1)!} v(S,t) \quad &+ \quad e^{-r(T-t)} v_t^\alpha(S,t) \\ &= \quad e^{-r(T-t)} v(S,t) \frac{t^{1-\alpha}}{(\alpha-1)!} - qSe^{-r(T-t)} v_S(S,t) \frac{t^{1-\alpha}}{(\alpha-1)!} \\ &\quad -\frac{\Gamma(1+\alpha)}{2} \sigma^2 S^2 e^{-r(T-t)} v_{SS}(S,t) \end{aligned} \tag{4.2.15}$$

which after simplifying yield,

$$v_t^\alpha(S,t) = -qSv_S(S,t) \frac{t^{1-\alpha}}{(\alpha-1)!} - \frac{\Gamma(1+\alpha)}{2} \sigma^2 S^2 v_{SS}(S,t), \quad 0 < \alpha \leq 1, \tag{4.2.16}$$

with terminal condition,

$$v(S,T) = V(S,T).$$

Now, since we want to obtain a pde with constant coefficients, to eliminate the

$Sv_S(S,t)$ and $S^2v_{SS}(S,t)$ terms from (4.2.16), we consider the transformation

$$s = e^{S-\tau}, \text{ for some constant } \tau, \tag{4.2.17}$$

resulting in a pde with the solution of the form

$$v(S,t) \equiv v(s,t),$$

and terminal condition

$$v(s,T) = v(S,T) = V(S,T).$$

Therefore,

$$v_t^{\alpha}(s,t) = \left(\frac{\Gamma(1+\alpha)}{2}\sigma^2 - q\frac{t^{1-\alpha}}{(\alpha-1)!}\right)v_s(s,t) - \frac{\Gamma(1+\alpha)}{2}\sigma^2 v_{ss}(s,t). \tag{4.2.18}$$

The general solution to (4.2.18) takes the form

$$v(s,t) \equiv p(s,t) = \phi(s - qt + \frac{1}{2}\sigma^2 t^2). \tag{4.2.19}$$

Which suggest for the following transformation (*again without loss of notations*)

$$s = s - ln(c) + r(T-t) - \frac{1}{2}\sigma^2(T^{\alpha} - t^{\alpha}), \tag{4.2.20}$$

and terminal condition

$$v(s,T) = c(e^s - 1) = c(e^{s-ln(c)+r(T-t)-\frac{1}{2}\sigma^2(T^{\alpha}-t^{\alpha})} - 1). \tag{4.2.21}$$

Choosing the constant τ in (4.2.17) as $\tau = -ln(c) + rT - \frac{1}{2}\sigma^2 T^{\alpha}$ for some constant c and substituting the new variable (s) of (4.2.19) back into (4.2.18) eliminates the

term $v_s(s,t)$ from (4.2.18) resulting into the following fractional heat equation

$$p_t^{\alpha}(s,t) = -\frac{\Gamma(1+\alpha)\sigma^2}{2} p_{ss}(s,t), \tag{4.2.22}$$

which can be simplified to

$$\frac{\partial^{\alpha} p(s,t)}{\partial t^{\alpha}} = \psi \frac{\partial^2 p(s,t)}{\partial s^2}, \tag{4.2.23}$$

where $\psi = -\frac{\Gamma(1+\alpha)\sigma^2}{2}$, with European put option initial and boundary conditions in terms of the original variables

$$\left.\begin{aligned} p(s,0) &= V(S,0) = \max(K - Ke^{rt}, 0), \\ p(0,t) &= V(0,T) = Ke^{-rt}, \\ \lim_{s\to\infty} p(s,t) &= \lim_{S\to\infty} V(S,t) = 0, \end{aligned}\right\} \tag{4.2.24}$$

where K is the strike price of the option and T is the maturity time.

For the remainder of this chapter equation (4.2.23) is referred to as the time-fractional Black-Scholes heat equation.

4.3 Numerical method and its analysis

This section presents the fundamental aspects and design of the proposed numerical scheme for solving equation (4.2.23).

To begin, Let L and N be some positive integers, and define $h = S_{max}/L$ and $k = T/N$ as the spatial and temporal grid sizes. Further denote $s_l \in [0, S_{max}]$ and $t_n \in [0, T]$ as the grid points in the asset and time directions, such that $s_l = lh$ and $t_n = nk$ for $l = 0, 1, 2, 3, ..., L$ and $n = 0, 1, 2, ..., N-1$.

Denote the value of the option p at grid point (t_n, s_l) by

$$p_l^n = p(t_n, s_l), \tag{4.3.1}$$

and also, define

$$C(t,s) := \frac{1}{\Gamma(1+\alpha)} \int_0^t \frac{p(\tau,s)}{(t-\tau)} dz, \tag{4.3.2}$$

such that

$$\frac{\partial^\alpha p(t_{n+1/2}, s_l)}{\partial t^\alpha} = \frac{\partial C(t_{n+1/2}, s_l)}{\partial t}, \tag{4.3.3}$$

which is defined in the Caputo sense, then,

$$\frac{\partial^\alpha p(t_{n+1/2}, s_l)}{\partial t^\alpha} = \frac{\partial C(t_{n+1/2}, s_l)}{\partial t} = \frac{C(t_{n+1}, s_l) - C(t_n, s_l)}{k} + \mathcal{O}(k^2). \tag{4.3.4}$$

Using the Caputo derivative in Definition 2.2.1, $C(t_{n+1}, s_l)$ can be represented as follow;

$$\begin{aligned}
C(t_{n+1}, s_l) &= \frac{1}{\Gamma(1+\alpha)} \int_0^{t_{n+1}} \frac{p(\tau, s_l)}{(t_{n+1}-\tau)^\alpha} dz, \\
&= \frac{1}{\Gamma(1-\alpha)} \sum_{j=1}^{n+1} \int_{(j-1)k}^{jk} \frac{p(\tau, s_l)}{(t_{n+1}-\tau)^\alpha} dz, \\
&= \frac{1}{\Gamma(1-\alpha)} \sum_{j=1}^{n+1} \left(\frac{(\tau - t_j)}{-k} p_l^{j-1} + \frac{(\tau - t_{j-1})}{k} p_l^j + \mathcal{O}(k^2) \right) \frac{1}{(t_{n+1}-\tau)^\alpha} dz, \\
&= \sum_{j=0}^{n} (\delta_j - j\beta_j)\, p_l^{n-j} - k \sum_{j=0}^{n} (\delta_j - (j+1)\beta_j)\, p_l^{n-j+1} + E_{n+1},
\end{aligned} \tag{4.3.5}$$

where

$$\begin{aligned}
E_{n+1} &= \frac{1}{\Gamma(1-\alpha)} \sum_{j=1}^{n+1} \int_{(j-1)k}^{jk} \mathcal{O}(k^2) \frac{dz}{(t_{n+1}-\tau)^\alpha} \\
&= \frac{1}{(\alpha-1)!} \mathcal{O}(k^2) \sum_{j=1}^{n+1} \left((n+2-j)^{1-\alpha} - (n+1-j)^{1-\alpha} \right) k^{1-\alpha} \\
&= \frac{(n+1)^{1-\alpha}}{(\alpha-1)!} \mathcal{O}(k^2),
\end{aligned} \tag{4.3.6}$$

$$\delta_j = \frac{1}{k^\alpha(2-\alpha)\Gamma(1-\alpha)}\left((j+1)^{2-\alpha} - j^{2-\alpha}\right), \tag{4.3.7}$$

and

$$\beta_j = \frac{1}{k^\alpha(\alpha-1)!}\left((j+1)^{1-\alpha} - j^{1-\alpha}\right). \tag{4.3.8}$$

Similarly,

$$\begin{aligned} C(t_n, s_l) &= \frac{1}{\Gamma(1+\alpha)}\int_0^{t_n} \frac{p(\tau, s_l)}{(t_n-\tau)^\alpha} dz, \\ &= \sum_{j=1}^{n}(\delta_{j-1} - (j-1)\beta_{j-1})p_l^{n-j} - k\sum_{j=1}^{n}(\delta_{j-1} - j\beta_{j-1})p_l^{n-j+1} \\ &\quad + E_n. \end{aligned} \tag{4.3.9}$$

We can therefore approximate

$$\frac{\partial^\alpha p(t_{n+1/2}, s_l)}{\partial t^\alpha}$$

as follow

$$\begin{aligned}
\frac{\partial^\alpha p(t_{n+1/2}, s_l)}{\partial t^\alpha} &= \frac{C(t_{n+1}, s_l) - C(t_n, s_l)}{k} + \mathcal{O}(k^2), \\
&= \sum_{j=0}^{n} (\delta_j - j\beta_j) p_l^{n-j} - \sum_{j=0}^{n} (\delta_j - (j+1)\beta_j) p_l^{n-j+1} \\
&\quad - \sum_{j=1}^{n} (\delta_{j-1} - (j-1)\beta_{j-1})\, p_l^{n-j} + \sum_{j=1}^{n} (\delta_j - j\beta_{j-1})\, p_l^{n-j+1} \\
&\quad + \frac{E_{n+1} - E_n}{k} + \mathcal{O}(k^2), \\
&= \sum_{j=0}^{n} \{(\delta_j - \delta(j-1)) + ((j-1)\beta_{j-1} - j\beta_j)\}\, p_l^{n-j} \\
&\quad + \sum_{j=0}^{n} \{(\delta_{j-1} - \delta_j) + ((j+1)\beta_{j+1} - j\beta_j)\}\, p_l^{n-j+1} \\
&\quad + \frac{E_{n+1} - E_n}{k} + \mathcal{O}(k^2), \\
&= \sum_{j=0}^{n} \sigma_j p_l^{n-j+1} + \frac{1}{(\alpha-1)!} \left(\frac{(n+1)^{1-\alpha} - n^{1-\alpha}}{k} \right) \mathcal{O}(k^2) + \mathcal{O}(k^2), \\
&= \sum_{j=0}^{n} \sigma_j p_l^{n-j+1} + \mathcal{O}(k^2), \qquad (4.3.10)
\end{aligned}$$

where

$$\sigma_j = \delta_{j+1} - 2\delta_j + \delta_{j-1}, \text{ for } j > 1, \qquad (4.3.11)$$

since

$$j\beta_j = \delta_j.$$

Therefore, using an appropriate second order approximation in the asset direction, (4.2.23) yield

$$\begin{aligned}
\sum_{j=0}^{n} \sigma_j p_l^{n-j+1} + \mathcal{O}(k^2) &= \frac{\psi}{2h^2} \left\{ p_{l+1}^{n+1} - 2p_l^{n+1} + p_{l-1}^{n+1} + p_{l+1}^{n} - 2p_l^{n} + p_{l-1}^{n} \right\} \\
&\quad + \mathcal{O}(h^2), \qquad (4.3.12)
\end{aligned}$$

where

$$0 \leq n \leq N-1, \text{ and, } 1 \leq l \leq L-1.$$

Which can be simplified to the following difference scheme

$$-\frac{\psi}{2h^2}p_{l+1}^1 + \left(\frac{\psi}{h^2}+\sigma_0\right)p_l^1 - \frac{\psi}{2h^2}p_{l-1}^1 = \frac{\psi}{2h^2}p_{l+1}^0 - \frac{\psi}{h^2}p_l^0 + \frac{\psi}{2h^2}p_{l-1}^0, \quad (4.3.13)$$

for $n = 0$ and,

$$-\frac{\psi}{2h^2}p_{l+1}^{n+1} + \left(\frac{\psi}{h^2}+\sigma_0\right)p_l^{n+1} - \frac{\psi}{2h^2}p_{l-1}^{n+1} = \frac{\psi}{2h^2}p_{l+1}^n - \left(\frac{\psi}{h^2}+\sigma_0\right)p_l^n + \frac{\psi}{2h^2}p_{l-1}^n - \sum_{j=1}^{n}\sigma_j p_l^{n-j+1}, \quad (4.3.14)$$

for $n \geq 1$, with an European put initial and boundary conditions

$$\left.\begin{aligned} p_l^0 &= \max(K - Ke^{rt}, 0), \\ p_0^n &= Ke^{-rt}, \\ p_L^n &= 0, \ 0 \leq n \leq N. \end{aligned}\right\} \quad (4.3.15)$$

4.3.1 Stability analysis

Let $P_l^n; l = 0, 1, 2, \cdots L$; $n = 0, 1, 2, \cdots N$; be an approximate solution to the difference scheme (4.3.13)-(4.3.14), and define $\epsilon_l^n = p_l^n - P_l^n$ as the truncation error, such that $\epsilon_0^n = \epsilon_L^n = 0$ for all n. Substituting ϵ_l^n into (4.3.13)-(4.3.14) we obtain

$$-\frac{\psi}{2h^2}\epsilon_{l+1}^1 + \left(\frac{\psi}{h^2}+\sigma_0\right)\epsilon_l^1 - \frac{\psi}{2h^2}\epsilon_{l-1}^1 = \frac{\psi}{2h^2}\epsilon_{l+1}^0 - \frac{\psi}{h^2}\epsilon_l^0 + \frac{\psi}{2h^2}\epsilon_{l-1}^0 = 0 \quad (4.3.16)$$

for $n = 0$ and,

$$-\frac{\psi}{2h^2}\epsilon_{l+1}^{n+1} + \left(\frac{\psi}{h^2} + \sigma_0\right)\epsilon_l^{n+1} - \frac{\psi}{2h^2}\epsilon_{l-1}^{n+1} = \frac{\psi}{2h^2}\epsilon_{l+1}^{n} - \left(\frac{\psi}{h^2} + \sigma_0\right)\epsilon_l^{n} + \frac{\psi}{2h^2}\epsilon_{l-1}^{n} - \sum_{j=1}^{n}\sigma_j\epsilon_l^{n-j+1},\ n \geq 1. \tag{4.3.17}$$

Let us define the following grid functions,

$$\epsilon^n(S) = \begin{cases} \epsilon_l^n, & \text{when} \quad S_l - \frac{h}{2} < S \leq S_l + \frac{h}{2}, \quad l = 1, 2, ..., L-1, \\ 0, & \text{when} \quad 0 \leq S < \frac{h}{2} \quad \text{or} \quad S_{max} - \frac{h}{2} < S \leq S_{max} + \frac{h}{2}. \end{cases} \tag{4.3.18}$$

Then $\epsilon^n(S)$ can be represented by the following Fourier series;

$$\epsilon^n(S) = \sum_{j=1}^{\infty} \varrho_n(j) e^{i2\pi jS/S_{max}}, \quad n = 1, 2, ..., N, \tag{4.3.19}$$

where

$$\varrho_n(j) = \frac{1}{S_{max}} \int_0^{Smax} \epsilon^n(S) e^{-i2\pi jS/S_{max}} dS, \quad n = 1, 2, ..., N. \tag{4.3.20}$$

Let $\epsilon^n = (\epsilon_1^n, \epsilon_2^n, \cdots, \epsilon_{L-1}^n)^T$ and, defining it's norm

$$\left\|\epsilon^n\right\|_2 = \left(\sum_{l=1}^{L-1} h|\ \epsilon_l^n\ |^2\right)^{1/2} = \left(\int_0^{S_{max}} |\ \epsilon^n(S)\ |^2 dS\right)^{1/2}, \tag{4.3.21}$$

and, applying the Parseval equality

$$\int_0^{S_{max}} |\ \epsilon^n(S)^2\ |\ dS = \sum_{j=-\infty}^{\infty} |\ \varrho_n(j)\ |^2, \tag{4.3.22}$$

we obtain that

$$\left\|\epsilon^n\right\|_2^2 = \int_0^{S_{max}} \mid \epsilon^n(S) \mid^2 dS = \sum_{j=-\infty}^{\infty} \mid \varrho_n(j) \mid^2 . \tag{4.3.23}$$

Therefore, we can propose the solution to (4.3.16) and (4.3.17) takes the following form

$$\epsilon^n = \varrho_n e^{i\beta lh}, \tag{4.3.24}$$

where $\beta = 2\pi j/S_{max}$ and $i = \sqrt{-1}$. Substituting the expression for ϵ^n into (4.3.16) and (4.3.17), we obtain

$$\begin{aligned} -\frac{\psi}{2h^2}\varrho_1 e^{i\beta(l+1)h} + \left(\frac{\psi}{h^2}+\sigma_0\right)\varrho_1 e^{i\beta lh} - \frac{\psi}{2h^2}\varrho_1 e^{i\beta(l-1)h} &= \frac{\psi}{2h^2}\varrho_0 e^{i\beta(l+1)h} \\ &\quad - \left(\frac{\psi}{h^2}+\sigma_0\right)\varrho_0 e^{i\beta lh} \\ &\quad + \frac{\psi}{2h^2}\varrho_0 e^{i\beta(l-1)h}; \end{aligned} \tag{4.3.25}$$

for $n = 0$ and,

$$\begin{aligned} -\frac{\psi}{2h^2}\varrho_{n+1} e^{i\beta(l+1)h} + \left(\frac{\psi}{h^2}+\sigma_0\right)\varrho_{n+1} e^{i\beta lh} - \frac{\psi}{2h^2}\varrho_{n+1} e^{i\beta(l-1)h} &= \frac{\psi}{2h^2}\varrho_n e^{i\beta(l+1)h} - \left(\frac{\psi}{h^2}+\sigma_0\right)\varrho_n e^{i\beta lh} \\ &\quad + \frac{\psi}{2h^2}\varrho_n e^{i\beta(l-1)h} - \sum_{j=1}^{n}\sigma_j \varrho_{n-j+1} e^{i\beta lh}; \; n \geq 1. \end{aligned} \tag{4.3.26}$$

Which after simplifications, leads to

$$\begin{aligned} \varrho_1\left(-\frac{\psi}{2h^2}e^{i\beta h} + e^{-i\beta h}\right) + \left(\frac{\psi}{h^2}+\sigma_0\right) &= \varrho_0\frac{\psi}{2h^2}\left(e^{i\beta h} + e^{-i\beta h}\right) \\ &\quad - \left(\frac{\psi}{h^2}+\sigma_0\right), \; n = 0, \end{aligned} \tag{4.3.27}$$

and

$$\varrho_{n+1}\left(-\frac{\psi}{2h^2}e^{i\beta h}+e^{-i\beta h}\right)+\left(\frac{\psi}{h^2}+\sigma_0\right) = \varrho_n\left(\frac{\psi}{2h^2}e^{i\beta h}+e^{-i\beta h}\right)-\left(\frac{\psi}{h^2}+\sigma_0\right) - \sum_{j=1}^{n}\sigma_j\varrho_{n-j+1},\ n\geq 1. \tag{4.3.28}$$

These implies that

$$\varrho_1\left(-\frac{\psi}{h^2}\cos\beta h+\frac{\psi}{h^2}+\sigma_0\right)=\varrho_0\left(\frac{\psi}{h^2}\cos\beta h-\left(\frac{\psi}{h^2}+\sigma_0\right)\right),\ n=0, \tag{4.3.29}$$

and

$$\varrho_{n+1}\left(-\frac{\psi}{h^2}\cos\beta h+\frac{\psi}{h^2}+\sigma_0\right) = \varrho_n\left(\frac{\psi}{h^2}\cos\beta h-\left(\frac{\psi}{h^2}+\sigma_0\right)\right) - \sum_{j=1}^{n}\sigma_j\varrho_{n-j+1};\ n\geq 1. \tag{4.3.30}$$

Proposition 4.3.1. *Suppose* ϱ_{n+1} *satisfy* (4.3.29) *and* (4.3.30)*, then* $\mid \varrho_{n+1} \mid \leq \mid \varrho_0 \mid$ *for all* $n=0,1,2,\cdots,N$.

Proof. Suppose $n=0$, from (4.3.29) we have

$$\begin{aligned}\mid \varrho_1 \mid &= \left|\frac{-\frac{\psi}{h^2}\cos\beta h+\left(\frac{\psi}{h^2}+\sigma_0\right)}{\frac{\psi}{h^2}\cos\beta h-\left(\frac{\psi}{h^2}+\sigma_0\right)}\varrho_0\right|,\\ &= \left|\frac{-\left(\frac{\psi}{h^2}\cos\beta h-\left(\frac{\psi}{h^2}+\sigma_0\right)\right)}{\frac{\psi}{h^2}\cos\beta h-\left(\frac{\psi}{h^2}+\sigma_0\right)}\varrho_0\right|,\\ &= \mid -\varrho_0 \mid,\\ &\leq \mid \varrho_0 \mid .\end{aligned} \tag{4.3.31}$$

Now, suppose $\mid \varrho_n \mid \leq \mid \varrho_0 \mid$ for $n=1,2,3,...,N$. We need to show that $\mid \varrho_{n+1} \mid \leq \mid \varrho_0 \mid$. From (4.3.30)

$$
\begin{aligned}
\mid \varrho_{n+1} \mid &\leq \left| \frac{\varrho_n \left(\frac{\psi}{h^2}\cos\beta h - \left(\frac{\psi}{h^2}+\sigma_0\right)\right)}{-\left(\frac{\psi}{h^2}\cos\beta h - \left(\frac{\psi}{h^2}+\sigma_0\right)\right)} \right| + \left| \frac{-\sum_{j=1}^{n}\sigma_j\varrho_{n-j+1}}{-\left(\frac{\psi}{h^2}\cos\beta h - \left(\frac{\psi}{h^2}+\sigma_0\right)\right)} \right|, \\
&\leq \left| \frac{\varrho_n \left(\frac{\psi}{h^2}\cos\beta h - \left(\frac{\psi}{h^2}+\sigma_0\right)\right)}{\left(\frac{\psi}{h^2}\cos\beta h - \left(\frac{\psi}{h^2}+\sigma_0\right)\right)} \right| + \left| \frac{\sum_{j=1}^{n}\sigma_j\varrho_{n-j+1}}{\left(\frac{\psi}{h^2}\cos\beta h - \left(\frac{\psi}{h^2}+\sigma_0\right)\right)} \right|, \\
&= \mid \varrho_n \mid + \frac{1}{\left|\left(\frac{\psi}{h^2}\cos\beta h - \left(\frac{\psi}{h^2}+\sigma_0\right)\right)\right| \sum_{j=1}^{n}|\sigma_j\varrho_{n-j+1}|}, \\
&\leq \mid \varrho_n \mid + \sum_{j=1}^{n} \mid \sigma_j\varrho_{n-j+1} \mid, \left(\because \frac{1}{\mid \frac{\psi}{h^2}\cos\beta h - \left(\frac{\psi}{h^2}+\sigma_0\right) \mid} \leq 1 \right), \\
&= \mid \varrho_n \mid + \sigma_1 \mid \varrho_n \mid + \sigma_2 \mid \varrho_{n-1} \mid + \cdots + \sigma_n \mid \varrho_1 \mid\mid, \\
&\leq \mid \varrho_0 \mid + \sigma_1 \mid \varrho_0 \mid + \sigma_2 \mid \varrho_0 \mid + \cdots + \varphi_n \mid \varrho_0 \mid, \\
&= \sum_{j=1}^{n} \sigma_j \mid \varrho_0 \mid \\
&= \mid \varrho_0 \mid \ (\because \sum_{j=1}^{n} \sigma_j = 1). \qquad (4.3.32)
\end{aligned}
$$

From Proposition 4.3.1 coupled with the Parseval equality, we obtain, $\left\|\epsilon^n\right\|_2 \leq \left\|\epsilon^0\right\|_2$ for all $n = 1, 2, \cdots, N-1$, which lead us to the following theorem.

Theorem 4.3.2. *The difference scheme* (4.3.13)-(4.3.14) *is unconditionally stable.*

The proof to Theorem 4.3.2 follows from results from equation 4.3.16 through to equation 4.3.32.

4.3.2 Convergence analysis

The concept of Fourier analysis was used to studying the convergence properties of the scheme. To begin, let us denote the truncation error at grid point (t_{n+1}, s_l) by R_l^{n+1}, then, from equation (4.3.5) and part of (4.3.12), we have that

$$\left|R_l^n\right| \leq C(k^2+h^2),\ l = 1, 2, \cdots, L-1;\ n = 0, 1, 2, \cdots, N-1, \qquad (4.3.33)$$

where C is a constant given by

$C = \max_{1\leq l\leq L-1, 0\leq n\leq N-1}\{C_l^n\}$, for some constants C_l^n independent of h and k.

Let $\xi_l^n = p(s_l, t_n) - p_l^n$ denote the approximation error at grid point (t_n, s_l), such that $\xi_L^n = 0$, for $n = 1, 2, \cdots, N$ and $\xi_l^0 = 0$, for $l = 0, 1, \cdots, L$. By substituting ξ_l^n into the scheme (4.3.13)-(4.3.14), we obtain

$$-\frac{\psi}{2h^2}\xi_{l+1}^1 + (\frac{\psi}{h^2} + \sigma_0)\xi_l^1 - \frac{\psi}{2h^2}\xi_{l-1}^1 = R_l^1, \tag{4.3.34}$$

for $n = 0$ and,

$$\begin{aligned} -\frac{\psi}{2h^2}\xi_{l+1}^{n+1} + (\frac{\psi}{h^2} + \sigma_0)\xi_l^{n+1} - \frac{\psi}{2h^2}\xi_{l-1}^{n+1} &= \frac{\psi}{2h^2}\xi_{l+1}^n - (\frac{\psi}{h^2} + \sigma_0)\xi_l^n + \frac{\psi}{2h^2}\xi_{l-1}^n \\ &\quad - \sum_{j=1}^{n}\sigma_j\xi_l^{n-j+1} + R_l^{n+1};\ n \geq 1. \end{aligned} \tag{4.3.35}$$

Similar to stability analysis, we define the following grid functions

$$\xi^n(S) = \begin{cases} \xi_l^n, & \text{when} \quad S_l - \frac{h}{2} < S \leq S_l + \frac{h}{2}, \quad l = 1, 2, ..., L-1, \\ 0, & \text{when} \quad 0 \leq S < \frac{h}{2} \quad \text{or} \quad S_{max} - \frac{h}{2} < S \leq S_{max} + \frac{h}{2}, \end{cases} \tag{4.3.36}$$

$$R^n(S) = \begin{cases} R_l^n, & \text{when} \quad S_l - \frac{h}{2} < S \leq S_l + \frac{h}{2}, \quad l = 1, 2, ..., L-1, \\ 0, & \text{when} \quad 0 \leq S < \frac{h}{2} \quad \text{or} \quad S_{max} - \frac{h}{2} < S \leq S_{max} + \frac{h}{2}, \end{cases} \tag{4.3.37}$$

which imply $\xi^n(S)$ and R_l^n have the following Fourier series representations

$$\xi^n(S) = \sum_{j=1}^{\infty}\tau_n(j)e^{i2\pi jS/S_{max}}; \quad n = 1, 2, ..., N, \tag{4.3.38}$$

$$R^n(S) = \sum_{j=1}^{\infty}\nu_n(j)e^{i2\pi jS/S_{max}}; \quad n = 1, 2, ..., N, \tag{4.3.39}$$

where

$$\tau_n(j) = \frac{1}{S_{max}} \int_0^{Smax} \xi^n(S) e^{-i2\pi jS/S_{max}} dS; \quad n = 1, 2, ..., N. \tag{4.3.40}$$

$$\nu_n(j) = \frac{1}{S_{max}} \int_0^{Smax} R^n(S) e^{-i2\pi jS/S_{max}} dS; \quad n = 1, 2, ..., N. \tag{4.3.41}$$

Let $\xi^n = (\xi_1^n, \xi_2^n, \cdots, \xi_{L-1}^n)^T$ and $R^n = (R_1^n, R_2^n, \cdots, R_{L-1}^n)^T$, and let us define their norms as follow

$$\left\| \xi^n \right\|_2 = \left(\sum_{l=1}^{L-1} h | \ \xi_l^n \ |^2 \right)^{1/2} = \left(\int_0^{S_{max}} | \ \xi^n(S) \ |^2 dS \right)^{1/2}, \tag{4.3.42}$$

$$\left\| R^n \right\|_2 = \left(\sum_{l=1}^{L-1} h | \ R_l^n \ |^2 \right)^{1/2} = \left(\int_0^{S_{max}} | \ R^n(S) \ |^2 dS \right)^{1/2}, \tag{4.3.43}$$

and, apply the following Parseval equalities

$$\int_0^{S_{max}} | \ \xi^n(S)^2 \ | \, dS = \sum_{j=-\infty}^{\infty} | \ \tau_n(j) \ |^2; \quad n = 1, 2, ..., N, \tag{4.3.44}$$

$$\int_0^{S_{max}} | \ R^n(S)^2 \ | \, dS = \sum_{j=-\infty}^{\infty} | \ \nu_n(j) \ |^2; \quad n = 1, 2, ..., N, \tag{4.3.45}$$

to obtain

$$\left\| \xi^n \right\|_2^2 = \sum_{j=-\infty}^{\infty} | \ \tau_n(j) \ |^2; \quad n = 1, 2, ..., N, \tag{4.3.46}$$

$$\left\| R^n \right\|_2^2 = \sum_{j=-\infty}^{\infty} | \ \nu_n(j) \ |^2; \quad n = 1, 2, ..., N. \tag{4.3.47}$$

We can therefore propose that

$$\xi^n = \tau_n e^{i\beta lh} \quad \text{and} \quad R^n = \nu_n e^{i\beta lh}, \tag{4.3.48}$$

where $\beta = 2\pi j/S_{max}$ and $i = \sqrt{-1}$. Substituting the expressions in (4.3.48) into (4.3.34) and (4.3.35), we obtain

$$-\frac{\psi}{2h^2}\tau_1 e^{i\beta(l+1)h} + \left(\frac{\psi}{h^2} + \sigma_0\right)\tau_1 e^{i\beta lh} - \frac{\psi}{2h^2}\tau_1 e^{i\beta(l-1)h} = \nu_1 e^{i\beta lh},\ n = 0, \tag{4.3.49}$$

and

$$\begin{aligned} -\frac{\psi}{2h^2}\tau_{n+1}e^{i\beta(l+1)h} \quad + \quad & \left(\frac{\psi}{h^2} + \sigma_0\right)\tau_{n+1}e^{i\beta lh} - \frac{\psi}{2h^2}\tau_{n+1}e^{i\beta(l-1)h} \\ = \quad & \frac{\psi}{2h^2}\tau_n e^{i\beta(l+1)h} \\ & - \left(\frac{\psi}{h^2} + \sigma_0\right)\tau_n e^{i\beta lh} \\ & + \frac{\psi}{2h^2}\tau_n e^{i\beta(l-1)h} - \sum_{j=1}^{n}\sigma_j\tau_{n-j+1}e^{i\beta lh} \\ & + \nu_{n+1}e^{i\beta lh};\ n \geq 1. \end{aligned} \tag{4.3.50}$$

Which after simplifications, leads to

$$\tau_1\left(-\frac{\psi}{2h^2}\left(e^{i\beta h} + e^{-i\beta h}\right) + \left(\frac{\psi}{h^2} + \sigma_0\right)\right) = \nu_1, \tag{4.3.51}$$

and

$$\begin{aligned} \tau_{n+1}\left(-\frac{\psi}{2h^2}\left(e^{i\beta h} + e^{-i\beta h}\right) + \left(\frac{\psi}{h^2} + \sigma_0\right)\right) \quad = \quad & \tau_n\left(\frac{\psi}{2h^2}\left(e^{i\beta h} + e^{-i\beta h}\right) - \left(\frac{\psi}{h^2} + \sigma_0\right)\right) \\ & - \sum_{j=1}^{n}\sigma_j\tau_{n-j+1} + \nu_{n+1},\ n \geq 1. \end{aligned} \tag{4.3.52}$$

These implies that for $n = 0$,

$$\tau_1 \left(-\frac{\psi}{h^2} \cos \beta h + \frac{\psi}{h^2} + \sigma_0 \right) = \nu_1, \tag{4.3.53}$$

and for $n \geq 1$,

$$\begin{aligned} \tau_{n+1} \left(-\frac{\psi}{h^2} \cos \beta h + \frac{\psi}{h^2} + \sigma_0 \right) &= \tau_n \left(\frac{\psi}{h^2} \cos \beta h - \left(\frac{\psi}{h^2} + \sigma_0 \right) \right) - \sum_{j=1}^{n} \sigma_j \tau_{n-j+1} \\ &\quad + \nu_{n+1}. \end{aligned} \tag{4.3.54}$$

Which leads to the following equalities,

$$\tau_1 = -\frac{\nu_1}{\left(\frac{\psi}{h^2} \cos \beta h - \left(\frac{\psi}{h^2} + \sigma_0 \right) \right)}, \tag{4.3.55}$$

and

$$\tau_{n+1} = -\left(\tau_n + \frac{\sum_{j=1}^{n} \sigma_j \tau_{n-j+1} + \nu_{n+1}}{\left(\frac{\psi}{h^2} \cos \beta h - \left(\frac{\psi}{h^2} + \sigma_0 \right) \right)} \right). \tag{4.3.56}$$

Proposition 4.3.3. *Suppose τ_n for $n = 0, 1, \cdots, N$ is a solution to equations (4.3.55) and (4.3.56), then there exists a positive constant C_1 such that $|\tau_n| \leq C_1 |\nu_1|$ for all n.*

Proof. Notice that when $n = 0$, from (4.3.55) we have

$$|\tau_1| \leq \left| \frac{\nu_1}{(\frac{\psi}{h^2} \cos \beta h - (\frac{\psi}{h^2} + \sigma_0))} \right| \leq C_1 |\nu_1|, \tag{4.3.57}$$

Suppose $|\tau_n| \leq C_0 |\nu_1|$, for $n = 1, 2, \cdots, N$, for some constant C independent of h

and k. Then,

$$\begin{aligned}
|\tau_{n+1}| &\leq \left|\tau_n + \frac{\sum_{j=1}^{n}\sigma_j\tau_{n-j+1}+\nu_{n+1}}{(\frac{\psi}{h^2}\cos\beta h-(\frac{\psi}{h^2}+\sigma_0))}\right|,\\
&\leq |\tau_n| + \left|\frac{\sum_{j=1}^{n}\sigma_j\tau_{n-j+1}+\nu_{n+1}}{(\frac{\psi}{h^2}\cos\beta h-(\frac{\psi}{h^2}+\sigma_0))}\right|,\\
&\leq C_0|\nu_1| + \sum_{j=1}^{n}\frac{1}{\left|(\frac{\psi}{h^2}\cos\beta h-(\frac{\psi}{h^2}+\sigma_0))\right|}(\sigma_j\left|\tau_{n-j+1}\right| + \left|\nu_{n+1}\right|),\\
&\leq C_0|\nu_1| + \sum_{j=1}^{n}C_j(\sigma_j\left|\tau_{n-j+1}\right| + \left|\nu_{n+1}\right|),\\
&\leq C_0|\nu_1| + \sum_{j=1}^{n}\sigma_jC_j\left|\tau_{n-j+1}\right| + C_{n+1}\left|\nu_1\right|,\\
&\leq C_0|\nu_1| + \sum_{j=1}^{n}\sigma_jC_j\left|\nu_1\right| + C_{n+1}\left|\nu_1\right|,\\
&= C_0|\nu_1| + \sigma_1C_1\left|\nu_1\right| + \sigma_2C_2\left|\nu_1\right| + \cdots + \sigma_nC_n\left|\nu_1\right| + C_{n+1}\left|\nu_1\right|,\\
&\leq \hat{C}(|\nu_1| + \sum_{j=1}^{n}\sigma_j|\nu_1| + \nu_1), (\hat{C} = \max_{0\leq j\leq n+1}\{C_j\}),\\
&= \hat{C}(2+\sum_{j=1}^{n}\sigma_j)|\nu_1|,\\
&= C|\nu_1|. \qquad (4.3.58)
\end{aligned}$$

The following theorem therefore holds,

Theorem 4.3.4. *The difference scheme* (4.3.13)-(4.3.14) *is convergent and converge with order* $\mathcal{O}(k^2, h^2)$.

The proof to Theorem 4.3.4 follows from equation (4.3.34) through to equation (4.3.58).

4.4 Numerical experiments

In this section we investigate the pricing of European put options using the time-fractional Black-Scholes (tfBS) PDE (4.2.23) which is implemented via scheme (4.3.13)-

(4.3.14) with initial and boundary conditions (4.3.15). We consider two distinct examples with varying dividend yields and order of the fractional derivative (α) fixed at $0.3, 0.5, 0.7$ and 0.9. The numerical solutions obtained using the proposed method shows that the option maturity payoff curves obtained are in very good coincidence with the European put option intrinsic payoff curves obtained under all possible parameter settings.

Example 4.4.1. *Consider equation* (4.2.23) *subject to conditions* (4.3.15) *on pricing a European put option with the following parameters:* $K = 150$, $r = 0.08$, $\sigma = 0.1$, $T = 1$, $S_{\max} = 450$, $L = 100$, $N = 200$, $\delta = 0.035$, 0.05 *and* 0.10.

Below we present numerical results for the case when $\delta = 0.035$ considered at all four values of α i.e. ($\alpha = 0.3, 0.5, 0.7$ and 0.9).

The maturity payoff curves for $\delta = 0.035$ are as shown in fig. 4.4.1 below,

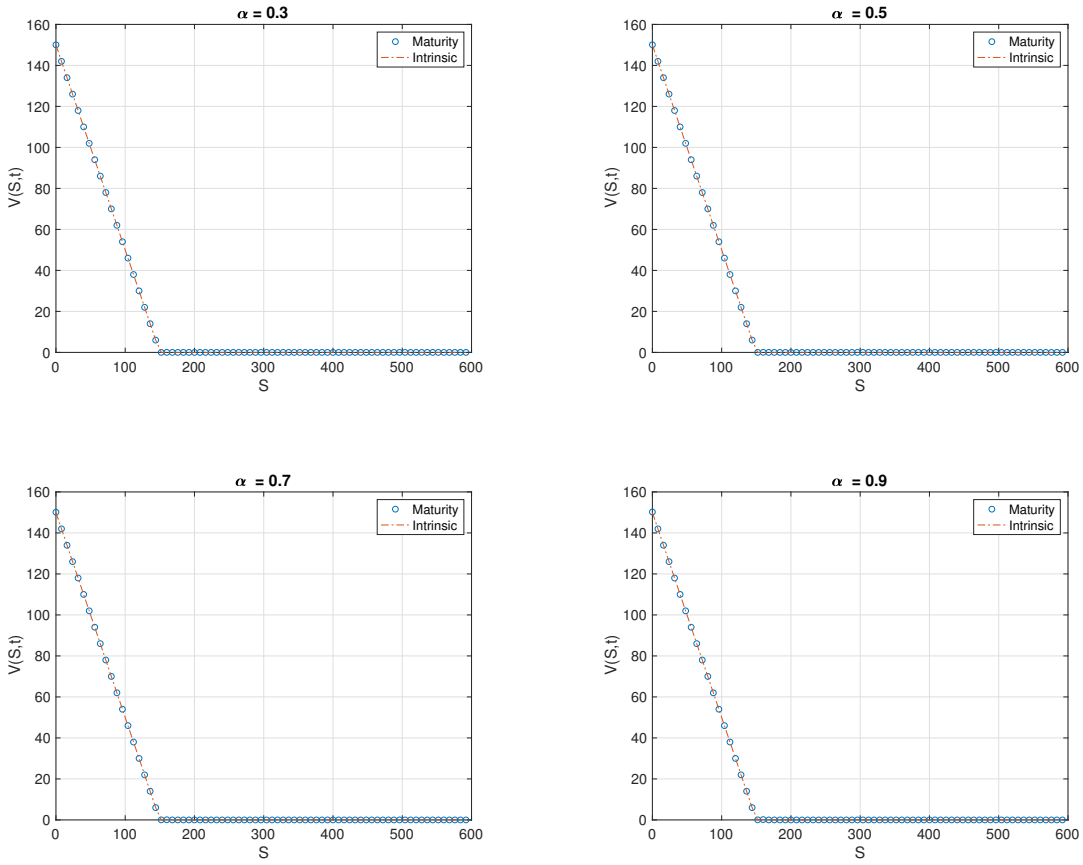

Figure 4.4.1: Maturity payoffs for $\delta = 0.035$ with $\alpha = 0.3\,, 0.5\,, 0.7\,\&\,0.9$ respectively,

and the general payoffs throughout the lifespan of the option at all considered sets of α are as appearing in Figure 4.4.2 below

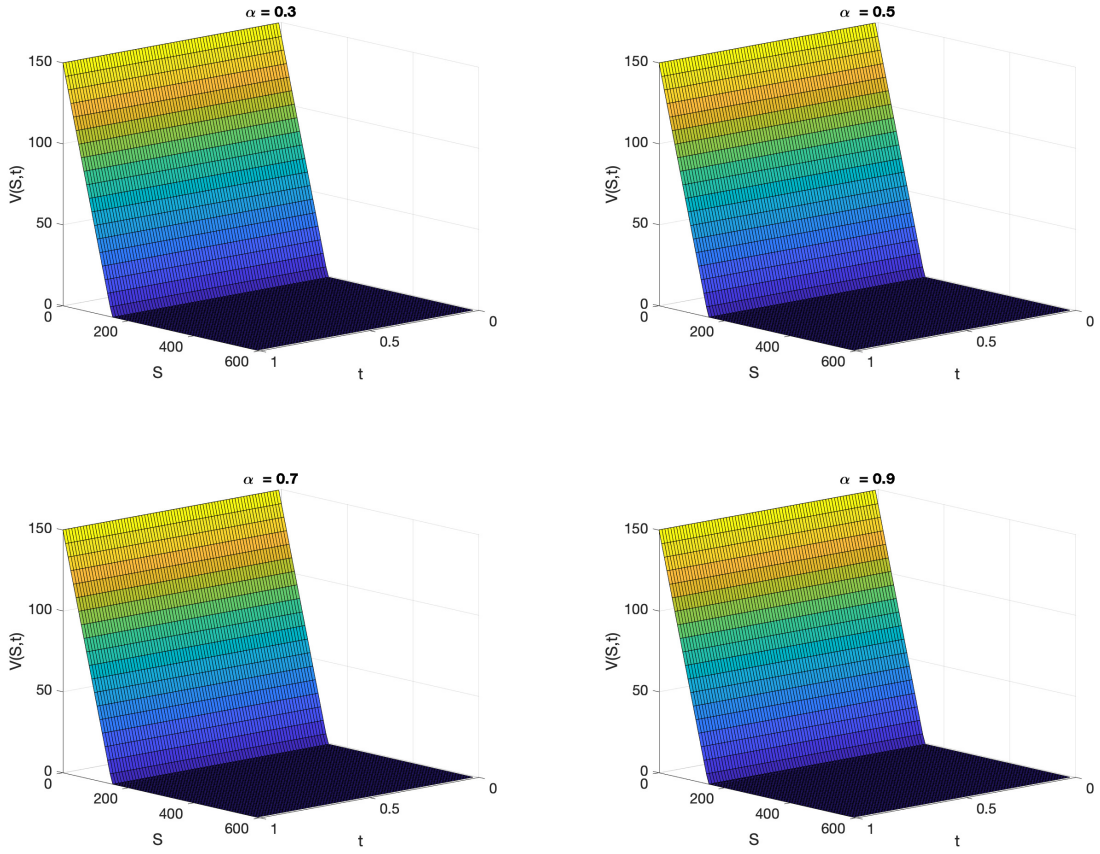

Figure 4.4.2: General payoffs for $\delta = 0.035$ with $\alpha = 0.3\,, 0.5\,, 0.7\,\&\,0.9$ respectively.

Example 4.4.2. *Consider* (4.2.23)*, again, subject to conditions* (4.3.15) *but under the following parameters:*$K = 150, \quad r = .065$, $\sigma = .13$, $T = 1$, $S_{\max} = 600$, $L = 30$, $N = 100, \delta = 0.045,\ 0.085,$ *and* 0.11.

Similar to Example 4.4.1 in this Example 4.4.2 we only present payoff results for when $\delta = 0.045$ at all four considered values of α. The maturity payoff curves for $\delta = 0.045$ at all four values of α are presented in fig. 4.4.3 and their respective general payoffs presented in fig. 4.4.4 below.

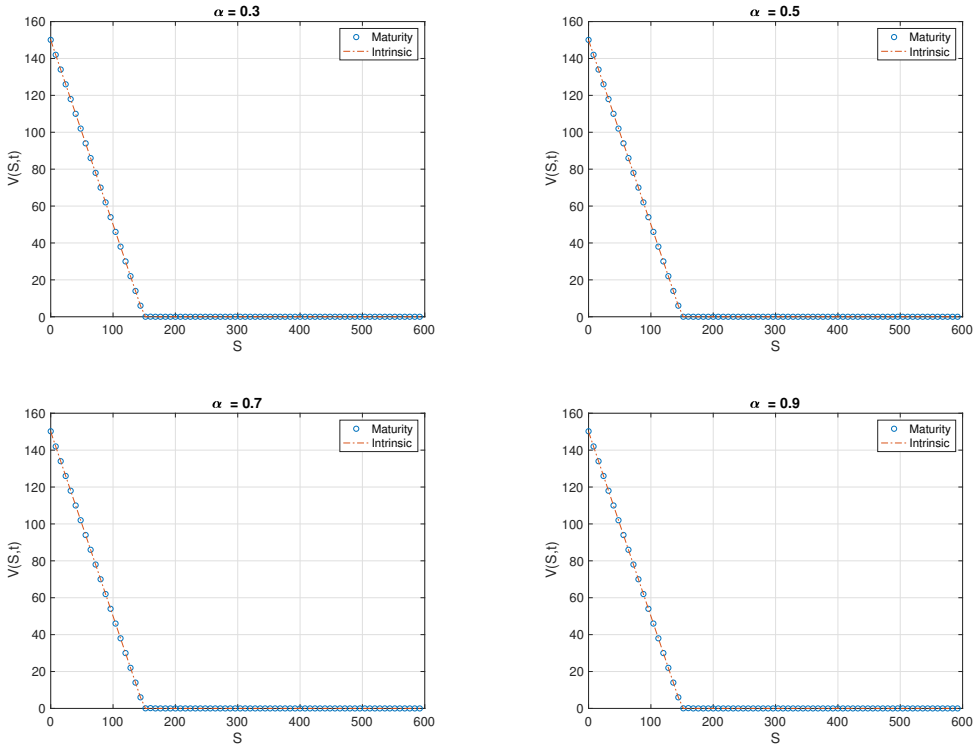

Figure 4.4.3: Maturity payoffs for $\delta = 0.045$ with $\alpha = 0.3\,, 0.5\,, 0.7\,\&\,0.9$ respectively.

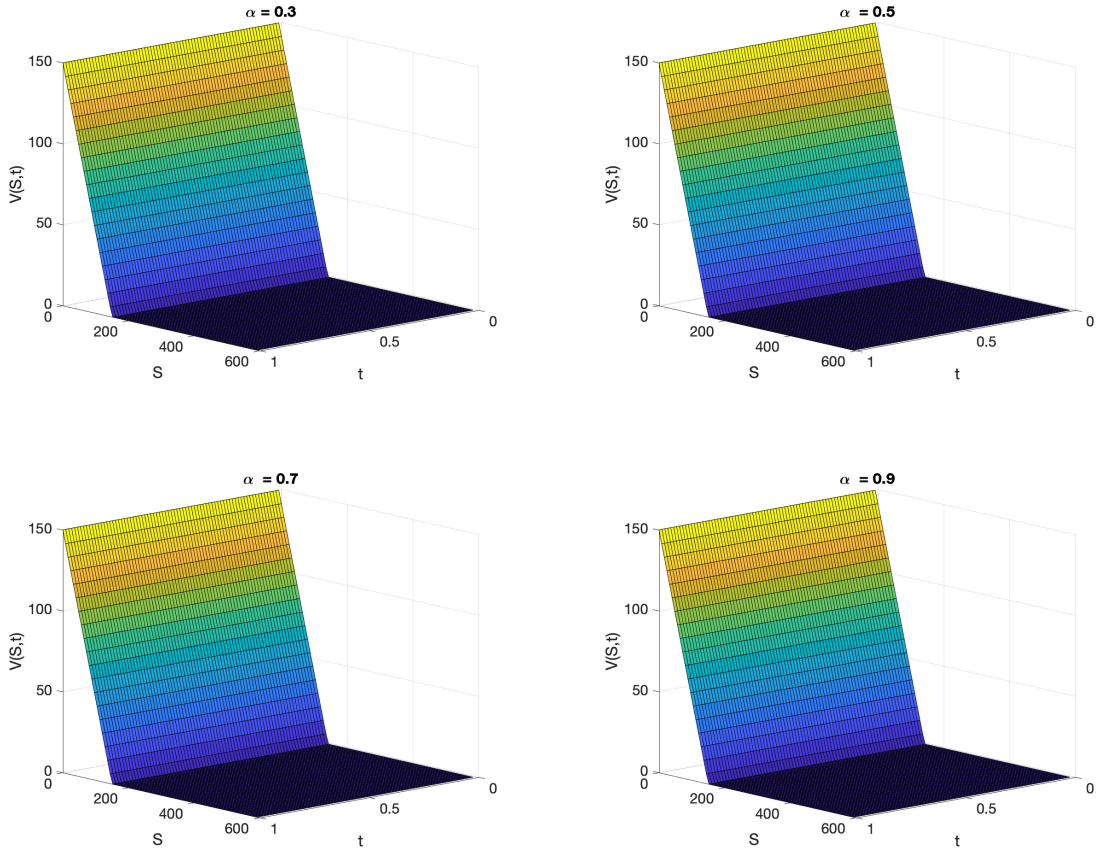

Figure 4.4.4: General payoffs for $\delta = 0.045$ with $\alpha = 0.3\,, 0.5\,, 0.7\,\&\,0.9$ respectively.

The tabular results for example 4.4.1 and example 4.4.2, with N starting from 30 for example 4.4.1 and 50 for example 4.4.2 are presented in tables 4.4.2, 4.4.3, 5.5.3 and 5.5.4 below. Numerical results herein confirms that our results are in excellent agreement with our theoretical deductions presented in section 4.3.1 and theorem 4.3.4 under section 4.3.1 and section 4.3.2 respectively.

Table 4.4.1: Maximum absolute errors for example 4.4.1 with $r = 0.08$ and $\delta = 0.035$.

α	$N = 30$	$N = 60$	$N = 120$	$N = 240$	$N = 480$
0.1	7.5592e-03	1.8952e-03	4.7712e-04	1.1987e-04	3.0128e-05
0.2	6.8088e-03	1.8694e-03	4.7170e-04	1.1825e-04	3.3784e-05
0.3	6.2147e-03	1.6191e-03	4.3368e-04	1.1698e-04	3.1352e-05
0.4	5.7443e-03	1.5001e-03	4.0358e-04	1.1684e-04	2.9426e-05
0.5	5.3746e-03	1.4966e-03	3.7993e-04	1.1651e-04	2.7912e-05
0.6	5.0893e-03	1.4044e-03	3.6167e-04	1.1619e-04	2.1544e-05
0.7	4.8773e-03	1.3880e-03	3.4810e-04	1.1607e-04	2.1676e-05
0.8	4.7318e-03	1.2500e-03	3.3879e-04	1.1405e-04	1.9950e-05
0.9	4.6499e-03	1.1682e-03	2.9355e-04	7.3797e-05	1.8575e-05
1.0	4.6328e-03	1.1645e-03	3.0246e-04	7.5988e-05	1.9670e-05

Table 4.4.2: Convergence rates for example 4.4.1 with $r = 0.08$ and $\delta = 0.035$.

α	$N = 60$	$N = 120$	$N = 240$	$N = 480$
0.1	1.67	1.86	1.88	1.89
0.2	1.66	1.87	1.88	1.89
0.3	1.68	1.87	1.89	1.90
0.4	1.68	1.87	1.89	1.91
0.5	1.68	1.88	1.89	1.95
0.6	1.68	1.88	1.89	1.96
0.7	1.78	1.88	1.89	1.98
0.8	1.89	1.88	1.89	1.98
0.9	1.89	1.88	1.89	1.98
1.0	1.89	1.87	1.89	1.98

Table 4.4.3: Maximum absolute errors for example 4.4.2 with $r = 0.065$ and $\delta = 0.045$.

α	$N = 50$	$N = 100$	$N = 200$	$N = 400$	$N = 800$
0.1	1.4714e-03	3.5691e-04	8.8754e-05	2.2298e-05	5.6053e-06
0.2	1.3394e-03	3.2352e-04	7.9308e-05	2.0162e-05	5.0648e-06
0.3	1.1162e-03	2.6506e-04	6.6025e-05	1.6549e-05	4.1509e-06
0.4	9.6623e-04	2.5089e-04	6.2188e-05	1.5578e-05	3.7253e-06
0.5	8.6515e-04	2.1632e-04	5.5720e-05	1.3942e-05	3.5015e-06
0.6	8.1315e-04	2.1216e-04	5.2393e-05	1.3100e-05	3.2885e-06
0.7	7.6609e-04	2.0126e-04	4.9381e-05	1.2439e-05	3.0859e-06
0.8	7.4065e-04	1.9183e-04	4.7753e-05	1.1927e-05	2.9817e-06
0.9	7.2436e-04	1.9170e-04	4.6711e-05	1.1663e-05	2.9350e-06
1.0	7.2202e-04	1.8911e-04	4.6561e-05	1.1625e-05	2.9254e-06

Table 4.4.4: Convergence rates for example 4.4.2 with $r = 0.065$ and $\delta = 0.045$.

α	$N = 100$	$N = 200$	$N = 400$	$N = 800$
0.1	1. 78	1.89	1.97	1.97
0.2	1.79	1.92	1.96	1.98
0.3	1.79	1.93	1.97	1.98
0.4	1.80	1.94	1.97	1.99
0.5	1.88	1.95	1.98	1.99
0.6	1.88	1.96	1.98	1.99
0.7	1.88	1.96	1.98	1.99
0.8	1.88	1.97	1.98	1.99
0.9	1.89	1.97	1.98	1.99
1.0	1.89	1.97	1.98	1.99

4.5 Summary and discussions

The fractional approach is a very effective approach to asset pricing as it provides a unique framework, one that has a potential to transform conventional thinking in asset pricing theory and applications. The non-local derivatives and integral operators as well as the accompanying fractional stochastic dynamics provides the best tools for explaining trend and noise memory effects as well as non-localised information about the stock price movements, something that the classical models may fail to explain. Since the fractional derivatives operators are of a non-local nature, there is little to none existing knowledge of analytic solutions to fractional BS models. As such, numerical methods are the only available avenues to help understand the nature of solutions to these models.

In this chapter, we transformed a standard tfBS-PDE into a solvable tfBS-PDE in the form of a heat equation. In general, the transformation is necessary as it helps in easing the mathematical difficulties and complexity involved in solving the original tfBS-PDE using the high order numerical method presented herein. We constructed a robust and high order numerical scheme for solving the resultant model. From the simulation, we considered two examples, Example 4.4.1, and Example 4.4.2 as well as their numerical results in Tables 4.4.1 to 4.4.4. The above stated results are in

agreement with theoretical observations that, the method is unconditional stable and converges to up to order $\mathcal{O}(k^2)$. We further observe that, our approach provides a very efficient, effective and powerful mathematical tool for option pricing.

Though the asymptotic long-term behaviours of markets tends to be similar for when the dynamics are driven by the usual Gaussian processes as compared to non-Gaussian processes (i.e fractal processes), we observe that, incorporating the fractional parameters describes the dynamics much better and with greater flexibility. Such fact does holds most specifically in markets with empirical evidence of memory or those that presents some non-random power law properties which are often not predictable using ordinary Gaussian assumptions.

The application of the approach to other models and their calibration to real-time market data remain the subject of future research. In the next chapter we formulate an American option pricing fractional Black-Scholes equation as well as propose a front-fixing transformation based numerical method for solving the resultant model.

Chapter 5

A Robust Numerical Simulation of an American Put Option Pricing Time Fractional Black-Scholes Equation

In this chapter we propose a robust finite difference numerical scheme for solving a time-fractional Black-Scholes equation for pricing American put options. The numerical method herein is based on front-fixing transformation, whereby the early exercise boundaries are transformed into fixed boundaries allowing for the simultaneous computation of the option premiums as well as the corresponding optimal exercise boundaries.

5.1 Introduction

After the discovery of fractal structures of financial markets, fractional partial differential equations became very popular in studying financial derivative pricing problems. The available research results includes two key aspects, firstly, derivation of a better realistic pricing model, one that closely reflects the actual dynamics of financial markets. Secondly, the design of a robust numerical method for solving the resultant models become important, since in most cases, the resultant models are often of nonlinear nature and as such, no reliable analytic methods have thus far been documented. therefore

numerical methods become vitally important in understanding the nature of solutions to these models. The difficulty in evaluating American options accurately lies on the unknown free boundaries associated with these type of options. The free boundaries emanates from the flexibility of early exercise features associated with the American options. To the best of our knowledge, there are no extensive literatures on numerical methods for pricing of American option problems from a fractional point of view.

This chapter is organised as follow, Section 5.2 present a brief derivation of the involved time-fractional Black-Scholes (tfBS) PDE for pricing American put options. In Section 5.3 we propose a finite difference discretisation of the transformed tfBS-PDE while further elaborating on the construction of the numerical scheme. The theoretical analysis of the scheme are presented in Section 5.4, while in Section 5.5 we present some American option pricing numerical experiments. Concluding remarks as well as scope for further research are presented in Section 5.6.

5.2 The tfBS-PDE for American put options

5.2.1 A time-fractional PDE describing an American option problem

Let $v(S,t)$ denote the value of an American put option, S the price of the underlying stock and K the option's strike price. Assume the stock price dynamics follow the following fractal process, driven by the usual Gaussian white noise $\omega(t)$

$$dS = (r-\delta)Sdt + \sigma S\omega(t)(dt)^{\alpha/2}, \;\; 0 < \alpha \leq 1, \tag{5.2.1}$$

where r is the risk-free interest rate, δ the dividend yield, and $\omega(t)$ the Gaussian white noise. Using (5.2.1) and the Generalized Taylor series expansion of $v(S,t)$ with some algebraic manipulations, leads to the following time-fractional Black-Scholes (tfBS)

PDE with initial and boundary conditions for American put option.

$$\frac{\partial^\alpha v}{\partial t^\alpha} = \left(rv - (r-\delta)S\frac{\partial v}{\partial S}\right)\frac{t^{1-\alpha}}{\Gamma(2-\alpha)} - \frac{\Gamma(1+\alpha)}{2}\sigma^2 S^2\frac{\partial^2 v}{\partial S^2}, \quad S > b(t),\ 0 < \alpha \leq 1, \tag{5.2.2}$$

$$\begin{aligned} v(S,0) &= max(K-S,0),\ S \geq 0, \\ \frac{\partial v}{\partial S}(b(t),t) &= -1, \\ v(b(t),t) &= K - b(t), \\ \lim_{S\to\infty} v(S,t) &= 0, \\ b(0) &= K, \\ v(S,t) &= K - S,\ 0 \leq S < b(t). \end{aligned} \tag{5.2.3}$$

With a change of variable $\tau = T - t$ (time to maturity), the equation (5.2.2) become

$$\frac{\partial^\alpha v}{\partial \tau^\alpha} = \left(rv - (r-\delta)S\frac{\partial v}{\partial S}\right)\frac{\tau^{1-\alpha}}{\Gamma(2-\alpha)} - \frac{\Gamma(1+\alpha)\tau^{1-\alpha}}{2(T-\tau)^{1-\alpha}}\sigma^2 S^2\frac{\partial^2 v}{\partial S^2}, \quad S > b(\tau),\ 0 < \alpha \leq 1,\ t > 0, \tag{5.2.4}$$

$$\begin{aligned} v(S,0) &= max(K-S,0),\ S \geq 0, \\ \frac{\partial v}{\partial S}(b(\tau),\tau) &= -1, \\ v(b(\tau),\tau) &= K - b(\tau), \\ \lim_{S\to\infty} v(S,\tau) &= 0, \\ b(0) &= K, \\ v(S,\tau) &= K - S,\ 0 \leq S < b(\tau), \end{aligned} \tag{5.2.5}$$

where $b(\tau)$ is the moving exercise boundary.

It is worth noting that, when $S \leq b(\tau)$ it is optimal to exercise a put option.

Whereas, when $b(\tau) < S$, the optimal exercising strategy would be to hold the option when $b(\tau) < S$.

The value matching condition $v(b(\tau), \tau) = K - b(\tau)$ and the smooth pasting condition $\frac{\partial v}{\partial S}(b(\tau), \tau) = -1$ are necessary for preserving financial interpretation of the continuity of $v(b(\tau), \tau)$ and $\frac{\partial v}{\partial S}(b(\tau), \tau)$ across the optimal exercise boundary $b(\tau)$. This is done to avoid arbitrage opportunities, because after purchasing an American put an investor can exercise the option once the asset price falls below $b(\tau)$, or purchase it back whenever the asset price rises above $b(\tau)$. Since the transactions of converting the put option into holding of cash plus a short position in asset and vice versa all occur on the early exercise boundary, we require the value matching and smooth pasting conditions in order to ensure that these transactions are self-financing, that is, each portfolio revision undertaken is exactly financed by the proceeds from the sale of the previous position ([53]).

The underlying concept of the front-fixing approach is to remove the moving exercise boundary $b(\tau)$ by change of variables which then leads to a non-linear tfBS-PDE posed on a fixed domain. With this formulation, the position of the boundary is given but some of the boundary conditions remain unknown and must be simultaneously computed with the value of the option.

To transform the tfBS-PDE (5.2.4) and for the convenience of numerical implementation, we consider the following change of variables

$$u(x, \tau) = \frac{v(S, \tau)}{K}, \; b_f(\tau) = \frac{b(\tau)}{K}, \; x = ln\left(\frac{S}{b_f}\right). \tag{5.2.6}$$

The so-called Landau transformation of the spatial variable ($x = ln\left(\frac{S}{b_f}\right)$) serves to ensure that $x = 0$ whenever $S = b(\tau)$, which transform the then free boundary conditions to fixed boundary conditions. Under this transformation, the free boundary $S = b(\tau)$ become the fixed boundary $x = 0$, hence the name of the method. Using the

new random variable x, the underlying stock dynamic equation (5.2.1) change to

$$dx = \left(q - \frac{\sigma^2}{2} - \frac{b_f'(\tau)}{b_f(\tau)}\right) dt + \sigma\omega(t)(dt)^{\alpha/2},\ q = r - \delta,\ 0 < \alpha \leq 1. \tag{5.2.7}$$

By using (5.2.7) and replicating a derivation parallel to the one presented in chapter 2, the tfBS-PDE (5.2.4) is transformed into the following fractional linear complementary problem (FLCP) under a new random variable x

$$\frac{\partial^\alpha u}{\partial \tau^\alpha} = \phi(\tau)\left(\left(ru - (q - \frac{\sigma^2}{2})\frac{\partial u}{\partial x}\right)\frac{(T-\tau)^{1-\alpha}}{\Gamma(2-\alpha)} - \frac{\Gamma(1+\alpha)}{2}\sigma^2\frac{\partial^2 u}{\partial x^2} + \frac{b_f'}{b_f}\frac{\partial u}{\partial x}\right), \tag{5.2.8}$$

$$x > 0,\ \phi(\tau) = \tau^{1-\alpha}(T-\tau)^{\alpha-1},\ 0 < \alpha \leq 1, \text{ and, } 0 < \tau \leq T.$$

This FPDE can further be simplified into

$$\frac{\partial^\alpha u}{\partial \tau^\alpha} = \theta_\tau\left(ru - \mu\frac{\partial u}{\partial x}\right) - \omega_\tau\frac{1}{2}\sigma^2\frac{\partial^2 u}{\partial x^2} + \frac{b_f'}{b_f}\frac{\partial u}{\partial x},\ x > 0,\ 0 < \alpha \leq 1,\ 0 < \tau \leq T,$$
$$\theta_\tau = \frac{\tau^{1-\alpha}}{\Gamma(2-\alpha)},\ \omega_\tau = \frac{\Gamma(1+\alpha)\tau^{1-\alpha}}{(T-\tau)^{1-\alpha}},\ \mu = r - \delta - \frac{\sigma^2}{2}, \tag{5.2.9}$$

with initial and boundary conditions for an American put option

$$u(x,0) = \max(1 - e^{-x}, 0),\ x \geq 0, \tag{5.2.10}$$
$$\frac{\partial v}{\partial x}(0,\tau) = -b_f(\tau), \tag{5.2.11}$$
$$u(0,\tau) = 1 - b_f(\tau), \tag{5.2.12}$$
$$\lim_{x\to\infty} u(x,\tau) = 0, \tag{5.2.13}$$
$$b_f(0) = 1, \tag{5.2.14}$$

where b_f' is the derivative (of the free boundary b_f) with respect to τ.

5.3 Discretization of the tfBS-PDE and construction of the numerical scheme

In this section, we introduce a finite difference method for solving the time fractional Black Scholes (tfBS) initial boundary value problem (IBVP) (5.2.9) with a free boundary $b_f(\tau)$. Not only do we compute the solution to the fractional IBVP (5.2.9) but simultaneously compute the position of the free boundary $b_f(\tau)$.

5.3.1 Discretization of the tfBS-PDE

Let L and N be positive integers and define $h = x_{max}/L$ and $k = T/N$ as the space and time step sizes respectively. Define $x_l = lh; l = 1, 2, ..., L$ and $\tau_n = nk; n = 0, 1, 2, ..., N$, such that $x_l \in [x_{min}, x_{max}]$ and $\tau_n \in [0, T]$. Furthermore, define $u_l^n = u(x_l, \tau_n)$ as the solution at the grid point $(x_l, \tau_n) = (lh, nk)$.

We evaluate the α-derivative in (5.2.6) by the following quadrature

$$\frac{\partial^\alpha u(x_l, \tau_n)}{\partial \tau^\alpha} = \rho_\alpha \sum_{j=1}^{n} \beta_j (u_l^{n-j+1} - u_l^{n-j}) + \frac{\tau_n^{1-\alpha}}{\Gamma(2-\alpha)} k, \tag{5.3.1}$$

where

$$\rho_\alpha = \frac{1}{\Gamma(2-\alpha)} \frac{1}{k^\alpha}, \tag{5.3.2}$$

and

$$\beta_j = j^{1-\alpha} - (j-1)^{1-\alpha}, \; j = 1, 2, \cdots, n, \tag{5.3.3}$$

such that, $1 = \beta_1 > \beta_2 > \beta_3 > \cdots > \to 0$ as $j \to n$.

Simplifying (5.3.1) we obtain

$$\frac{\partial^\alpha u(x_l, \tau_n)}{\partial \tau^\alpha} = \rho_\alpha \sum_{j=1}^{n} \beta_j (u_l^{n-j+1} - u_l^{n-j}) + \mathcal{O}(k). \tag{5.3.4}$$

It can be shown that, for $j = 1$ and $\alpha = 1$, (5.3.4) reduces to the classical backward finite difference formula.

The other derivative terms in (5.3.1) are approximated by

$$\frac{\partial u(x_l, \tau_n)}{\partial x} = \frac{u_{l+1}^n - u_{l-1}^n}{2h} + \mathcal{O}(h^2), \tag{5.3.5}$$

$$\frac{\partial^2 u(x_l, \tau_n)}{\partial x^2} = \frac{u_{l+1}^n - 2u_l^n + u_{l-1}^n}{h^2} + \mathcal{O}(h^2), \tag{5.3.6}$$

$$\frac{\partial b_f}{\partial \tau} = \frac{b_f^n - b_f^{n-1}}{k} + \mathcal{O}(k). \tag{5.3.7}$$

5.3.2 Construction of the numerical scheme

To obtain the full numerical scheme, we substitute (5.3.4), (5.3.5),(5.3.6) and (5.3.7) into (5.2.9). After simplifying, we obtain

for $n = 1$

$$au_{l-1}^1 + bu_l^1 + cu_{l+1}^1 - \left(\frac{b_f^1 - b_f^0}{b_f^1}\right)\frac{u_{l+1}^1 - u_{l-1}^1}{2h} = 0, \tag{5.3.8}$$

and for $n \geq 2$

$$au_{l-1}^n + bu_l^n + cu_{l+1}^n - \left(\frac{b_f^n - b_f^{n-1}}{b_f^n}\right)\frac{u_{l+1}^n - u_{l-1}^n}{2h} = \sum_{j=1}^{n-1} \varphi_j u_l^{n-j}, \tag{5.3.9}$$

where

$$\begin{aligned} a &= \chi_\alpha \left(\frac{\sigma^2\omega_\tau}{4h} - \frac{\theta_\tau \mu}{2h}\right), \\ b &= 1 - \chi_\alpha \left(\theta_\tau r - \frac{1}{2h}\sigma^2\omega_\tau\right), \\ c &= \chi_\alpha \left(\frac{\sigma^2\omega_\tau}{4h} + \frac{\theta_\tau \mu}{2h}\right), \end{aligned} \tag{5.3.10}$$

where

$$\chi_\alpha = k\rho_\alpha = \frac{1}{\Gamma(2-\alpha)}k^{1-\alpha}, \tag{5.3.11}$$

and

$$\varphi_j \quad = \quad \beta_j - \beta_{j+1},\ j = 1, 2, \cdots, n. \tag{5.3.12}$$

From boundary conditions in (5.2.10) we obtain

$$\frac{u_1^n - u_{-1}^n}{2h} = -b_f^n, \text{ and, } u_0^n = 1 - b_f^n. \tag{5.3.13}$$

Consider (5.2.9) for $x_0 = 0, \tau > 0$ and substitute (5.3.13) into (5.2.9) at $(0, \tau)$ to obtain

$$\frac{1}{2}\sigma^2\omega_\tau\frac{\partial^2}{\partial x^2}u(0,\tau) - \theta_\tau(\delta + \frac{\sigma^2}{2})b_f(\tau) + \theta_\tau r = 0, \tag{5.3.14}$$

with its central discretization given by

$$\frac{1}{2}\sigma^2\omega_\tau\frac{u_1^n - 2u_0^n + u_{-1}^n}{h^2} - \theta_\tau(\delta + \frac{\sigma^2}{2})b_f^n + \theta_\tau r = 0. \tag{5.3.15}$$

Equation (5.3.15) follow directly from the definition of a fractional derivative of a differentiable function $u(x, \tau)$ at $x = 0$.

Now (5.3.13) implies

$$u_0^n \quad = \quad 1 - b_f^n, \tag{5.3.16}$$

$$u_{-1}^n \quad = \quad u_1^n + 2hb_f^n. \tag{5.3.17}$$

After some algebraic manipulations, we obtain the following expression in terms of

u_1^n

$$u_1^n = \zeta + \gamma b_f^n;\ n \geq 1, \tag{5.3.18}$$

whereby

$$\zeta = \kappa(1 + \frac{h^2}{\sigma^2}r), \text{ and } \gamma = \kappa(1 + h + \frac{h^2}{2}),\ \text{ for } \kappa = -\frac{\theta_\tau}{\omega_\tau}. \tag{5.3.19}$$

Using scheme(5.3.8)-(5.3.9) for $l = 1$, and evaluating (5.3.19) at n^{th}- step, the free boundary b_f^n can be expressed as

$$b_f^n = \psi_{n-1} b_f^{n-1},\ 1 \leq n \leq N, \tag{5.3.20}$$

where

$$\psi_n = \frac{\zeta - (au_0^n + bu_1^n + cu_2^n - (u_2^n - u_0^n)/2h)}{(u_2^n - u_0^n)/2h + \gamma b_f^n}, \tag{5.3.21}$$

therefore the final schemes for u_l^n and b_f^n are given by

$$\begin{aligned}
b_f^n &= \psi_{n-1} b_f^{n-1}, && (5.3.22)\\
u_0^n &= 1 - b_f^n, && (5.3.23)\\
u_1^n &= \zeta - \gamma b_f^n;\ n \geq 1, && (5.3.24)\\
\bar{a}^n u_{l-1}^1 + b u_l^1 + \bar{c}^n u_{l+1}^1 &= \beta_1 u_l^0,\ l = 2, \cdots, L,\ n = 1, && (5.3.25)\\
\bar{a}^n u_{l-1}^n + b u_l^n + \bar{c}^n u_{l+1}^n &= \sum_{j=1}^{n-1} \varphi_j u_l^{n-j} + \beta_n u_l^0,\ l = 2, \cdots, L,\ n \geq 2, && (5.3.26)
\end{aligned}$$

for

$$\bar{a}^n = a + \frac{b_f^n - b_f^{n-1}}{2hb_f^n},\ b = 1 - \chi_\alpha \left(\theta_\tau r - \frac{1}{2h}\sigma^2\omega_\tau\right) \text{ and } \bar{c}^n = c - \frac{b_f^n - b_f^{n-1}}{2hb_f^n}, \tag{5.3.27}$$

with initial and boundary conditions

$$b_f^0 = 1,\ u_l^0 = max(1 - e^{-x}, 0),\ \text{with}\, u_0^0 = 0,\ \text{and}\, u_{L+1}^n = 0,\ \text{for}\ 0 \leq l \leq L+1 \quad (5.3.28)$$

The above scheme can be represented in the following tridiagonal matrix system

$$\mathbf{A}^1\mathbf{U}^1 = \beta_1\mathbf{U}^0, \qquad \text{for } n = 1, \quad (5.3.29)$$

and

$$\mathbf{A}^n\mathbf{U}^n = \varphi_1\mathbf{U}^{n-1} + \varphi_2\mathbf{U}^{n-2} + \cdots + \varphi_{n-1}\mathbf{U}^1, \qquad \text{for } n \geq 2, \quad (5.3.30)$$

where

$$\mathbf{A}^n = \begin{pmatrix} b & \hat{c}^2 & \cdots & \cdots & \cdots & 0 \\ \hat{a}^1 & b & \hat{c}^3 & \cdots & \cdots & 0 \\ 0 & \hat{a}^2 & b & \hat{c}^4 & \cdots & 0 \\ \vdots & \ddots & \ddots & \ddots & \ddots & \vdots \\ 0 & \cdots & \cdots & \hat{a}^{N-3} & b & \hat{c}^N \\ 0 & \cdots & \cdots & \cdots & \hat{a}^{N-1} & b \end{pmatrix},$$

and

$$\mathbf{U}^n = \left(u_1^n, u_2^n, \cdots, b_{L-1}^n\right)^T. \quad (5.3.31)$$

5.4 Analysis of the numerical method

In this section, we present theoretical results on the positivity and non-increasing spatial monotonicity properties of the numerical solution as well as those of the moving boundary which then establish the stability results. To begin, we show that the coefficients a, b, and c satisfy the two conditions in lemma 5.4.1 below.

5.4.1 Positivity of the solution and boundary conditions

Lemma 5.4.1. *The positivity conditions for the coefficients a, b, and c in the schemes (5.3.8) and (5.3.9), with regards to descritization stepsizes h and k are*

Cond. 1. $\frac{3\sigma^2}{2} \geq |r-\delta|$, *for any* $h>0$, *and*

Cond. 2. $k \leq \left(\tau^{1-\alpha}r - \frac{\sigma^2}{2h}\frac{\Gamma(1+\alpha)^2}{(T-\tau)^\alpha}\right)^{-\alpha}$.

Proof. From equation (5.3.14), the non-negativity of a, implies

$$\begin{aligned}
\frac{\sigma^2\omega_\tau}{4h} - \frac{\theta_\tau\mu}{2h} &= \frac{1}{4h}\left(\sigma^2\omega_\tau - 2\theta_\tau\mu\right), \\
&= \frac{1}{4h}\left(\sigma^2\omega_\tau - 2\theta_\tau\mu\right), \\
&= \frac{1}{4h}\left(\sigma^2\omega_\tau - 2\theta_\tau\mu\right), \\
&= \frac{\Gamma(1+\alpha)\Gamma(2-\alpha)}{4h(T-\tau)^{1-\alpha}}\left(\sigma^2 - \left((r-\delta) - \frac{\sigma^2}{2}\right)\right), \\
&= \frac{\Gamma(1+\alpha)^2}{4h(T-\tau)^{1-\alpha}}\left(\sigma^2 - \left((r-\delta) - \frac{\sigma^2}{2}\right)\right) > 0. \qquad (5.4.1)
\end{aligned}$$

therefore the positivity condition for coefficient a is that

$$\frac{3\sigma^2}{2} \geq r-\delta, \text{ for any } h>0, \qquad (5.4.2)$$

whereas for b, we have

$$\begin{aligned}
1 - k^\alpha\Gamma(2-\alpha)\left(\frac{\tau^{1-\alpha}}{\Gamma(2-\alpha)}r - \frac{\sigma^2}{2h}\frac{\Gamma(1+\alpha)}{(T-\tau)^\alpha}\right) &\geq 0, \\
1 &\geq k^\alpha\left(\tau^{1-\alpha}r - \frac{\sigma^2}{2h}\frac{\Gamma(1+\alpha)^2}{(T-\tau)^\alpha}\right). \qquad (5.4.3)
\end{aligned}$$

Therefore the positivity condition for b is that

$$k \leq \left(\tau^{1-\alpha}r - \frac{\sigma^2}{2h}\frac{\Gamma(1+\alpha)^2}{(T-\tau)^\alpha}\right)^{-\alpha}, \qquad (5.4.4)$$

and the positivity of c follows directly from (5.3.14) when

$$\frac{3\sigma^2}{2} \leq r - \delta, \text{ for any } h > 0. \tag{5.4.5}$$

To establish results on positivity of the numerical solution u_l^n and the moving boundary b^n, we propose lemma 5.4.2 and its proof together with other subsequent results therein leads to the desired positivity results.

Lemma 5.4.2. *Let $\{u_l^n, b_f^n\}$ be the numerical solution to the scheme (5.3.22)-(5.3.26) for the American put option problem in (5.2.9) and let ψ_n be defined as in (5.3.21). Then from lemma 5.4.1, for any $h > 0$ we obtain that*

1). For every fixed n,

$$0 < \psi_n \leq 1. \tag{5.4.6}$$

2). $u_l^n \geq u_{l+1}^n$ for $l = 0, \cdots, L; n = 0, \cdots, N-1$.

3). $u_l^n \geq 0$ for $l = 0, \cdots, L-1; n = 0, \cdots, N-1$.

Proof. Given $n = 0$, then from initial conditions in (5.3.28), we have $u_l^0 \geq 0$ and $b_f^0 \geq 0$, and from (5.3.19), (5.3.21), (5.3.27) and *Cond.*1. of lemma 5.4.1, we obtain

$$0 \leq \psi_0 = \frac{\zeta}{\gamma} \leq 1, \tag{5.4.7}$$

since

$$\lim_{h\to 0} \frac{\zeta}{\gamma} = \lim_{h\to 0} \frac{\kappa}{\kappa} \left(\frac{1 + \frac{h^2}{\sigma^2} r}{1 + h + \frac{h^2}{2}} \right) = 1. \tag{5.4.8}$$

Note that, from (5.3.22)-(5.3.24) and (5.4.7) we have

$$0 < b_f^1 = \psi_0 b_f^0 \leq 1, \tag{5.4.9}$$

$$u_0^1 = 1 - \psi_0 \geq 0, \tag{5.4.10}$$

$$u_1^1 = \zeta - \gamma b_f^1 = \zeta - \gamma\psi_0 = \zeta - \gamma\frac{\zeta}{\gamma} = 0, \tag{5.4.11}$$

and from (5.3.25) and (5.3.28) we have $u_j^1 \geq 0$ for all $j = 2, \cdots, L$.

Now

$$\begin{aligned} \psi_1 &= \frac{\zeta - (au_0^1 + cu_2^1 - (u_2^1 - u_0^1)/2h)}{(u_2^1 - u_0^1)/2h + \gamma b_f^1}, \\ &= \frac{\zeta - (a - 1/2h)u_0^1}{\gamma b_f^1}, \\ &= 1 - a\kappa\frac{h + h^2(1/2 - r/\sigma^2)}{1/2 + h(3/4 + r/2\sigma^2) + \mathcal{O}(h^2))}, \end{aligned} \tag{5.4.12}$$

which implies $0 < \psi_1 \leq 1$.

To show that $u_2^2 = 0$, we consider (5.3.26) for $n = 2$ and $l = 2$, which give

$$\bar{a}^2 u_1^2 + bu_2^2 + \bar{c}^2 u_3^2 = \sum_{j=1}^{1} \varphi_j u_2^0 + \beta_2 u_2^0 = 0,$$

which implies

$$bu_2^2 = -\bar{a}^2(u_3^2 - u_1^2) = 0. \tag{5.4.13}$$

Since $\bar{a}^2$ and b are positive we have $u_2^2 = 0$, hence

$$0 < \psi_2 \leq 1.$$

Let $n > 2$ and by induction hypothesis, we assume the conclusions holds true for $n-1$, such that

$$0 < \psi_{n-1} \leq 1, \quad u_l^{n-1} \geq 0, \quad u_l^{n-1} \geq u_{l+1}^{n-1}. \tag{5.4.14}$$

Now let us define

$$p_n = \kappa\left(1 + \frac{h^2}{\sigma^2}r\right) + \frac{u_0^n - u_2^n}{2h} - au_0^n - bu_1^n - cu_2^n, \tag{5.4.15}$$

and

$$d_n = \frac{u_2^n - u_0^n}{2h} + \kappa\left(1 + h + \frac{h^2}{2}\right)b_f^n, \tag{5.4.16}$$

which yields

$$\psi_n = \frac{p_n}{d_n}.$$

When $l = 2$, combining the Taylor expansion of (5.3.14) with (5.4.15) coupled with the value matching and smooth pasting conditions ((5.2.11) and (5.2.12)), we obtain

$$u_2^n = \kappa\left(\frac{\sigma^2 + 2rh^2}{\sigma^2} - \frac{(2 + 2h + h^2)}{2}b_f^n\right) + \mathcal{O}(h^3). \tag{5.4.17}$$

Using (5.3.16), (5.3.18) and (5.4.17) in (5.4.15) we obtain

$$\begin{aligned} p_n &= \kappa\left(\frac{\sigma^2 + rh^2}{\sigma^2}\right)(1 - b - c) + \left(\frac{1 - 2ha}{2h}\right)(1 - b_f^n) \\ &\quad + \left(\frac{1 - 2hb\kappa - 2hc\kappa}{2h}\right)\left(\frac{2 + 2h + h^2}{2}\right)b_f^n, \end{aligned} \tag{5.4.18}$$

and

$$d_n = \frac{\kappa\left(\sigma^2 + 2rh^2\right)}{2h\sigma^2} + \frac{b_f^n - 1}{2h} + \left(\frac{2h - 1}{2h}\right)\left(\frac{2 + 2h + h^2}{2}\right)\kappa b_f^n. \tag{5.4.19}$$

To show the positivity of the solution $\{u^n\}$ and consequently that of ψ_n as well as it's boundedness, it suffices to show that, the coefficients $\bar{a}^n$ and $\bar{c}^n$ in (5.3.27) are positive.

The coefficients are positive because

$$\bar{a}^n = a + \frac{b_f^n - b_f^{n-1}}{2hb_f^n} = a + \frac{1 - \frac{1}{\psi_{n-1}}}{2h} = a + \frac{\psi_{n-1} - 1}{2h\psi_{n-1}} = a - \frac{1 - \psi_{n-1}}{2h\psi_{n-1}}, \tag{5.4.20}$$

and by induction assumption $0 < \psi_{n-1} \leq 1$, then $0 < 1 - \psi_{n-1} \leq 0$, we obtain

$$\bar{a}^n = a + \frac{b_f^n - b_f^{n-1}}{2hb_f^n} = a - \frac{1 - \psi_{n-1}}{2h\psi_{n-1}} \geq 0. \tag{5.4.21}$$

Similarly, for $\bar{c}^n$ we have

$$\bar{c}^n = c - \frac{b_f^n - b_f^{n-1}}{2hb_f^n} = c + \frac{1 - \psi_{n-1}}{2h} \geq c \geq 0, \tag{5.4.22}$$

therefore

$$0 < \psi_n \leq 1.$$

Moreover, the solution $\{u_l^n\}$ is an increasing function of l since a put option become worthless as it approach maturity.

The following theorem follows from the results above

Theorem 5.4.3. *Under the assumptions of lemma 5.4.2, the scheme (5.3.22)-(5.3.26) guarantees the following properties about the free boundary condition and the numerical solution*

i. monotonicity and positivity of b_f^n, $n = 0, \cdots, N$;

ii. monotonicity and positivity of the solution $u^n = (u_0^n, \cdots, u_l^n)$ *for* $n = 0, \cdots, N$.

5.4.2 Stability and consistency analysis

In this section, we study the stability and consistency properties of the scheme (5.3.22)-(5.3.26).

Numerical stability

We note that

Definition 5.4.4. *The numerical scheme (5.3.22)-(5.3.26) with initial and boundary conditions (5.2.10) is said to be $\|.\|_\infty$ stable in the fixed domain $[0, x_\infty] \times [0, T]$, if for every partition with $k = 1/N$, $h = 1/L$ and $(L+1)h = x_\infty$,*

$$\|u^n\| \leq M,\ 0 \leq n \leq N, \tag{5.4.23}$$

where $\|.\|_\infty$ is the supremum norm and M some constant independent of h, k and N.

Theorem 5.4.5. *Under assumptions of lemma 5.4.2, the numerical scheme (5.3.22)-(5.3.26) for solving the tfBS PDE (5.2.9) is $\|.\|_\infty$-stable.*

Proof. Since for each fixed n, the sequence of solutions u_l^n is non-increasing with respect to l, then according to the boundary condition (5.3.23) and based on the positivity results of b_f^n established under lemma 5.4.1, we get

$$\|u^n\|_\infty = u_0^n = 1 - b_f^n < 1,\ 0 \leq n \leq N. \tag{5.4.24}$$

therefore the numerical scheme (5.3.22)-(5.3.26) is $\|.\|_\infty$-stable.

Consistency of the numerical schemes

To analyze for numerical consistency of a numerical scheme to a partial differential equation, one look at how well the numerical solution approximate the exact theoretical solution as the discretization stepsizes approach zero ([86]). In our case however, on top

of matching the behaviour of the numerical scheme (5.3.25)-(5.3.26) to the tfBS PDE (5.2.9), we also extend the approach to the moving boundary condition (5.2.11)-(5.2.12) with its numerical scheme (5.3.20).

To assess the numerical consistency of the scheme (5.3.25)-(5.3.26) we first define $\hat{u}_l^n = u(x_l, \tau_n)$ and $\hat{b}_f^n = b_f(\tau_n)$ as the exact solutions to the tfBS PDE (5.2.9) and moving boundary at time τ_n, respectively. As follow, redefine the scheme to (5.2.9)

$$\begin{aligned} S(u_l^n, b_f^n) &= \rho_\alpha \sum_{j=1}^{n} \beta_j \left(u_l^{n-j+1} - u_l^{n-j}\right) - \theta_\tau \left(r u_l^n - \mu \frac{u_{l+1}^n - u_{l-1}^n}{2h}\right) \\ &\quad + \omega_\tau \frac{1}{2}\sigma^2 \left(\frac{u_{l+1}^n - 2u_l^n + u_{l-1}^n}{h^2}\right) \\ &\quad - \left(\frac{b_f^n - b_f^{n-1}}{k b_f}\right) \frac{u_{l+1}^n - u_{l-1}^n}{2h}. \end{aligned} \tag{5.4.25}$$

The scheme (5.4.25) is consistent with equation (5.4.26) below

$$F(u, b_f) = \frac{\partial^\alpha u}{\partial \tau^\alpha} - \theta_\tau \left(r u - \mu \frac{\partial u}{\partial x}\right) + \omega_\tau \frac{1}{2}\sigma^2 \frac{\partial^2 u}{\partial x^2} - \frac{b_f'}{b_f}\frac{\partial u}{\partial x} = 0, \tag{5.4.26}$$

if the local truncation error is given by

$$\begin{aligned} T_l^n(\hat{u}_l, \hat{b}_f^n) &= S(\hat{u}_l, \hat{b}_f^n) - F(\hat{u}_l, \hat{b}_f^n), \\ &= \rho_\alpha \sum_{j=1}^{n} \beta_j \left(u_l^{n-j+1} - u_l^{n-j}\right) - \frac{\partial^\alpha u}{\partial \tau^\alpha} - \theta_\tau \mu \left(\frac{u_{l+1}^n - u_{l-1}^n}{2h} - \frac{\partial u}{\partial x}\right) \\ &\quad + \omega_\tau \frac{1}{2}\sigma^2 \left(\frac{u_{l+1}^n - 2u_l^n + u_{l-1}^n}{h^2} - \frac{\partial^2 u}{\partial x^2}\right) \\ &\quad - \frac{1}{b_f}\left(\left(\frac{b_f^n - b_f^{n-1}}{k}\right) \frac{u_{l+1}^n - u_{l-1}^n}{2h} + b_f' \frac{\partial u}{\partial x}\right), \end{aligned} \tag{5.4.27}$$

such that

$$\lim_{h,k \to 0} T_l^n(\hat{u}, \hat{b}_f^n) = 0. \tag{5.4.28}$$

Suppose $u(x, \tau)$ is α-differentiable up to order 2α $(0 < \alpha \leq 1)$ in time, and differ-

entiable up to order four in space then, applying the generalised Taylor expansion of $T_l^n(\hat{u}, \hat{b}_f^n)$ about (x_l, τ_n) yield

$$\begin{aligned} T_l^n(\hat{u}_l, \hat{b}_f^n) &= k^\alpha R_l^n(1) - \theta_\tau \mu h^2 R_l^n(2) + \omega_\tau \frac{1}{2}\sigma^2 h^2 R_l^n(3) + k R_l^n(4)\frac{\partial u}{\partial x}(x_l, \tau_n) \\ &\quad + h^2 R_l^n(2)\frac{1}{\hat{b}_f^n}\frac{db_f}{d\tau}(\tau_n) - k h^2 R_l^n(4) R_l^n(2), \end{aligned} \tag{5.4.29}$$

where

$$\left.\begin{aligned} R_l^n(1) &= \tfrac{1}{(2\alpha)!}\tfrac{\partial^{2\alpha} u}{\partial \tau^{2\alpha}}(x_l, \tau_n), \quad R_l^n(2) = \tfrac{1}{6}\tfrac{\partial^3 u}{\partial x^3}(x_l, \tau_n), \\ R_l^n(3) &= \tfrac{1}{12}\tfrac{\partial^4 u}{\partial x^4}(x_l, \tau_n), \quad R_l^n(4) = \tfrac{k}{2\hat{b}_f}\tfrac{d^2 b_f}{d\tau^2}(\tau_n). \end{aligned}\right\} \tag{5.4.30}$$

From (5.4.29)-(5.4.30) we observe that the local truncation error of the numerical scheme (5.3.25)-(5.3.26) for the tfBS-PDE (5.2.9) is of order $\mathcal{O}(k)$ in time and $\mathcal{O}(h^2)$ in space.

To complete the consistency analysis of the solution of the free boundary, we rewrite the boundary conditions (5.2.11)-(5.2.12) and (5.3.14) in the following form

$$\begin{aligned} F_1(u, b_f) &= \frac{\partial v}{\partial x}(0, \tau) + b_f(\tau) = 0, \\ F_2(u, b_f) &= u(0, \tau) + b_f(\tau) - 1 = 0, \\ F_3(u, b_f) &= \frac{1}{2}\sigma^2 \omega_\tau \frac{\partial^2}{\partial x^2} u(0, \tau) - \theta_\tau \left(\delta + \frac{\sigma^2}{2}\right) b_f(\tau) + \theta_\tau r = 0, \end{aligned} \tag{5.4.31}$$

and their respective numerical approximations are as follow

$$\begin{aligned} S_1(u, b_f) &= \frac{u_1^n - u_{-1}^n}{2h} + b_f^n = 0, \\ S_2(u, b_f) &= u_0^n + b_f^n - 1 = 0, \\ S_3(u, b_f) &= \frac{1}{2}\sigma^2 \omega_\tau \frac{u_1^n - 2u_0^n + u_{-1}^n}{h^2} - \theta_\tau \left(\delta + \frac{\sigma^2}{2}\right) b_f^n + \theta_\tau r = 0. \end{aligned} \tag{5.4.32}$$

Using Taylor expansion it is trivial to show that

$$\begin{aligned} T_1(u, b_f) &= S_1(u, b_f) - F_1(u, b_f) = 0, \\ T_2(u, b_f) &= S_2(u, b_f) - F_2(u, b_f) = \mathcal{O}(h^2), \\ T_3(u, b_f) &= S_3(u, b_f) - F_3(u, b_f) = \mathcal{O}(h^2). \end{aligned} \tag{5.4.33}$$

therefore the local truncation error for the boundary condition is of order $\mathcal{O}(h^2)$ in space. The above observations suffice as proof to the following results.

Theorem 5.4.6. *Suppose the solution $u(x, \tau)$ to the tfBS-PDE (5.2.9) with initial and boundary conditions (5.2.10)-(5.2.14) is α-differentiable up to order 2α in time as well as differentiable up to order four in space, then, the numerical solution obtained via the scheme(5.3.22)-(5.3.26) is consistent with the tfBS-PDE (5.2.9) with initial and boundary conditions (5.2.10)-(5.2.14). therefore from the Lax equivalence theorem, the scheme converges and is second-order accurate in space as well as first-order accurate in time.*

5.5 Numerical experiments

Example 5.5.1. *Consider an American put option with the following market parameters $\delta = 0.02 \,\&\, 0.2$, $r = 0.10$, $\sigma = 0.02$, and $K = 150$.*

Graphical results are presented in the following figures.

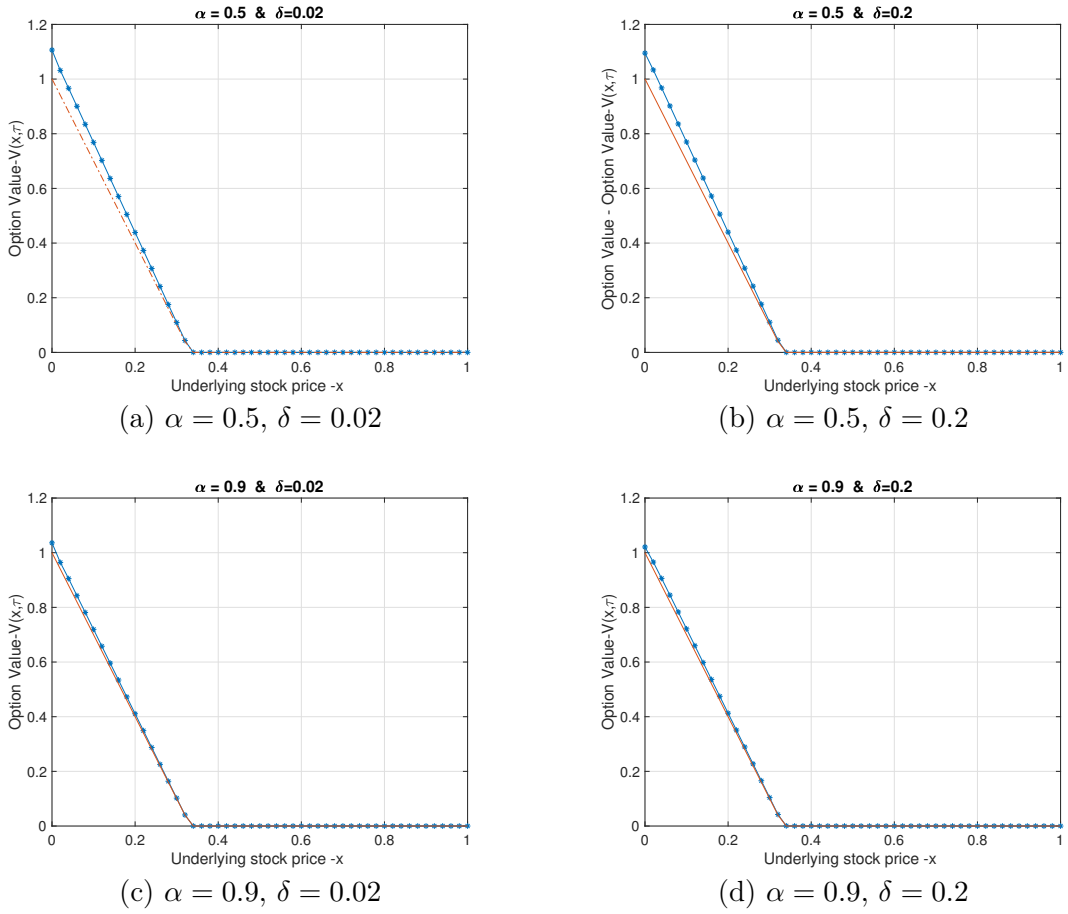

(a) $\alpha = 0.5$, $\delta = 0.02$

(b) $\alpha = 0.5$, $\delta = 0.2$

(c) $\alpha = 0.9$, $\delta = 0.02$

(d) $\alpha = 0.9$, $\delta = 0.2$

Figure 5.5.1: American put option maturity payoffs for $\alpha = 0.5$ and $\alpha = 0.9$ at different dividend yields.

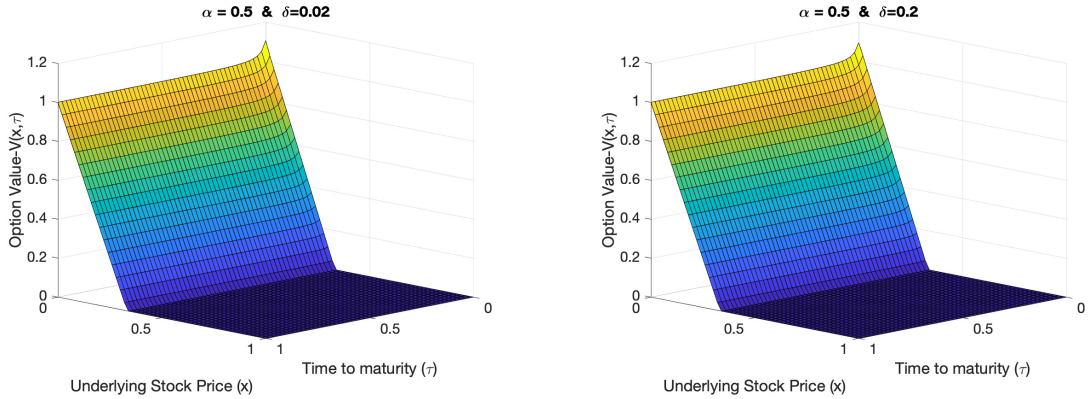

(a) $\alpha = 0.5$, $\delta = 0.02$ (b) $\alpha = 0.5$, $\delta = 0.2$

(c) $\alpha = 0.9$, $\delta = 0.02$ (d) $\alpha = 0.9$, $\delta = 0.2$

Figure 5.5.2: American put option general payoffs for $\alpha = 0.5$ and $\alpha = 0.9$ at different dividend yields.

Results from fig. 5.5.1 through to fig. 5.5.2 suggest that the approach is more effective for larger values of α ($\alpha > 0.5$). This is not surprising because $\alpha > 0.5$ represent the case when the underlying stock increments are persistently positively correlated.

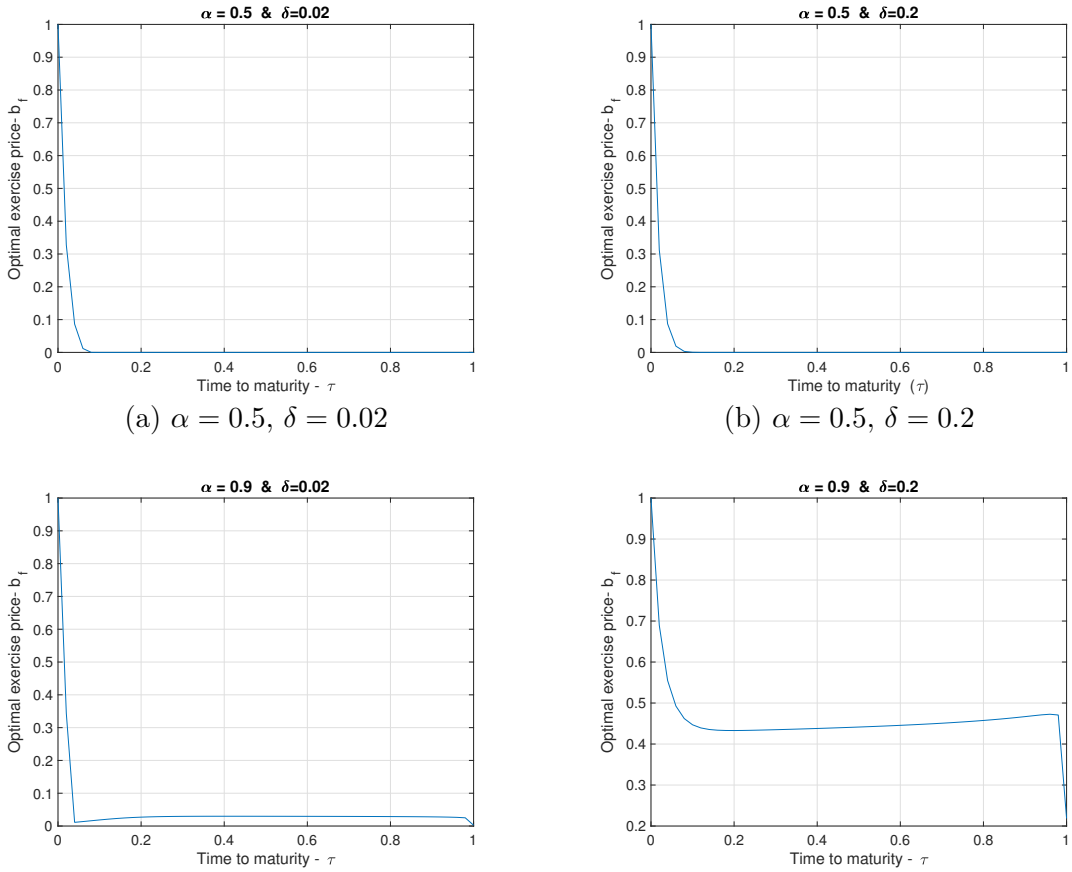

(a) $\alpha = 0.5$, $\delta = 0.02$ (b) $\alpha = 0.5$, $\delta = 0.2$

(c) $\alpha = 0.9$, $\delta = 0.02$ (d) $\alpha = 0.9$, $\delta = 0.2$

Figure 5.5.3: American put option exercise boundaries for $\alpha = 0.5$ and $\alpha = 0.9$ at different dividend yields.

Figure 5.5.3 above show the early exercise boundaries for the four considered combinations of α and δ. It is evident from the results that, the option holder must keep track of specific points in time and for a specific price of the stock to maximise the benefit of holding these specific stock options. Tabular results are presented in the following tables.

Table 5.5.1: Maximum absolute errors for example 5.5.1 with $r = 0.10$ and $\delta = 0.02$.

α	$N = 10$	$N = 20$	$N = 40$	$N = 80$	$N = 160$	$N = 320$
0.1	4.6360e-02	2.3559e-02	1.1972e-02	5.9859e-03	2.9929e-03	1.4965e-03
0.2	4.7227e-02	2.4000e-02	1.2196e-02	6.0979e-03	3.0490e-03	1.5245e-03
0.3	4.7745e-02	2.4263e-02	1.2330e-02	6.1648e-03	3.0824e-03	1.5412e-03
0.4	4.8015e-02	2.4400e-02	1.2399e-02	6.1997e-03	3.0999e-03	1.5499e-03
0.5	4.8093e-02	2.4440e-02	1.2420e-02	6.2098e-03	3.1049e-03	1.5524e-03
0.6	4.7972e-02	2.4378e-02	1.2388e-02	6.1941e-03	3.0971e-03	1.5485e-03
0.7	4.7591e-02	2.4184e-02	1.2290e-02	6.1449e-03	3.0724e-03	1.5362e-03
0.8	4.6903e-02	2.3835e-02	1.2112e-02	6.0561e-03	3.0280e-03	1.5140e-03
0.9	4.5976e-02	2.3364e-02	1.1873e-02	5.9363e-03	2.9682e-03	1.4841e-03
1.0	4.5000e-02	2.2838e-02	1.1621e-02	5.8104e-03	2.9052e-03	1.4526e-03

Table 5.5.2: Convergence rates for example 5.5.1 with $r = 0.10$ and $\delta = 0.02$.

α	$N = 10$	$N = 20$	$N = 40$	$N = 80$	$N = 160$
0.1	0.98	0.98	1.00	1.00	1.00
0.2	0.98	0.98	1.00	1.00	1.00
0.3	0.98	0.98	1.00	1.00	1.00
0.4	0.98	0.98	1.00	1.00	1.00
0.5	0.98	0.98	1.00	1.00	1.00
0.6	0.98	0.98	1.00	1.00	1.00
0.7	0.98	0.98	1.00	1.00	1.00
0.8	0.98	0.98	1.00	1.00	1.00
0.9	0.98	0.98	1.00	1.00	1.00
1.0	0.98	0.98	1.00	1.00	1.00

Table 5.5.3: Maximum absolute errors for example 5.5.1 with $r = 0.10$ and $\delta = 0.2$.

α	$N = 10$	$N = 20$	$N = 40$	$N = 80$	$N = 160$	$N = 320$
0.1	4.6168e-02	2.3471e-02	1.1922e-02	5.9611e-03	2.9806e-03	1.4903e-03
0.2	4.6826e-02	2.3806e-02	1.2092e-02	6.0462e-03	3.0231e-03	1.5115e-03
0.3	4.7119e-02	2.3924e-02	1.2168e-02	6.0839e-03	3.0420e-03	1.5210e-03
0.4	4.7151e-02	2.3951e-02	1.2176e-02	6.0881e-03	3.0440e-03	1.5220e-03
0.5	4.7002e-02	2.3865e-02	1.2138e-02	6.0688e-03	3.0344e-03	1.5172e-03
0.6	4.6728e-02	2.3726e-02	1.2067e-02	6.0335e-03	3.0167e-03	1.5084e-03
0.7	4.6370e-02	2.3564e-02	1.1975e-02	5.9873e-03	2.9936e-03	1.4968e-03
0.8	4.5954e-02	2.3323e-02	1.1867e-02	5.9336e-03	2.9668e-03	1.4834e-03
0.9	4.5496e-02	2.3108e-02	1.1749e-02	5.8744e-03	2.9372e-03	1.4686e-03
1.0	4.5000e-02	2.2838e-02	1.1621e-02	5.8104e-03	2.9052e-03	1.4526e-03

Table 5.5.4: Convergence rates for example 5.5.1 with $r = 0.10$ and $\delta = 0.2$.

α	$N = 10$	$N = 20$	$N = 40$	$N = 80$	N= 160
0.1	0.98	0.98	1.00	1.00	1.00
0.2	0.98	0.98	1.00	1.00	1.00
0.3	0.98	0.98	1.00	1.00	1.00
0.4	0.98	0.98	1.00	1.00	1.00
0.5	0.98	0.98	1.00	1.00	1.00
0.6	0.98	0.98	1.00	1.00	1.00
0.7	0.98	0.98	1.00	1.00	1.00
0.8	0.98	0.98	1.00	1.00	1.00
0.9	0.98	0.98	1.00	1.00	1.00
1.0	0.98	0.98	1.00	1.00	1.00

To illustrate the order of convergence in the space direction, we fixed $N = 30$ for varying N and obtain the following results.

Table 5.5.5: Maximum absolute errors for Example 5.5.1 with $r = 0.10$ and $\delta = 0.2$. for a fixed N.

α	$M = 30$	$M = 60$	$M = 120$	$M = 240$	$M = 480$
0.1	7.6512e-02	1.9962e-02	5.1892e-03	1.3597e-03	3.4953e-04
0.2	6.7988e-03	1.8944e-02	5.0170e-03	1.2673e-03	3.1784e-04
0.3	6.2147e-02	1.7191e-02	4.3368e-03	1.0940e-03	2.7652e-04
0.4	5.7443e-02	1.4701e-02	4.0358e-03	1.0137e-03	2.5926e-04
0.5	5.3746e-02	1.4566e-02	2.7993e-03	7.0810e-04	1.7202e-04
0.6	4.0893e-02	1.0948e-02	2.6167e-03	6.7192e-04	1.6889e-04
0.7	4.0773e-02	1.0880e-02	2.4898e-03	6.1752e-04	1.5688e-04
0.8	4.0318e-02	1.0498e-02	2.3779e-03	6.0115e-04	1.5576e-04
0.9	4.0499e-02	1.0338e-02	2.4355e-03	6.0039e-04	1.5495e-04
1.0	4.0328e-02	1.0295e-02	2.4246e-03	5.9881e-04	1.5047e-04

Table 5.5.6: Convergence rates for Example 5.5.1 with $r = 0.10$ and $\delta = 0.2$ for a fixed N.

α	$M = 30$	$M = 60$	$M = 120$	$M = 240$
0.1	1.95	1.88	1.99	1.98
0.2	1.96	1.88	1.99	1.98
0.3	1.96	1.98	1.99	1.98
0.4	1.96	1.98	1.99	1.98
0.5	1.97	1.98	1.99	1.98
0.6	1.97	1.98	1.99	1.98
0.7	1.97	1.98	1.99	1.98
0.8	1.97	1.98	1.99	1.98
0.9	1.97	1.98	1.99	1.98
1.0	1.97	1.98	1.99	1.98

The maximum norm errors presented in table 5.5.1, table 5.5.3 and table 5.5.5 above indicates that, the numerical method converges for all α values. These observations validates our theoretical observations that, the method is indeed convergent. It can also be observed from table 5.5.2, table 5.5.4 and table 5.5.6 above, that, in all possible states of the world (parameterisation), the method converges up to first-order in time as well as second order in space.

5.6 Summary and discussions

Over the past decade, the financial literature has proposed a multitude of different models to capture the dynamics of financial assets. The use of fractal processes and models based on these processes has proven to be an excellent tool that strikes the right balance between capturing the desired properties of stock price evolution and mathematical tractability. Though the mathematical complexity of these models may pose some serious challenges in terms of designing analytical solutions, in this chapter we demonstrate that numerical techniques can save the day when using the approach to price nonlinear American option problems.

In this chapter, a front-fixing method for American put option was considered. Our results indicate that the numerical scheme is stable under the stability and positivity

conditions presented in Lemma 5.4.1 and Lemma 5.4.2. In addition to positivity and monotonicity of solution, we also demonstrate and confirm via numerical results in fig. 5.5.3 that the associated free boundaries are also positive and monotone. Over all our results suggest that the approach is very robust, effective and efficient for pricing American put option for when the order of the fractional derivative $\alpha > 0.5$. This is not surprising because $\alpha > 0.5$ represent the case when increments of the underlying stock process are persistently and positively correlated. This in essence justify our prior assumption that, indeed stock markets have memory.

In the next chapter, we present an investigation on the pricing of double barrier options under a time-fractional Black-Scholes setup. Furthermore, a corresponding high order numerical method (both in time and space) to the resultant fractional model is proposed.

Chapter 6

A Robust Numerical Method for a Time Fractional Black-Scholes Equation for Pricing Double Barrier Options

This chapter presents an investigation on the numerical pricing of double barrier options. Herein we focus on those options written on underlying asset(s) whose dynamics are governed by a non-standard fractal stochastic processes. The resultant model is of a time fractional nature referred to as a time-fractional Black-Scholes equation. We extend the concept of double barrier options pricing in a time-fractional Black-Scholes scope. A robust numerical scheme is implemented and its' stability and convergence properties are studied. Results suggest that, the numerical method is unconditionally stable and and converges with order $\mathcal{O}(h^4 + k^2)$. To substantiate the theoretical findings, we further present some numerical experiments on pricing of double knock-in barrier option problems.

6.1 Introduction

After the discovery of fractal features of financial markets, alot of efforts has been dedicated to finding accurate and stable numerical methods for solving the already involved asset pricing fractional differential equations. In the chapter we suggest a numerical scheme for solving a double barrier option pricing governed by time-fractional Black-Scholes equation. The time-fractional derivative in the model helps in capturing the time-decaying effects of the underlying asset and also in capturing the global nature of the change in underlying asset price as well as the involved barriers.

The underlying motivation for pricing double barrier options via the time-fractional Black-Scholes framework is justified by the evidence of "long memory" in the time direction observed in many assets time series, see for example ([84, 57, 59]). Its has been substantiated, see for example [25], that the long decay in the underlying asset in the time direction does not deteriorate the no-arbitrage constraints of asset pricing theory, which may invalidate herein.

The combination of time-fractional Black-Scholes and double barriers conditions in this chapter, adds on an additional degrees of complexity in the design of solution(s) to the model. Albeit the complexity involved, we designed a new robust numerical scheme for solving time-fractional Black-Scholes model for pricing discrete-monitored double-barrier European options. This chapter therefore present an efficient numerical scheme for solving a time-fractional Black-Scholes model for pricing discrete double barrier option problems.

The rest of this chapter is organised as follow, Section 6.2 present the model under consideration, while Section 6.3, present the detailed construction of the numerical scheme. A comprehensive theoretical analysis of the method in terms of convergence and stability is presented in Section 6.4. Two practical examples on the use of the approach for pricing double knock-in European put stock options can be found in Section 6.5. And lastly, Section 6.6 present some concluding remarks and set the scope for future research.

6.2 Model

To the best of our knowledge there is limited number of literature on the subject of high order solution schemes for barrier options pricing time-fractional Black-Scholes PDEs as the topic is still quite relatively new and limited to vanilla option problems. In this chapter, we will consider the following time fractional Black-Scholes (tfBS)-PDE for pricing double barrier put options

$$\left.\begin{array}{l} \frac{\partial^\alpha v}{\partial t^\alpha} = \left(rv - (r-\delta)\frac{S\partial v}{\partial S}\right)\frac{t^{1-\alpha}}{\Gamma(2-\alpha)} - \frac{\sigma^2\Gamma(1+\alpha)}{2}\frac{S^2\partial^2 v}{\partial S^2},\ 0<\alpha<1, \\ \\ B_l \le S \le B_u, t \in (0,T), \\ v(B_l,t) = R_l,\ V(B_u,t) = R_u, \end{array}\right\} \tag{6.2.1}$$

whereby B_l and B_u are the lower and upper knock-out barriers with R_l and R_u denoting the respective rebates paid when the corresponding barriers are hit, while r represent the risk-free interest rate and δ the dividend yield paid by the underlying stock.

Using variable transform ($\tau = T - t$) time to maturity, we obtain the following initial value problem (IVP)

$$\tau^{\alpha-1}(T-\tau)^{1-\alpha}\frac{\partial^\alpha v}{\partial \tau^\alpha} - \left(\frac{rv}{\Gamma(2-\alpha)} - (r-\delta)S^\alpha\frac{\partial^\alpha v}{\partial S^\alpha}\right)(T-\tau)^{1-\alpha} + \frac{\Gamma(1+\alpha)\sigma^2S^2}{2}\frac{\partial^2 v}{\partial S^2} = 0,$$

which simplifies to

$$\frac{\partial^\alpha v}{\partial \tau^\alpha} - \left(\frac{rv}{\Gamma(2-\alpha)} - (r-\delta)S\frac{\partial v}{\Gamma(2-\alpha)\partial S}\right)\tau^{1-\alpha} + \frac{\Gamma(1+\alpha)\sigma^2S^2}{2}\frac{\partial^2 v}{\partial S^2} = 0, \quad 0<\alpha<1, \tag{6.2.2}$$

with initial and boundary conditions

$$\left.\begin{aligned} &S \in (B_l, B_u)\,, \\ &\tau \in (T, 0)\,, \\ &v\,(B_l, \tau) = R_l,\ v\,(B_u, \tau) = R_u. \end{aligned}\right\} \tag{6.2.3}$$

Considering the following change of variables $x = ln(S)$ and $v(x,\tau) = e^{r\tau}v(S,\tau)$ and without loss of notations, after simplification we obtain

$$\frac{\partial^\alpha v(x,\tau)}{\partial \tau^\alpha} = \left(\frac{rv(x,\tau)}{\Gamma(2-\alpha)} - (r-\delta)x\frac{\partial v(x,\tau)}{\Gamma(2-\alpha)\partial x}\right)\tau^{1-\alpha} - \frac{\Gamma(1+\alpha)\sigma^2x^2}{2}\frac{\partial^2 v}{\partial S^2}, \quad 0<\alpha<1, \tag{6.2.4}$$

with the following initial and barrier conditions

$$\left.\begin{aligned} &v(x,0) = \max(K - e^x, 0),\ 0 < \tau < T, \\ &v\,(b_l, \tau) = r_l,\ v\,(b_u, \tau) = r_u,\ \ b_l < x < b_u. \end{aligned}\right\} \tag{6.2.5}$$

6.3 Numerical scheme

This section present the construction of the involved numerical scheme in solving (6.2.4) subject to initial and barrier conditions (6.2.5).

6.3.1 Model discretization

Let L and N be positive integers and define $h = (b_u - b_l)/L$ and $k = T/N$ the space and time step-sizes respectively. Denote $x_l = b_l + lh$; for $l = 0, 1, 2, ..., L$ and $\tau_n = nk$; $n = 0, 1, 2, ..., N$, such that $x_l \in [b_l, b_u]$ and $\tau_n \in [0, T]$. Furthermore, define $v_l^n = v(x_l, \tau_n)$ as the solution at the grid point $(x_l, \tau_n) = (b_l + lh, nk)$.

Temporal discretization

Let us define

$$\Delta_t v_l^n = \Delta_t v(x_l, \tau_n) = \frac{v(x_l, \tau_n) - v(x_l, \tau_{n-1})}{k^\alpha} = \frac{v_l^n - v_l^{n-1}}{k^\alpha}, \tag{6.3.1}$$

and discretize the time-fractional derivative in (6.2.4) at the grid point (x_l, τ_{n+1}) by the following quadrature formula

$$\begin{aligned} \frac{\partial^\alpha v(x_l, \tau_{n+1})}{\partial \tau^\alpha} &= \frac{k^{-\alpha}}{\Gamma(2-\alpha)} \sum_{j=0}^{n} \sigma_j \left(v(x_l, \tau_{n-j+1}) - v(x_l, \tau_{n-j}) \right) + \frac{\tau_n^{1-\alpha}}{\Gamma(2-\alpha)} k^2, \\ &= \frac{1}{\Gamma(2-\alpha)} \sum_{j=0}^{n} \sigma_j \Delta_t v(x_l, t_{n-j+1}) + \mathcal{O}(k^2), \end{aligned} \tag{6.3.2}$$

where

$$\sigma_j = (j+1)^{1-\alpha} - j^{1-\alpha},\ j = 0, 1, 2, \cdots, n, \tag{6.3.3}$$

such that, $1 = \sigma_0 > \sigma_1 > \sigma_2 > \cdots > \to 0$ as $j \to n$.

Spatial discretization

We approximate the spatial derivatives in (6.2.4) as follow

$$\frac{\partial v(x_l, \tau_{n+1})}{\partial x} = \frac{v(x_{l+1}, \tau_{n+1}) - v(x_{l-1}, \tau_{n+1})}{2h} - \frac{h^2}{6} \frac{\partial^3 v(x_l, \tau_{n+1})}{\partial x^3} + \mathcal{O}(h^4), \tag{6.3.4}$$

and

$$\begin{aligned} \frac{\partial^2 v(x_l, \tau_{n+1})}{\partial x^2} &= \frac{v(x_{l+1}, \tau_{n+1}) - 2v(x_l, \tau_{n+1}) + v(x_{l-1}, \tau_{n+1})}{h^2} - \frac{h^2}{12} \frac{\partial^4 v(x_l, \tau_{n+1})}{\partial x^4} \\ &\quad + \mathcal{O}(h^4). \end{aligned} \tag{6.3.5}$$

6.3.2 The full scheme

To obtain the full numerical scheme we substitute (6.3.2), (6.3.4) and (6.3.5) into (6.2.4) we obtain the following scheme

$$\begin{aligned}\frac{1}{\Gamma(2-\alpha)}\sum_{j=0}^{n}\sigma_j\Delta_t v_l^{n-j+1} &= \left(rv_l^{n+1}-q\Delta_x v_l^{n+1}\right)\frac{\tau^{1-\alpha}}{\Gamma(2-\alpha)}\\ &\quad -\omega(\alpha)\Delta_{xx}v_l^{n+1}-R_l^{n+1}\\ &\quad q=r-\delta,\ n\geq 0,\ \omega(\alpha)=\frac{\Gamma(1+\alpha)\sigma^2x^2}{2},\end{aligned} \tag{6.3.6}$$

which after some algebraic manipulations can be simplified into

$$\sum_{j=1}^{n+1}\varphi_{j-1}v_l^{n-j+1} = av_{l-1}^{n+1}+bv_l^{n+1}+cv_{l+1}^{n+1}+R_l^{n+1}, \tag{6.3.7}$$

where by $a=-k^\alpha q\frac{\tau^{1-\alpha}-\omega'}{h^2}$, $b=k^\alpha\frac{\tau^{1-\alpha}r+2\omega'}{h^2}$, $c=-k^\alpha q\frac{\tau^{1-\alpha}-\omega'}{h^2}-1$, $\omega'=k^\alpha\Gamma(2-\alpha)\omega(\alpha)$, and $\varphi_j=\sigma_j-\sigma_{j+1}$.

The final scheme is explicitly given by

$$\varphi_0v_l^n+\cdots+\varphi_{n-1}v_l^1+\varphi_nv_l^0 = av_{l-1}^{n+1}+bv_l^{n+1}+cv_{l+1}^{n+1}, \tag{6.3.8}$$

where the left hand side of the scheme (6.3.8) capture the memory effects.

R_l^{n+1} represent the remainder after truncation which is given by

$$R_l^{n+1}=\frac{h^2}{12}\left(\frac{\tau^{1-\alpha}}{\Gamma(2-\alpha)}\frac{\partial^3v_l^{n+1}}{\partial x^3}+\omega(\alpha)\frac{\partial^4v_l^{n+1}}{\partial x^4}\right)+\mathcal{O}\left(h^4+k^2\right), \tag{6.3.9}$$

therefore,

$$\left|R_l^{n+1}\right|=C\left(h^4,k^2\right). \tag{6.3.10}$$

For some constant C independent of h and k. The proof to this result follows in the next section.

6.4 Analysis of the numerical method

In this section we present the stability and convergence properties of the proposed difference scheme (6.3.8).

6.4.1 Stability analysis

The stability properties of the proposed scheme (6.3.8) will be discussed using the concept of Fourier analysis. Suppose $\hat{v}_l^n$ is an approximate solution to the scheme (6.3.8) such that $v_l^n - \hat{v}_l^n = \epsilon_l^n$ for $l = 0, 1, \cdots, L$, then the following theorem holds.

Theorem 6.4.1. *The difference scheme in (6.3.8) is unconditional stable*

Proof: Substituting the roundoff error ϵ_l^n into (6.3.8) we obtain

$$\sum_{j=1}^{n+1} \varphi_{j-1} \epsilon_l^{n-j+1} = a\epsilon_{l-1}^{n+1} + b\epsilon_l^{n+1} + c\epsilon_{l+1}^{n+1}, \tag{6.4.1}$$

such that $\epsilon_0^n = \epsilon_L^n = 0$.

Let us define the grid function as follow,

$$\epsilon^n(x) = \begin{cases} \epsilon_l^n, & \text{when } x_l - \frac{h}{2} < x \leq x_l + \frac{h}{2}, \ l = 1, 2, ..., L-1, \\ 0, & \text{when } b_l \leq x \leq b_l + \frac{h}{2} \text{ or } b_u - \frac{h}{2} < x \leq b_u + \frac{h}{2}, \end{cases} \tag{6.4.2}$$

which can be expanded in terms of the following Fourier series representation

$$\epsilon^n(x) = \sum_{j=1}^{\infty} \varrho_n(j) e^{i2\pi jx/b_u - b_l}, \quad n = 1, 2, ..., N, \tag{6.4.3}$$

where

$$\varrho_n(j) = \frac{1}{b_u - b_l} \int_0^{b_u - b_l} \epsilon^n(x) e^{-i2\pi jx/b_u - b_l} dx, \quad n = 1, 2, ..., N, \tag{6.4.4}$$

and $i = \sqrt{-1}$.

Let $\epsilon^n = (\epsilon_1^n, \epsilon_2^n, \cdots, \epsilon_{L-1}^n)^T$ and, define it's norm

$$\|\epsilon^n\|_2 = \left(\sum_{l=1}^{L-1} h|\ \epsilon_l^n\ |^2\right)^{1/2} = \left(\int_0^{b_u-b_l} |\ \epsilon^n(x)\ |^2 dx\right)^{1/2}. \tag{6.4.5}$$

Then apply the Parseval equality to obtain

$$\int_0^{b_u-b_l} |\ \epsilon^n(x)^2\ |\ dx = \sum_{j=-\infty}^{\infty} |\ \varrho_n(j)\ |^2, \tag{6.4.6}$$

to obtain

$$\|\epsilon^n\|_2^2 = \int_0^{b_u-b_l} |\ \epsilon^n(x)\ |^2 dx = \sum_{j=-\infty}^{\infty} |\ \varrho_n(j)\ |^2\ . \tag{6.4.7}$$

Therefore, the solution to (6.4.1) takes the following form

$$\epsilon_l^n = \varrho_n e^{i\beta lh}, \tag{6.4.8}$$

for $\beta := 2\pi j/b_u - b_l$ and $i = \sqrt{-1}$. Substituting the expression for ϵ^n into (6.4.1), after simplifying we obtain

$$\left(\varphi_0\varrho_n + \cdots + \varphi_{n-1}\varrho_1 + \varphi_n\varrho_0\right) e^{i\beta lh} \;=\; e^{i\beta lh}\varrho_{n+1}\left(ae^{-i\beta h} + ce^{i\beta h} + b\right), \tag{6.4.9}$$

and

$$\varphi_0\varrho_n + \cdots + \varphi_{n-1}\varrho_1 + \varphi_n\varrho_0 \;=\; \varrho_{n+1}\left(a\left(e^{-i\beta h} + e^{i\beta h}\right) + b - 1\right), \tag{6.4.10}$$

since $\beta_0 = 1$ and $a = c - \beta_0$.

From the Fourier series representation of $\cos\beta h$ we obtain

$$\varphi_0\varrho_n + \cdots + \varphi_{n-1}\varrho_1 + \varphi_n\varrho_0 \;=\; \varrho_{n+1}\left(a\cos\beta h + b - 1\right). \tag{6.4.11}$$

Now we have

Proposition 6.4.2. *Suppose* ϱ_{n+1} *satisfy* (6.4.11), *then* $|\varrho_{n+1}| \leq |\varrho_0|$ *for all* $n = 0, 1, 2, \cdots, N$

Proof: Let $n = 0$, then from (6.4.11) we have

$$|\varrho_1 (a \cos \beta h + b - 1)| = |\varphi_0 \varrho_0| , \tag{6.4.12}$$

which implies that

$$\begin{aligned} |\varrho_1| &= \left| \frac{\varphi_0 \varrho_0}{a \cos \beta h + b - 1} \right| , \\ &\leq \frac{\varphi_0}{|a \cos \beta h + b - 1|} |\varrho_0| , \\ &\leq \frac{1 - \beta_1}{|a \cos \beta h + b - 1|} |\varrho_0| , \\ &< \frac{1}{|a \cos \beta h + b - 1|} |\varrho_0| , \ (\because 1 - \beta_1 < 1) , \\ &< |\varrho_0| , \ \left(\because \frac{1}{|a \cos \beta h + b - 1|} < 1 \right) . \end{aligned} \tag{6.4.13}$$

We therefore have,

$|\varrho_1| \leq |\varrho_0| .$

For $n = 1$, we suppose $|\varrho_n| \leq |\varrho_0|$ for all $n = 1, 2, \cdots, N$, and show that the same is true for $|\varrho_{n+1}| \leq |\varrho_0|$ for all n.

Proof:

$$\begin{aligned}
|\varrho_{n+1}| &= \left|\frac{\sum_{j=1}^{n+1}\varphi_{j-1}\varrho_{n-j+1}}{a\cos\beta h+b-1}\right|,\\
&\leq \frac{1}{|a\cos\beta h+b-1|}\sum_{j=1}^{n+1}|\varphi_{j-1}\varrho_{n-j+1}|,\\
&\leq \sum_{j=1}^{n+1}|\varphi_{j-1}\varrho_{n-j+1}|,\left(\because \frac{1}{|a\cos\beta h+b-1|}\right)<1,\\
&= \varphi_0|\varrho_n|+\varphi_1|\varrho_{n-1}|+\cdots+\varphi_{n-1}|\varrho_1|+\varphi_n|\varrho_0|,\\
&\leq \varphi_0|\varrho_0|+\varphi_1|\varrho_0|+\cdots+\varphi_{n-1}|\varrho_0|+\varphi_n|\varrho_0|,\\
&= (\varphi_0+\varphi_1+\cdots+\varphi_{n-1}+\varphi_n)|\varrho_0|,\\
&= \sum_{j=1}^{n+1}\varphi_{j-1}|\varrho_0|,\\
&= |\varrho_0|,\left(\because\sum_{j=1}^{n+1}\varphi_{j-1}=1\right). \qquad (6.4.14)
\end{aligned}$$

It therefore follow that, $\left\|\epsilon_l^{n+1}\right\|_2 \leq \|\epsilon_l^0\|_2$.

6.4.2 Convergence analysis

In this subsection we prove that the proposed scheme (6.3.8) converges with the spatial accuracy of fourth order. The analysis will follow the concept of Fourier analysis. Let R_l^{n+1} denote the truncation error of involved in the approximation at grid point (x_l, τ_{n+1}), then from (6.3.9) we obtain the following theorem

Theorem 6.4.3. *The difference scheme (6.3.8) is convergent and converges with order* $\mathcal{O}(k^2+h^4)$.

Let $\xi_l^n = v(x_l,t_n) - v_l^n$ denote the approximation error at grid point (t_n, x_l), such that $\xi_L^n = 0$, for $n = 1,2,\cdots,N$ and $\xi_l^0 = 0$, for $l = 0,1,\cdots,L$. By substituting ξ_l^n

into the scheme (6.3.8) we obtain

$$\sum_{j=1}^{n+1} \varphi_{j-1}\xi_l^{n-j+1} + R_l^{n+1} = a\xi_{l-1}^{n+1} + b\xi_l^{n+1} + c\xi_{l+1}^{n+1}, \tag{6.4.15}$$

Similar to stability analysis, we define the following grid functions

$$\xi^n(S) = \begin{cases} \xi_l^n, & \text{when} \quad x_l - \frac{h}{2} < x \leq S_l + \frac{h}{2}, \quad l = 1, 2, ..., L-1, \\ 0, & \text{when} \quad 0 \leq x < \frac{h}{2} \quad \text{or} \quad x_{max} - \frac{h}{2} < S \leq x_{max} + \frac{h}{2}, \end{cases} \tag{6.4.16}$$

$$R^n(x) = \begin{cases} C_l^n, & \text{when} \quad x_l - \frac{h}{2} < x \leq x_l + \frac{h}{2}, \quad l = 1, 2, ..., L-1, \\ 0, & \text{when} \quad 0 \leq x < \frac{h}{2} \quad \text{or} \quad x_{max} - \frac{h}{2} < x \leq x_{max} + \frac{h}{2}, \end{cases} \tag{6.4.17}$$

which imply $\xi^n(x)$ and C_l^n have the following Fourier series representations

$$\xi^n(x) = \sum_{j=1}^{\infty} \tau_n(j) e^{i2\pi jx/x_{max}}; \quad n = 1, 2, ..., N, \tag{6.4.18}$$

$$R^n(x) = \sum_{j=1}^{\infty} \nu_n(j) e^{i2\pi jx/x_{max}}; \quad n = 1, 2, ..., N, \tag{6.4.19}$$

where

$$\tau_n(j) = \frac{1}{x_{max}} \int_0^{xmax} \xi^n(x) e^{-i2\pi jx/x_{max}} dx; \quad n = 1, 2, ..., N. \tag{6.4.20}$$

$$\nu_n(j) = \frac{1}{x_{max}} \int_0^{xmax} R^n(x) e^{-i2\pi jx/x_{max}} dx; \quad n = 1, 2, ..., N. \tag{6.4.21}$$

Let $\xi^n = (\xi_1^n, \xi_2^n, \cdots, \xi_{L-1}^n)^T$ and $R^n = (R_1^n, R_2^n, \cdots, R_{L-1}^n)^T$, and let us define their

norms as follow

$$\left\|\xi^n\right\|_2 = \left(\sum_{l=1}^{L-1} h|\ \xi_l^n\ |^2\right)^{1/2} = \left(\int_0^{x_{max}} |\ \xi^n(x)\ |^2 dx\right)^{1/2}, \tag{6.4.22}$$

$$\left\|R^n\right\|_2 = \left(\sum_{l=1}^{L-1} h|\ R_l^n\ |^2\right)^{1/2} = \left(\int_0^{x_{max}} |\ R^n(x)\ |^2 dx\right)^{1/2}, \tag{6.4.23}$$

and, apply the following Parseval equalities

$$\int_0^{S_{max}} |\ \xi^n(S)^2\ |\ dS = \sum_{j=-\infty}^{\infty} |\ \tau_n(j)\ |^2; \quad n = 1, 2, ..., N, \tag{6.4.24}$$

$$\int_0^{S_{max}} |\ R^n(S)^2\ |\ dS = \sum_{j=-\infty}^{\infty} |\ \nu_n(j)\ |^2; \quad n = 1, 2, ..., N, \tag{6.4.25}$$

to obtain

$$\left\|\xi^n\right\|_2^2 = \sum_{j=-\infty}^{\infty} |\ \tau_n(j)\ |^2; \quad n = 1, 2, ..., N, \tag{6.4.26}$$

$$\left\|R^n\right\|_2^2 = \sum_{j=-\infty}^{\infty} |\ \nu_n(j)\ |^2; \quad n = 1, 2, ..., N. \tag{6.4.27}$$

Now let us define

$$\xi^n = \tau_n e^{i\beta lh} \quad \text{and} \quad R^n = \nu_n e^{i\beta lh}, \tag{6.4.28}$$

where $\beta = 2\pi j/S_{max}$ and $i = \sqrt{-1}$, and use these expressions in (6.4.15) such that

$$\begin{aligned}\sum_{j=1}^{n+1} \varphi_{j-1}\tau_{n-j+1}e^{i\beta lh} &= a\tau_{n+1}e^{i\beta(l-1)h} + b\tau_{n+1}e^{i\beta lh} + c\tau_{n+1}e^{i\beta(l+1)h}, \\ &\quad -\nu_{n+1}e^{i\beta lh} \end{aligned} \tag{6.4.29}$$

which implies

$$\left(\sum_{j=1}^{n+1} \varphi_{j-1}\tau_{n-j+1}\right) e^{i\beta lh} = e^{i\beta lh}\tau_{n+1}\left(\left(ae^{-i\beta h} + ce^{i\beta h} + b\right) - \nu_{n+1}\right). \tag{6.4.30}$$

simpifying into

$$\sum_{j=1}^{n+1} \varphi_{j-1}\tau_{n+1-j} = \tau_{n+1}\left(a\cos\beta h + b - 1\right) - \nu_{n+1}. \tag{6.4.31}$$

Therefore,

$$\tau_{n+1} = \frac{\sum_{j=1}^{n+1} \varphi_{j-1}\tau_{n+1-j} + \nu_{n+1}}{\left(a\cos\beta h + b - 1\right)}. \tag{6.4.32}$$

Now we have

Proposition 6.4.4. *Suppose τ_n for $n = 0, 1, \cdots, N$ is a solution to (6.4.32), then there exists some positive constant C such that $|\tau_n| \leq C|\nu_1|$ for all n.*

Proof. It is trivial to show that for $n = 0$, from (6.4.32) we have

$$|\tau_1| = \left|\frac{\varphi_0\tau_0 + \nu_1}{\left(a\cos\beta h + b - 1\right)}\right| \leq \nu_1. \tag{6.4.33}$$

Suppose $|\tau_n| \leq C_0|\nu_1|$, for $n = 1, 2, \cdots, N$, for some constant C independent of h

and k. Then,

$$\begin{aligned}
|\tau_{n+1}| &\leq \left| \frac{\sum_{j=1}^{n+1} \varphi_{j-1}\tau_{n+1-j} + \nu_{n+1}}{(a\cos\beta h + b - 1)} \right|, \\
&\leq \sum_{j=1}^{n+1} \frac{1}{|(a\cos\beta h + b - 1)|}(\sigma_{j-1}\,|\tau_{n-j+1}| + |\nu_{n+1}|), \\
&\leq \sum_{j=1}^{n+1} C_{j-1}(\sigma_{j-1}\,|\tau_{n-j+1}| + |\nu_{n+1}|), \\
&\leq \sum_{j=1}^{n+1} \sigma_{j-1}C_{j-1}\,|\tau_{n-j+1}| + C_{n+1}\,|\nu_1|\,, \\
&\leq \sum_{j=1}^{n+1} \sigma_{j-1}C_{j-1}\,|\nu_1| + C_{n+1}\,|\nu_1|\,, \\
&= \sigma_0 C_0|\nu_1| + \sigma_1 C_1\,|\nu_1| + \sigma_2 C_2\,|\nu_1| + \cdots + \sigma_n C_n\,|\nu_1| + C_{n+1}\,|\nu_1|\,, \\
&\leq \hat{C}(\sum_{j=1}^{n+1} \sigma_{j-1}|\nu_1| + \nu_1), (\hat{C} = \max_{0\leq j\leq n+1}\{C_j\}) \\
&= \hat{C}(\sum_{j=0}^{n+1} \sigma_j)|\nu_1| \\
&= C|\nu_1|. \qquad (6.4.34)
\end{aligned}$$

We can therefore conclude that the scheme (6.3.8) is convergent and this complete the proof to Theorem 6.4.3.

6.5 Numerical experiments

In this section, we present two double barrier knock-in put options examples.

Example 6.5.1. Consider equation (6.2.1) subject to conditions (6.2.5) for pricing double knock-in put option with the following parameters: $K = 80$, $r = 0.05$, $\sigma = 0.01$, $T = 1$, $S_{\max} = 120$, $L = 100$, $N = 50, \delta = 0.025$, and 0.075, $\alpha = 0.5,\ 0.7,\ 0.9,\ 1.0$, with lower barrier located at $B_l = 6$ and upper barrier located at $B_u = 110$.

To check for the effects of the change in some key option parameters on the efficiency of the model, as well as the numerical method herein, we consider a second example with two different set of dividend yields δ, two different sets of barriers, same interest rate r, same strike price, same maturity time and same set of α values.

Example 6.5.2. Consider equation (6.2.1) subject to conditions (6.2.5) for pricing double knock-in put options with the following parameters: $K = 80,\ r = 0.05,\ \sigma = 0.015,\ T = 1,\ S_{\max} = 120,\ L = 100,\ N = 100, \delta = 0.045$ and $0.10,\ \alpha = 0.5,\ 0.7,\ 0.9,\ 1.0,$ with lower barrier located at $B_l = 10$ and upper barrier located at $B_u = 130$.

Option maturity payoff curves for the two considered examples (considered examples (Example 6.5.1 and Example 6.5.2, above) are presented in figs. 6.5.1 and 6.5.2 below.

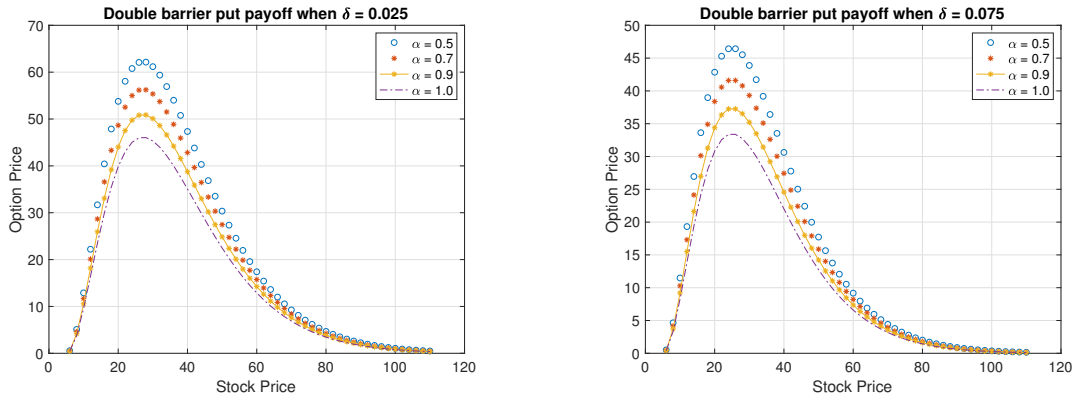

Figure 6.5.1: Double barrier put option payoffs for $\delta = 0.025,$ and $0.075,$ with $\alpha = 0.5,\ 0.7,\ 0.9,\ 1.0,$ and $B_l = 6,\ B_u = 110$ at $t = T$.

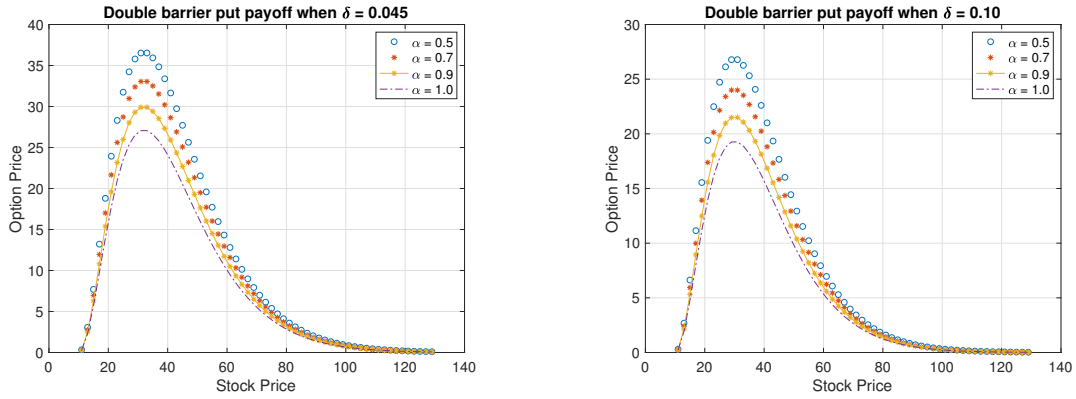

Figure 6.5.2: Double barrier put option payoffs for $\delta = 0.045$, and 0.10, with $\alpha = 0.5,\ 0.7,\ 0.9,\ 1.0$, and $B_l = 10$, $B_u = 130$ at $t = T$

The results in figs. 6.5.1 and 6.5.2 are well consistent with those obtained in [103] which was in terms of a call option. Figures 6.5.1 and 6.5.2 indicates that, change in the dividend yield has an effect on the option price (premium). A higher dividend yield (δ) yield a lower option premium. This is not strange because, the holder of the option with a higher dividend yield is compensated more through dividends as compared to the one with a lower dividend yield.

Moreover, the consider tfBS in (6.2.1) give high option price both for the in-the-money option and for when the underlying asset price (S) is close to the strike price (K) as compared to the classical BS model ($\alpha = 1$). This shows that, the tfBS model is of a *power-law* nature as compared to the classical BS model.

The tabular results for the two considered examples (Example 6.5.1 and Example 6.5.2, above) are presented in Tables 6.5.1 to 6.5.4 below.

Table 6.5.1: Maximum absolute errors for Example 6.5.1 with $r = 0.05$ and $\delta = 0.025$.

α	$N = 50$	$N = 100$	$N = 200$	$N = 400$	$N = 800$
0.1	7.1212e-03	1.7901e-03	4.4561e-04	1.1525e-04	2.9154e-05
0.2	7.1336e-03	1.8180e-03	4.4711e-04	1.1563e-04	2.9250e-05
0.3	7.3465e-03	1.8383e-03	4.5753e-04	1.1827e-04	2.9717e-05
0.4	7.4609e-03	1.9326e-03	4.8371e-04	1.2239e-04	3.0759e-05
0.5	8.1315e-03	2.0213e-03	5.1493e-04	1.3000e-04	3.2785e-05
0.6	8.4515e-03	2.1032e-03	5.4620e-04	1.3842e-04	3.4915e-05
0.7	9.5333e-03	2.3909e-03	6.1088e-04	1.5478e-04	3.7153e-05
0.8	1.1062e-02	2.5616e-03	6.4925e-04	1.6449e-04	4.1409e-05
0.9	1.2494e-02	3.1452e-03	7.8208e-04	2.0062e-04	5.0548e-05
1.0	1.3815e-02	3.4591e-03	8.7754e-04	2.2198e-04	5.5953e-05

Table 6.5.2: Convergence rates for Example 6.5.1 with $r = 0.05$ and $\delta = 0.025$.

α	$N = 100$	$N = 200$	$N = 400$	$N = 800$
0.1	1.91	1.95	1.98	1.99
0.2	1.92	1.96	1.98	1.99
0.3	1.93	1.96	1.98	1.99
0.4	1.93	1.96	1.98	1.99
0.5	1.93	1.97	1.98	1.99
0.6	1.94	1.97	1.98	1.99
0.7	1.94	1.97	1.98	1.99
0.8	1.94	1.97	1.98	1.99
0.9	1.94	1.97	1.98	1.99
1.0	1.94	1.97	1.98	1.99

Table 6.5.3: Maximum absolute errors for Example 6.5.2 with $r = 0.05$ and $\delta = 0.045$.

α	$N = 100$	$N = 200$	$N = 400$	$N = 800$	$N = 1600$
0.1	6.5512e-02	1.6492e-02	4.1892e-03	1.0597e-03	2.5953e-04
0.2	5.7988e-03	1.4694e-02	3.7170e-03	9.4025e-04	2.3784e-04
0.3	5.2147e-02	1.3191e-02	3.3368e-03	8.4408e-04	2.1352e-04
0.4	4.7443e-02	1.2001e-02	3.0358e-03	7.6794e-04	1.9426e-04
0.5	4.3746e-02	1.1066e-02	2.7993e-03	7.0810e-04	1.7912e-04
0.6	4.0893e-02	1.0344e-02	2.6167e-03	6.6192e-04	1.6544e-04
0.7	3.8773e-02	9.8080e-03	2.4898e-03	6.2752e-04	1.5688e-04
0.8	3.7318e-02	9.4300e-03	2.3779e-03	6.0305e-04	1.4980e-04
0.9	3.6499e-02	9.3328e-03	2.4355e-03	5.9979e-04	1.5745e-04
1.0	3.7328e-02	9.2895e-03	2.4246e-03	5.9803e-04	1.5670e-04

Table 6.5.4: Convergence rates for Example 6.5.2 with $r = 0.05$ and $\delta = 0.045$.

α	$N = 200$	$N = 400$	$N = 800$	$N = 1600$
0.1	1.95	1.98	1.99	1.99
0.2	1.96	1.98	1.99	1.99
0.3	1.96	1.98	1.99	1.99
0.4	1.96	1.98	1.99	2.00
0.5	1.97	1.98	1.99	2.00
0.6	1.97	1.98	1.99	2.00
0.7	1.97	1.98	1.99	2.00
0.8	1.97	1.98	1.99	2.00
0.9	1.97	1.98	1.99	2.00
1.0	1.97	1.98	1.99	2.00

To demonstrate the convergence properties of the scheme in the asset direction, we fix $N = 100$ and computer the error for varying M. The results are presented in the tables below

Table 6.5.5: Maximum absolute errors for Example 6.5.2 with $r = 0.05$ and $\delta = 0.045$ when N is fixed.

α	$M = 100$	$M = 200$	$M = 400$	$M = 800$	$M = 1600$
0.1	6.6630e-02	4.1642e-03	2.6892e-04	1.6297e-05	1.1165e-06
0.2	5.8987e-02	3.6294e-03	2.2672e-04	1.4025e-05	9.0211e-07
0.3	5.3146e-02	3.3591e-03	2.3168e-04	1.2638e-05	7.9527e-07
0.4	4.8442e-02	3.1629e-03	2.1086e-04	1.4057e-05	9.3715e-07
0.5	4.4745e-02	2.8924e-03	1.9124e-04	1.2644e-05	8.3602e-07
0.6	4.1892e-02	2.7038e-03	1.7877e-04	1.1820e-05	7.8149e-07
0.7	3.9772e-02	2.5636e-03	1.6950e-04	1.1207e-05	7.4098e-07
0.8	3.8317e-02	2.4674e-03	1.6314e-04	1.0786e-05	7.1317e-07
0.9	3.7498e-02	2.4132e-03	1.5956e-04	1.0550e-05	6.9752e-07
1.0	3.8327e-02	2.4680e-03	1.6318e-04	1.0789e-05	7.1336e-07

Table 6.5.6: Convergence rates for Example 6.5.2 with $r = 0.05$ and $\delta = 0.045$ when N is fixed.

α	$M = 200$	$M = 400$	$M = 800$	$M = 1600$
0.1	3.99	3.68	3.69	3.69
0.2	3.96	3.92	3.99	3.75
0.3	3.96	3.92	3.99	3.75
0.4	3.96	3.92	3.99	3.87
0.5	3.97	3.92	3.99	3.87
0.6	3.97	3.92	3.99	3.88
0.7	3.97	3.92	3.99	3.98
0.8	3.97	3.92	3.99	3.99
0.9	3.97	3.91	3.99	3.99
1.0	3.97	3.91	3.99	3.99

Numerical results herein confirms our theoretical deductions on the stability and convergence properties of the scheme as presented in Section 6.4.1 and Section 6.4.2 respectively. The scheme is unconditionally stable and converges with order two in time as well as order four in space.

6.6 Summary and discussions

This chapter considered a double barrier option pricing problem under the time-fractional Black-Scholes setup. We proposed a robust high order numerical scheme for solving a double barrier time-fractional Black-Scholes PDE. Two numerical examples were presented. Results indicates that, the fractional Black-Scholes approach is a very efficient valuation technique for barrier option as compared to usual/classical Black-Scholes approach. The barrier option tfBS model is sensitive to dividend payouts, it allocates lower put premiums to higher dividend yield options. This is well in-line with the theory of no arbitrage, investors who are compensated well in dividends should receive prices lower than those of investors with lower dividend yield options. Moreover, the numerical scheme herein, proves to be well efficient in solving the involved time-fractional Black-Scholes model.

On fractionalizing both temporal and spatial derivatives in the classical Black-Scholes model, Chapter 7 presents a discussion of the design and analysis of a time-space-fractional Black-Scholes PDE as well as its universal numerical scheme.

Chapter 7

A Universal Finite Difference Scheme for a Time-Space-Fractional Black-Scholes Equation

This chapter present a new kind of universal difference scheme for solving a time-space fractional B-S models. Theoretical analysis of the scheme suggest the scheme is conditionally stable, convergent, and uniquely solvable. Furthermore, numerical experiments indicates that the universal difference method is valid and efficient for solving the time-space fractional B-S equation. At the same time, numerical experiments indicates that the time-space fractional B-S equation and the proposed scheme provide superior results which are consistent with the actual financial market scenarios.

7.1 Introduction

The fractional Black-Scholes (B-S) equations are important mathematical models for modelling numerous physical phenomenons in science, finance and engineering. However the study of their numerical solutions has very significant practical applications.

This chapter focus on the numerical aspects of the solution methods to time-space fractional Black-Scholes partial differential equations (tfBS-PDE), something that ac-

cording to the best of our knowledge is not extensively documented in literature. We construct a universal difference scheme in Section 7.2. The discussion herein, focus on numerically solving a time-space fractional Black-Scholes equation subject to standard European put option initial and boundary conditions. The existence and uniqueness of the numerical method, its computational stability and convergence are discussed in Section 7.3. And lastly, some numerical examples are discussed in Section 7.4 which demonstrate the efficiency and robustness of the numerical method in solving time-space fractional Black-Scholes equations. Concluding remarks, further discussions and scope for further studies are presented in Section 7.5.

7.1.1 Model

Suppose the stock price S follow the following Ito-Maruyama fractional differential equation

$$d^{\alpha}S = (r-\delta)S\frac{(dt)^{\alpha}}{\Gamma(2-\alpha)}t^{1-\alpha} + \Gamma(1+\alpha)\sigma S\omega(t)(dt)^{\alpha/2},\ 0<\alpha\leq 1. \tag{7.1.1}$$

Using the following two fractional identities

$$\Gamma(1+\alpha)dS := d^{\alpha}S \tag{7.1.2}$$

and

$$\frac{d^{\alpha}t}{dt^{\alpha}} := \frac{1}{\Gamma(2-\alpha)}t^{1-\alpha},\ 0<\alpha\leq 1, \tag{7.1.3}$$

it is trivial to show that infact (7.1.1) is equivalent to

$$dS = (r-\delta)Sdt + \sigma S\omega(t)(dt)^{\alpha/2},\ 0<\alpha\leq 1, \tag{7.1.4}$$

for $\omega(t)$ a Gaussian white noise, whereas r and δ are the risk-free interest rate and continuous dividend yield respectively.

If we consider the standard case where the stock price dynamics are governed by the standard Brownian motion $B(t) = \int \omega(t)(dt)^{1/2}$, then (7.1.1) and (7.1.4) are generalizations of a geometric Brownian motion process with $B(t) = \int \omega(t)(dt)^{\alpha/2}$ as the governing stochastic process.

Let $v = v(S,t)$ denote the price of a European option such that $v(S,t)$ satisfy the following assumption

Assumption 7.1.1. *Assume the function $v(S,t)$ has a fractional partial derivative of order α with respect to t and fractional partial derivatives of order α and 2α with respect to S for some $0 < \alpha \leq 1$.*

Then, the generalized Taylor series in terms $v(S,t)$ up to remaining error term yields

$$dv = \frac{1}{\Gamma(1+\alpha)}\frac{\partial^\alpha v}{\partial t^\alpha}(dt)^\alpha + \frac{1}{\Gamma(1+\alpha)}\frac{\partial^\alpha v}{\partial S^\alpha}(dS)^\alpha + \frac{1}{\Gamma(1+2\alpha)}\frac{\partial^{2\alpha} v}{\partial S^{2\alpha}}(dS^\alpha)^2. \quad (7.1.5)$$

Using fractional identity (7.1.3) expressed in terms of S, we re-write (7.1.5) as

$$\begin{aligned} dv &= \frac{1}{\Gamma(1+\alpha)}\frac{\partial^\alpha v}{\partial t^\alpha}(dt)^\alpha + \frac{\Gamma(2-\alpha)}{\Gamma(1+\alpha)}S^{\alpha-1}\frac{\partial^\alpha v}{\partial S^\alpha}d^\alpha S \\ &\quad + \frac{\Gamma^2(2-\alpha)}{\Gamma(1+2\alpha)}S^{2\alpha-2}\frac{\partial^{2\alpha} v}{\partial S^{2\alpha}}(d^\alpha S)^2. \end{aligned} \quad (7.1.6)$$

Ito's lemma on $v(S,t)$ suggest we identify $\omega(t)^2$ with its variance such that $\omega(t)^2 = 1$, therefore from (7.1.1) we get

$$(d^\alpha S)^2 = \Gamma(1+\alpha)^2\sigma^2 S^2 (dt)^\alpha, \quad (7.1.7)$$

substituting into (7.1.7) we obtain

$$\alpha! dv = \left(\frac{\partial^\alpha v}{\partial t^\alpha} + (r-\delta)t^{1-\alpha}S^\alpha\frac{\partial^\alpha v}{\partial S^\alpha} + \Gamma^3(1+\alpha)\frac{\Gamma^2(2-\alpha)}{\Gamma(1+2\alpha)}\sigma^2 S^{2\alpha}\frac{\partial^{2\alpha} v}{\partial S^{2\alpha}}\right)(dt)^\alpha. \quad (7.1.8)$$

Using fractional identity (7.1.2), dividing both sides of equation (7.1.7) by $(dt)^\alpha$

and simplying we obtain the following time-space fractional Black-Scholes partial differential equation (tsfBS PDE)

$$\frac{\partial^\alpha v}{\partial t^\alpha} = \left(\frac{rv}{\Gamma(2-\alpha)} - (r-\delta)S^\alpha \frac{\partial^\alpha v}{\partial S^\alpha}\right) t^{1-\alpha} - \frac{\Gamma^3(1+\alpha)\Gamma^2(2-\alpha)}{\Gamma(1+2\alpha)}\sigma^2 S^{2\alpha}\frac{\partial^{2\alpha} v}{\partial S^{2\alpha}}, \quad 0 < \alpha \leq 1, \tag{7.1.9}$$

with standard European put options boundary conditions

$$\left.\begin{aligned} &v(S,t) = \max(K-S,0), \\ &v(0,t) = Ke^{-r(T-t)}, \\ &\lim_{S\to\infty} v(S,t) = 0, \end{aligned}\right\} \tag{7.1.10}$$

where K is the strike price of the option and T is the maturity time.

Let $x = e^S$, $t = T - \tau$, $v(x,t) = e^{-r\tau}v(s,\tau)$ be some change of notations. Without any loss of notations (7.1.9) simplify to

$$\frac{\partial^\alpha v}{\partial \tau^\alpha} = \left(\left(\gamma(\alpha)\frac{\Gamma(1-\alpha)}{\Gamma(1-2\alpha)}\sigma^2 + \kappa(\alpha)\right)\frac{\partial v}{\partial x} + \gamma(\alpha)\sigma^2\frac{\partial^2 v}{\partial x^2}\right)\tau(\alpha),\ 0 < \alpha \leq 1, \tag{7.1.11}$$

where $\gamma(\alpha) = \frac{\Gamma^3(1+\alpha)\Gamma^2(2-\alpha)}{\Gamma(1+2\alpha)}$, $\kappa(\alpha) = (r-\delta)(T-\tau)^{1-\alpha}$, and $\tau(\alpha) = \tau^{1-\alpha}(T-\tau)^{\alpha-1}$, subject to the following put option boundary conditions

$$\left.\begin{aligned} &v(x,\tau) = \max(K-e^x,0), \\ &v(0,\tau) = Ke^{-r\tau}, \\ &\lim_{x\to 1} v(x,\tau) = 0. \end{aligned}\right\} \tag{7.1.12}$$

7.2 Numerical scheme

Let L and N be positive integers and define $h = 1/L$ and $k = 1/N$ as the space and time grid size respectively. Define $x_l = lh$; $l = 0, 1, 2, ..., L$, and $\tau_n = nk$; $n = 0, 1, 2, ..., N$, such that $x_l \in [x_{min}, x_{max}]$ and $\tau_n \in [T, 0]$. Furthermore, define $v_l^n = v(x_l, \tau_n)$ as the solution at the grid point $(x_l, \tau_n) = (lh, nk)$.

The α-derivative in (7.1.11) is approximated using the following quadrature formula

$$\frac{\partial^\alpha v(x_l,\tau_n)}{\partial\tau^\alpha}=\frac{k^\alpha}{\Gamma(2-\alpha)}\sum_{j=1}^{n}\beta_j(v_l^{n-j+1}-v_l^{n-j})+\frac{\tau_n^{1-\alpha}}{\Gamma(2-\alpha)}k, \tag{7.2.1}$$

where

$$\beta_j=j^{1-\alpha}-(j-1)^{1-\alpha},\ j=1,2,\cdots,n, \tag{7.2.2}$$

such that, $1=\beta_1>\beta_2>\beta_3>\cdots>\to 0$ as $j\to n$.

The θ-method for solving (7.1.5) is designed by combining the classical explicit and implicit schemes of the right hand side of (7.1.5) using some parameter θ $(0\le\theta\le 1)$. Multiply the explicit scheme by $1-\theta$ and implicit by θ and add them together to obtain the following scheme after ignoring the truncation errors

$$\begin{aligned}\frac{\partial^\alpha v(x_l,\tau_{n+1})}{\partial\tau^\alpha} &= \frac{k^\alpha}{\Gamma(2-\alpha)}\sum_{j=1}^{n}\beta_j(v_l^{n-j+1}-v_l^{n-j})\\ &= (1-\theta)\Big((ab+(r-\delta)(T-k(n+1))^{1-\alpha})(k(n-1))^{1-\alpha}K^n\\ &\quad +a(k(n-1))^{1-\alpha}(T-k(n+1))^{\alpha-1}\frac{v_{l+1}^n-2v_l^n+v_{l-1}^n}{h^2}\Big)\\ &\quad +a(nk)^{1-\alpha}(T-nk)^{\alpha-1}\frac{v_{l+1}^{n+1}-2v_l^{n+1}+v_{l-1}^{n+1}}{h^2}\Big),\end{aligned} \tag{7.2.3}$$

where

$$K^n=(T-k(n+1))^{\alpha-1}\frac{v_{l+i}^n-v_{l-1}^n}{2h},\ a=\gamma(\alpha)\sigma^2,\ b=\frac{\Gamma(1-\alpha)}{\Gamma(1-2\alpha)},\ n=1,2,\cdots,N,$$

and

$$l=1,2,\cdots,L.$$

Let RHS be defined as follow

$$\begin{aligned} RHS: &= (-\mu_1(ab\varrho_{n+1}+(r-\delta)\psi_{n+1})-\mu_2\varrho_{n+1})\theta v_{l+1}^{n+1}+(1+2\theta\mu_2\varrho_{n+1})v_l^{n+1}+(\mu_1(ab\varrho_{n+1} \\ &\quad +(r-\delta)\psi_{n+1})-\mu_2\varrho_{n+1})\theta v_{l-1}^{n+1} \\ &= (1-\theta)(\mu_1(ab\varrho_n+(r-\delta)\psi_n)+\mu_2\varrho_n)v_{l+1}^n+(1-2\mu_2\varrho_n(1-\theta))v_l^n \qquad (7.2.4) \end{aligned}$$

Then, (7.2.3) is equivalent to

$$\begin{aligned} -\sum_{j=2}^{n-1}\varphi_j v_l^{n-j+1} &= RHS+(1-\theta)(-\mu_1(ab\varrho_n+(r-\delta)\psi_n)+\mu_2\varrho_n)v_{l-1}^n+(2^{1-\alpha})v_l^n+\beta_n v_l^1 \\ &= (1-\theta)(\mu_1(ab\varrho_n+(r-\delta)\psi_n)+\mu_2\varrho_n)v_{l+1}^n+(-2\mu_2\varrho_n(1-\theta)v_l^n \\ &\quad +(1-\theta)(-\mu_1(ab\varrho_n+(r-\delta)\psi_n)+\mu_2\varrho_n)v_{l-1}^n+\beta_n v_l^1 \qquad (7.2.5) \end{aligned}$$

where

$$\varphi_j = j^{1-\alpha}-(j-1)^{1-\alpha},\ \beta_j = j^{1-\alpha}-(j-1)^{1-\alpha},\ j=1,2,\cdots,n,$$

$$\varrho_n = (k(n-1))^{1-\alpha}(T-k(n+1))^{\alpha-1},\ \psi_n = (k(n-1))^{1-\alpha},\ j=1,2,\cdots,n.$$

This scheme can be simplified into the following simplest form

$$\begin{aligned} a_{n+1}v_{l-1}^{n+1}+b_{n+1}v_l^{n+1}+c_{n+1}v_{l+1}^{n+1} &= a_n v_{l-1}^n+b_n v_l^n+c_n v_{l+1}^n \\ &\quad +\sum_{j=1}^{n-1}\varphi_j v_l^{n-j+1}+\beta_n v_l^1, \qquad (7.2.6) \end{aligned}$$

where

$$\begin{aligned} a_{n+1} &= \theta[\mu_1(ab\varrho_{n+1} + (r-\delta)\psi_{n+1}) - \mu_2\varrho_{n+1}], \\ b_{n+1} &= 1 + 2\theta\mu_2\varrho_{n+1}, \\ c_{n+1} &= \theta[-\mu_1(ab\varrho_{n+1} + (r-\delta)\psi_{n+1}) - \mu_2\varrho_{n+1}], \\ a_n &= (1-\theta)[-\mu_1(ab\varrho_n + (r-\delta) + \mu_2\varrho_n) + \mu_2\varrho_n], \\ b_n &= -2(1-\theta)\mu_2\varrho_n, \\ c_n &= (1-\theta)[\mu_1(ab\varrho_n + (r-\delta)\psi_n) - \mu_2\varrho_n]. \end{aligned} \tag{7.2.7}$$

The general matrix form of the scheme is given by

$$\mathbf{A}^{n+1}\mathbf{U}^{n+1} = \mathbf{A}^n\mathbf{U}^n + \sum_{j=1}^{n} \varphi_j \mathbf{U}^{n-j+1} + \mathbf{C}^n, \text{ for all } n \geq 1, \tag{7.2.8}$$

with

$$\begin{aligned} \mathbf{A}^{n+1} &= \begin{pmatrix} b_{n+1} & c_{n+1} & & & \\ a_{n+1} & b_{n+1} & c_{n+1} & & \\ & \ddots & \ddots & \ddots & \\ & & a_{n+1} & b_{n+1} & c_{n+1} \\ & & & a_{n+1} & b_{n+1} \end{pmatrix}, \\ \mathbf{A}^{n} &= \begin{pmatrix} b_{n} & c_{n} & & & \\ a_{n} & b_{n} & c_{n} & & \\ & \ddots & \ddots & \ddots & \\ & & a_{n} & b_{n} & c_{n} \\ & & & a_{n} & b_{n} \end{pmatrix}, \end{aligned} \tag{7.2.9}$$

$$\mathbf{U}^{n+1} = \begin{pmatrix} v_2^{n+1} \\ v_3^{n+1} \\ \vdots \\ v_{L-1}^{n+1} \\ v_L^{n+1} \end{pmatrix}, \tag{7.2.10}$$

$$\mathbf{C}^n = \beta_n \mathbf{U}^1, \text{ for all } n \geq 1,$$

where

$$\mathbf{U}^1 = \begin{pmatrix} a_n v_1^n - a_{n+1} v_1^{n+1} \\ 0 \\ \vdots \\ 0 \\ c_n v_{L+1}^n - c_{n+1} v_{L+1}^{n+1} \end{pmatrix}. \tag{7.2.11}$$

7.3 Analysis of the numerical method

In this section we present a theoretical analysis of the scheme constructed in section 7.2. Four theoretical properties of the solution are investigated, namely; existence and uniqueness, it's stability as well as convergence.

7.3.1 Existence and uniqueness of the numerical solution

Theorem 7.3.1. *The θ-method (7.2.6) for solving the time-space fractional Black-Scholes PDE (7.1.11) is uniquely solvable.*

Proof.

From (7.2.7) we observe that $a_{n+1} < 0$, $c_{n+1} < 0$, $b_{n+1} > 0$, and that $b_{n+1} - |a_{n+1} + c_{n+1}| = 1$, so the coefficient matrix $\mathbf{A}^{n+1}$ is diagonally dominant and hence

invertible. Similar results are obtained in terms of the matrix $\mathbf{A}^n$, since $a_n > 0,\ b_n > 0$, and $c_n < 0$ with $|b_n| - |a_n + c_n| = 0$. Therefore, the θ-methodin (7.2.6) yield a unique solution. Therefore, theorem 7.3.1 follows.

7.3.2 Stability and convergence analysis

Stability analysis

Lemma 7.3.2. *Let $\tilde{v}_l^n$ be an approximate solution from the θ-method(7.2.6) in solving time-space fractional Black-Scholes PDE (7.1.11), and define $\varepsilon_l^n = \tilde{v}_l^n - v_l^n$ such that $\mathbf{E}_n = \left(\varepsilon_1^n, \cdots, \varepsilon_{l-1}^n\right)^T$, then, for $\frac{1}{2} \leq \theta \leq 1$ we have $\|\mathbf{E}_n\|_\infty \leq \|\mathbf{E}_1\|_\infty$ for all $1 \leq n \leq N+1$, for $0 \leq \theta < \frac{1}{2}$ and $\frac{a\Gamma(2-\alpha)}{h^2 k^\alpha} < 1$ we have $\|\mathbf{E}_n\|_\infty \leq \|\mathbf{E}_1\|_\infty$ for all $1 \leq n \leq N+1$.*

Proof. Suppose $n = 1$ and let

$$| \varepsilon_m^1 | = \max_{1 \leq l \leq L} | \varepsilon_l^1 | . \tag{7.3.1}$$

Then

$$\begin{aligned} \|E_2\|_\infty &= | \varepsilon_m^1 |, \\ &\leq | a_2 \varepsilon_{l-1}^2 + b_2 \varepsilon_l^2 + c_2 \varepsilon_{l+1}^2 |, \\ &= | \varepsilon_l^1 |, \\ &\leq \|\mathbf{E}_1\|_\infty, \end{aligned} \tag{7.3.2}$$

which implies that

$$\|\mathbf{E}_2\|_\infty \leq \|\mathbf{E}_1\|_\infty. \tag{7.3.3}$$

Now suppose for $n \geq 2$, then

$$\begin{aligned} a_{n+1}\varepsilon_{l-1}^{n+1} + b_{n+1}\varepsilon_l^{n+1} + c_{n+1}\varepsilon_{l+1}^{n+1} &= a_n\varepsilon_{l-1}^n + b_n\varepsilon_l^n + c_n\varepsilon_{l+1}^n \\ &\quad + \sum_{j=1}^{n-1} \varphi_j \varepsilon_l^{n-j} + \beta_n \varepsilon_l^1, \end{aligned} \tag{7.3.4}$$

and suppose

$$\|\mathbf{E}_n\|_\infty \leq \|\mathbf{E}_1\|_\infty. \tag{7.3.5}$$

If we define

$$| \varepsilon_m^n | = \max_{1 \leq l \leq L-1} | \varepsilon_l^n |, \tag{7.3.6}$$

and

$$| \varepsilon_m^{n+1} | = \max_{1 \leq l \leq L-1} | \varepsilon_l^{n+1} |, \tag{7.3.7}$$

then

$$
\begin{aligned}
\|E_{n+1}\|_\infty &= \mid \varepsilon_m^{n+1} \mid, \\
&\leq a_{n+1} \mid \varepsilon_{l-1}^{n+1} \mid + b_{n+1} \mid \varepsilon_l^{n+1} \mid + c_{n+1} \mid \varepsilon_{l+1}^{n+1} \mid, \\
&\leq \left| a_{n+1}\varepsilon_{l-1}^{n+1} + b_{n+1}\varepsilon_l^{n+1} + c_{n+1}\varepsilon_{l+1}^{n+1} \right|, \\
&= \left| a_n\varepsilon_{l-1}^{n} + b_n\varepsilon_l^{n} + c_n\varepsilon_{l+1}^{n} + \sum_{j=1}^{n-1} \varphi_j \varepsilon_l^{n-j} + \beta_n \varepsilon_l^1 \right|, \\
&\leq a_n \mid \varepsilon_{l-1}^{n} \mid + b_n \mid \varepsilon_l^{n} \mid + c_n \mid \varepsilon_{l+1}^{n} \mid + \sum_{j=1}^{n-1} \varphi_j \mid \varepsilon_l^{n-j} \mid + \beta_n \mid \varepsilon_l^1 \mid, \\
&\leq a_n \mid \varepsilon_{l}^{n} \mid + b_n \mid \varepsilon_l^{n} \mid + c_n \mid \varepsilon_{l}^{n} \mid + \sum_{j=1}^{n-1} \varphi_j \mid \varepsilon_l^{n} \mid + \beta_n \mid \varepsilon_l^{n} \mid, \\
&= a_n \mid \varepsilon_{l}^{n} \mid + b_n \mid \varepsilon_l^{n} \mid + c_n \mid \varepsilon_{l}^{n} \mid + \varphi_1 \mid \varepsilon_l^{n} \mid + \cdots + \varphi_{n-1} \mid \varepsilon_l^{n} \mid + \beta_n \mid \varepsilon_l^1 \mid, \\
&= (a_n + b_n + c_n) \mid \varepsilon_l^{n} \mid + (\varphi_n + \cdots + \varphi_{n-1}) \mid \varepsilon_l^{n} \mid + \beta_n \mid \varepsilon_l^1 \mid \\
&\leq (\varphi_n + \cdots + \varphi_{n-1} + \beta_n) \|\mathbf{E}_1\|_\infty \\
&= \left(\sum_{j=1}^{n-1} \varphi_j + \beta_n \right) \|\mathbf{E}_1\|_\infty, \\
&= (1 - \beta_n + \beta_n) \|\mathbf{E}_1\|_\infty, \\
&= \|\mathbf{E}_1\|_\infty. \qquad (7.3.8)
\end{aligned}
$$

,

Therefore

$$\|\mathbf{E}_n\|_\infty \leq \|\mathbf{E}_1\|_\infty \text{ for all } n = 1, 2, \cdots, N,$$

which completes the proof of the following theorem.

Theorem 7.3.3. *The θ-method (7.2.6) for solving the time-space fractional Black-Scholes PDE (7.1.5) is unconditionally stable when $\frac{1}{2} \leq \theta \leq 1$ and the condition $\frac{a\Gamma(2-\alpha)}{h^2 k^\alpha} < 1$ must hold for $0 \leq \theta < \frac{1}{2}$.*

Convergence Analysis

Lemma 7.3.4. *Let u_l^n be the exact solution to the time-space fractional Black-Scholes PDE (7.1.5) at grid point (x_l, τ_n). Define the truncation error by $e_l^n = u_l^n - v_l^n$, with $\mathbf{e}^n = (e_1^n, e_2^n, \cdots, e_{L-1}^n)^T$ and $\mathbf{e}^0 = 0$. Define $\|\mathbf{e}^n\|_\infty = \mid e_m^n \mid = \max\limits_{1\le l\le L-1} \mid e_l^n \mid$, when $\frac{1}{2} \le \theta \le 1$ we set $\|\mathbf{e}^n\|_\infty \le \hat{C}\beta_n^{-1}(k^{1+\alpha} + k^\alpha h)$; and when $0 \le \theta < \frac{1}{2}$ the condition $\frac{a\Gamma(2-\alpha)}{h^2k^\alpha} < 1$ holds and one also set $\|\mathbf{e}^n\|_\infty \le \hat{C}\beta_n^{-1}(k^{1+\alpha} + k^\alpha h)$.*

Since the errors e_l^n satisfy (7.2.6) we have

$$a_{n+1}e_{l-1}^{n+1} + b_{n+1}e_l^{n+1} + c_{n+1}e_{l+1}^{n+1} = a_n e_{l-1}^n + b_n e_l^n + c_n e_{l+1}^n + \sum_{j=1}^{n-1} \varphi_j e_l^{n-j} + R_l^n. \quad (7.3.9)$$

Define

$$L_k^\alpha v(x_l, \tau_{n+1}) := \frac{k^{-\alpha}}{\Gamma(2-\alpha)} \sum_{j=1}^{n-1} \beta_j \left[v(x_l, \tau_{n+1-j}) - v(x_l, \tau_{n-j}) \right], \quad (7.3.10)$$

then

$$\begin{aligned}
&\left| \frac{\partial^\alpha v(x_l, \tau_{n+1})}{\partial t^\alpha} - L_k^\alpha v(x_l, \tau_{n+1}) \right| \\
&\le \frac{1}{\Gamma(1-\alpha)} \sum_{j=1}^{n-1} \int_{(j-1)k}^{jk} \left| \frac{\partial v(x_l, \tau)}{\partial \tau} - \frac{(v(x_l, \tau_{n+1-j}) - v(x_l, \tau_{n-j}))}{k} \right| \frac{ds}{(\tau_{n+1} - s)^\alpha}, \\
&\le \frac{1}{\Gamma(1-\alpha)} k \sum_{j=1}^{n-1} \int_{(j-1)k}^{jk} \frac{ds}{(\tau_{n+1} - s)^\alpha}, \\
&\le \frac{C}{\Gamma(1-\alpha)} k \int_0^{jk} \frac{ds}{(\tau_n - s)^\alpha}, \\
&\le C_1 k, \qquad (7.3.11)
\end{aligned}$$

where C and C_1 are constants independent of h and k. Therefore

$$\begin{aligned} L_k^{\alpha} v(x_l, \tau_{n+1}) &= \frac{k^{-\alpha}}{\Gamma(2-\alpha)} \sum_{j=1}^{n-1} \beta_j \left[v(x_l, \tau_{n+1-j}) - v(x_l, \tau_{n-j}) \right] \\ &= \frac{\partial^{\alpha} v(x_l, \tau_{n+1})}{\partial t^{\alpha}} + C_1 k. \end{aligned} \tag{7.3.12}$$

We further note that

$$\frac{v(x_{l+1}, \tau_n) - v(x_l, \tau_n)}{h} = \frac{\partial v(x_l, \tau_n)}{\partial x} + C_2 h, \tag{7.3.13}$$

and

$$\frac{v(x_{l+1}, \tau_n) - 2v(x_l, \tau_n) + v(x_{l-1}, \tau_n)}{h^2} = \frac{\partial^2 v(x_l, \tau_n)}{\partial x^2} + C_3 h^2. \tag{7.3.14}$$

Combining (7.3.12)-(7.3.14) yield

$$\begin{aligned} R_l^n &= k^{\alpha}\Gamma(2-\alpha) \left[\frac{\partial^{\alpha} v(x_l, \tau_n)}{\partial t^{\alpha}} - \frac{\mu}{\Gamma(2-\alpha)} v(x_l, \tau_n) - \frac{\omega}{\Gamma(2-\alpha)} \frac{\partial v(x_l, \tau_n)}{\partial x} \right. \\ &\quad \left. + \beta \frac{\partial^2 v(x_l, \tau_n)}{\partial x^2} \right] + C_1 k^{1+\alpha} + C_2 k^{\alpha} h + C_3 k^{\alpha} h^2, \end{aligned} \tag{7.3.15}$$

where C_2 and C_3 are constants independent of h and k.

From (7.3.15), we have

$$\begin{aligned} \mid R_l^n \mid &\leq \hat{C}(k^{1+\alpha} + k^{\alpha}(h + h^2)), \\ &\leq \hat{C}(k^{1+\alpha} + k^{\alpha} h), \qquad (h^2 \leq h), \end{aligned} \tag{7.3.16}$$

where $\hat{C}$ is a generic constant.

We can now prove the following main result.

Theorem 7.3.5. *The θ-method (7.2.6) for solving the time-space fractional Black-Scholes PDE (7.1.5) is convergent when $\frac{1}{2} \leq \theta \leq 1$ and the condition $\frac{\alpha\Gamma(2-\alpha)k^{\alpha}}{h^2} N^{\alpha-1} < 1$ must for when $0 \leq \theta < \frac{1}{2}$. The scheme is first-order convergent in both time and*

space.

Proof. To proceed, define

$$\|\mathbf{e}^n\|_\infty = \mid e_m^n \mid = \max_{1\le l\le L-1} \mid e_l^n \mid .$$

For $n = 1$, we have

$$\begin{aligned}
\|\mathbf{e}^1\|_\infty &= \mid e_m^1 \mid, \\
&\le \mid a_1 e_{l-1}^1 + b_1 e_l^1 + c_1 e_{l+1}^1 \mid, \\
&= \mid R_l^1 \mid, \\
&\le \hat{C}\beta_1^{-1}(k^{1+\alpha} + k^\alpha h) \ \text{(using (7.3.16))}.
\end{aligned} \tag{7.3.17}$$

And, for $n \ge 2$, we have

$$\begin{aligned}
\|\mathbf{e}^n\|_\infty &= \mid e_m^n \mid, \\
&\le \mid a_{n+1} e_{l-1}^{n+1} + b_{n+1} e_l^n + c_{n+1} e_{l+1}^1 \mid, \\
&= \mid \varphi_1 \mathbf{e}^{n-1} + \varphi_2 \mathbf{e}^{n-2} + \cdots + \varphi_1 \mathbf{e}^1 + R_m^n \mid, \\
&\le \varphi_1 \mid \mathbf{e}^{n-1} \mid + \varphi_2 \mid \mathbf{e}^{n-2} \mid + \cdots + \varphi_{n-1} \mid \mathbf{e}^1 \mid + \mid R_m^n \mid, \\
&\le \varphi_1 \mid \mathbf{e}^{n-1} \mid + \varphi_2 \mid \mathbf{e}^{n-2} \mid + \cdots + \varphi_{n-1} \mid \mathbf{e}^1 \mid + \hat{C}(k^{1+\alpha} + k^\alpha h), \\
&\le \varphi_1 \|\mathbf{e}^{n-1}\|_\infty + \varphi_2 \|\mathbf{e}^{n-2}\|_\infty + \cdots + \varphi_{n-1} \|\mathbf{e}^1\|_\infty + \hat{C}(k^{1+\alpha} + k^\alpha h), \\
&\le (\varphi_1 + \varphi_2 + \cdots + \varphi_{n-1} + \beta_n)\beta_n^{-1}\hat{C}(k^{1+\alpha} + k^\alpha h), \\
&= \left(\sum_{j=1}^{n-1} \varphi_j + \beta_n\right) \beta_n^{-1}\hat{C}(k^{1+\alpha} + k^\alpha h), \\
&= (1 - \beta_n + \beta_n)\, \beta_n^{-1}\hat{C}(k^{1+\alpha} + k^\alpha h), \\
&= \hat{C}\beta_n^{-1}(k^{1+\alpha} + k^\alpha h).
\end{aligned} \tag{7.3.18}$$

It can be shown that

$$\begin{aligned}
\lim_{n\to\infty}\frac{\beta_n^{-1}}{n^{\alpha}} &= \lim_{n\to\infty}\frac{n^{-\alpha}}{n^{1-\alpha}-(n-1)^{1-\alpha}},\\
&= \lim_{n\to\infty}\frac{n^{-\alpha}}{n^{1-\alpha}}\left(\frac{1}{1-(1-\frac{1}{n})^{1-\alpha}}\right),\\
&= \lim_{n\to\infty}\frac{n^{-1}}{1-(1-\frac{1}{n})^{1-\alpha}},\\
&= \lim_{n\to\infty}\frac{n^{-1}}{(1-\alpha)n^{-1}},\\
&= \frac{1}{1-\alpha}. \qquad (7.3.19)
\end{aligned}$$

Therefore, (7.3.17) and (7.3.18) yield

$$\begin{aligned}
\|\mathbf{e}^n\|_{\infty} &\leq \hat{C}n^{\alpha}(k^{1+\alpha}+k^{\alpha}h),\\
&= \hat{C}n^{\alpha}k^{\alpha}(k+h),\\
&= \hat{C}t_n^{\alpha}(k+h) \ \text{ since } \ \tau_n = nk \leq T,\\
&= \widetilde{C}(k+h) \ \text{ where } \ \widetilde{C} = \hat{C}t_n^{\alpha}. \qquad (7.3.20)
\end{aligned}$$

This completes the proof to theorem 7.3.5.

7.4 Numerical experiments

In this section, we present some numerical results from scheme (7.2.6) for the time-space fractional Black-Scholes PDE in (7.1.11) subject to the option and market parameters in the example below.

Example 7.4.1. Consider a standard European put option with the following parameters: $K = 150,\ r = 0.055,\ \sigma = 0.01,\ T = 1,\ S_{\max} = 450,\ L = 100,\ N = 100, \delta = 0.025,\ 0.055$ and 0.065.

In order to practically understand the effects of the time-space fractional Black-Scholes PDE in (7.1.5) when used to price options as well the effectiveness of the

θ-method in solving the model, herein we present convergence results for three cases. This consist of two cases when the scheme is unconditional stable, i.e. $\theta = 1/2$ and $\theta = 1$ and another one when the scheme is conditionally stable, that is for $\theta = 1/3$. Convergence results in tables 7.4.1 to 7.4.6 indicates that the numerical scheme is convergent for $\frac{1}{2} \leq \alpha < 1$.

Results indicate that the time-space fractional PDE model provides superior results in terms of put options premium calculations, as compared to the classical Black-Scholes model (equivalent to $\alpha = 1$). The time-space fractional Black-Scholes (7.1.5) setup therefore, yields results which are consistent with the actual option market dynamics as compared to the classical Black-Scholes PDE obtained when $\alpha = 1$.

However the case when the fractional order $0 < \alpha < \frac{1}{2}$, provides weaker results. These is observations are not strange however. As far as financial markets dynamics and fractional Black-Scholes theory is concerned, $0 < \alpha < \frac{1}{2}$ correspond to an anti-persistent regime of the underlying stock price, characterised by a negative correlation between increments. Similar observations were made in Chapter 3 for a time-fractional Black-Scholes model in pricing European put options. Therefore, our general observation is that, fractional Black-Scholes models only out perform their classical counterparts when $\frac{1}{2} \leq \alpha < 1$.

Table 7.4.1: Maximum absolute errors for example 7.4.1 with $r = 0.10$, $\delta = 0.02$ and $\theta = 1/2$.

α	$N = 10$	$N = 20$	$N = 40$	$N = 80$	$N = 160$
0.1	5.9325e-06	2.8495e-06	1.3066e-06	5.3180e-07	1.3793e-07
0.2	5.6042e-06	2.6933e-06	1.2382e-06	5.1154e-07	1.4946e-07
0.3	5.2703e-06	2.5332e-06	1.1655e-06	4.8348e-07	1.4534e-07
0.4	4.9343e-06	2.3722e-06	1.0925e-06	4.5545e-07	1.4184e-07
0.5	4.6000e-06	2.2121e-06	1.0199e-06	4.2784e-07	1.3921e-07
0.6	4.2719e-06	2.0549e-06	9.4878e-07	4.0114e-07	1.3786e-07
0.7	3.9556e-06	1.9035e-06	8.8045e-07	3.7593e-07	1.3831e-07
0.8	3.6580e-06	1.7611e-06	8.1643e-07	3.5294e-07	1.4120e-07
0.9	3.3875e-06	1.6318e-06	7.5854e-07	3.3294e-07	1.4705e-07
1.0	3.1541e-06	1.5204e-06	7.0894e-07	3.1681e-07	1.5567e-07

Table 7.4.2: Convergence rates for example 7.4.1 with $r = 0.10$, $\delta = 0.02$ and $\theta = 1/2$.

α	$N = 10$	$N = 20$	$N = 40$	$N = 80$
0.1	1.06	1.12	1.30	1.25
0.2	1.06	1.12	1.28	1.18
0.3	1.06	1.12	1.27	1.33
0.4	1.06	1.12	1.26	1.28
0.5	1.06	1.12	1.25	1.32
0.6	1.06	1.11	1.24	1.24
0.7	1.06	1.11	1.23	1.24
0.8	1.05	1.11	1.21	122
0.9	1.05	1.11	1.19	1.18
1.0	1.05	1.10	1.16	1.03

Table 7.4.3: Maximum absolute errors for example 7.4.1 with $r = 0.10$, $\delta = 0.02$ and $\theta = 1$.

α	$N = 10$	$N = 20$	$N = 40$	$N = 80$	$N = 160$
0.1	1.2097e-05	5.9325e-06	2.8495e-06	1.3066e-06	5.3180e-07
0.2	1.1426e-05	5.6042e-06	2.6933e-06	1.2382e-06	5.1154e-07
0.3	1.0745e-05	5.2703e-06	2.5332e-06	1.1655e-06	4.8348e-07
0.4	1.0060e-05	4.9343e-06	2.3722e-06	1.0925e-06	4.5545e-07
0.5	9.3776e-06	4.6000e-06	2.2121e-06	1.0199e-06	4.2784e-07
0.6	8.7080e-06	4.2719e-06	2.0549e-06	9.4878e-07	4.0114e-07
0.7	8.0626e-06	3.9556e-06	1.9035e-06	8.8045e-07	3.7593e-07
0.8	7.4552e-06	3.6580e-06	1.7611e-06	8.1643e-07	3.5294e-07
0.9	6.9029e-06	3.3875e-06	1.6318e-06	7.5854e-07	3.3294e-07
1.0	6.4264e-06	3.1541e-06	1.5204e-06	7.0894e-07	3.1681e-07

Table 7.4.4: Convergence rates for example 7.4.1 with $r = 0.10$, $\delta = 0.02$ and $\theta = 1$.

α	$N = 10$	$N = 20$	$N = 40$	$N = 80$
0.1	1.03	1.06	1.12	1.30
0.2	1.03	1.06	1.12	1.28
0.3	1.03	1.06	1.12	1.27
0.4	1.03	1.06	1.12	1.26
0.5	1.03	1.06	1.11	1.25
0.6	1.03	1.06	1.11	1.24
0.7	1.03	1.05	1.11	1.23
0.8	1.03	1.05	1.11	1.21
0.9	1.03	1.05	1.11	1.19
1.0	1.03	1.05	1.10	1.16

Table 7.4.5: Maximum absolute errors for example 7.4.1 with $r = 0.10$, $\delta = 0.02$ and $\theta = 1/3$.

α	$N = 10$	$N = 20$	$N = 40$	$N = 80$	$N = 160$
0.1	2.4426e-05	1.2097e-05	5.9325e-06	2.8495e-06	1.3066e-06
0.2	2.3071e-05	1.1426e-05	5.6042e-06	2.6933e-06	1.2382e-06
0.3	2.1695e-05	1.0745e-05	5.2703e-06	2.5332e-06	1.1655e-06
0.4	2.0311e-05	1.0060e-05	4.9343e-06	2.3722e-06	1.0925e-06
0.5	1.8933e-05	9.3776e-06	4.6000e-06	2.2121e-06	1.0199e-06
0.6	1.7581e-05	8.7080e-06	4.2719e-06	2.0549e-06	9.4878e-07
0.7	1.6278e-05	8.0626e-06	3.9556e-06	1.9035e-06	8.8045e-07
0.8	1.5051e-05	7.4552e-06	3.6580e-06	1.7611e-06	8.1643e-07
0.9	1.3936e-05	6.9029e-06	3.3875e-06	1.6318e-06	7.5854e-07
1.0	1.2973e-05	6.4264e-06	3.1541e-06	1.5204e-06	7.0894e-07

Table 7.4.6: Convergence rates for example 7.4.1 with $r = 0.10$, $\delta = 0.02$ and $\theta = 1/3$.

α	$N = 10$	$N = 20$	$N = 40$	$N = 80$
0.1	0.93	0.95	0.96	0.99
0.2	1.00	0.99	0.98	1.12
0.3	1.01	1.03	1.01	1.12
0.4	1.01	1.03	1.02	1.12
0.5	1.01	1.03	1.03	1.12
0.6	1.01	1.03	1.02	1.11
0.7	1.01	1.03	1.03	1.11
0.8	1.01	1.03	1.05	1.11
0.9	1.01	1.03	1.05	1.11
1.0	1.01	1.03	1.05	1.10

7.5 Summary and discussions

In this chapter, a θ-method is used to solve a time-space fractional Black-Scholes equations on pricing a standard European put option problem. Theoretical results demonstrates that the scheme exhibits unconditional stability and convergence properties when $\frac{1}{2} \leq \theta \leq 1$ and is conditional stable when $1 < \theta \leq \frac{1}{2}$, with stability condition $(\frac{\alpha\Gamma(2-\alpha)k^{\alpha}}{h^2}N^{\alpha-1} < 1)$. Numerical results confirm these theoretical deductions. All in all the results indicates the time-space fractional Black-Scholes approach is appropriate for calculating fair put option premiums for $\frac{1}{2} \leq \alpha < 1$ compared to the classical Black-Scholes model. Like in the time-fractional Black-Scholes model expensively discussed in the earlier chapters, the time-space fractional Black-Scholes under performs when $0 < \alpha < \frac{1}{2}$ compared to its classical counter-party. Calibration of the time-space fractional Black-Scholes model and design of robust high order numerical method to solving such models remain a subject of future research.

Chapter 8

Concluding remarks and scope for future research

The discovery of fractal geometry and fractal dynamics of financial markets lead to a grate progress in the design of new mathematical modelling techniques. Of special interests are those models designed to circumvent some of the unrealistic assumptions in the classical Black-Scholes approach. At the centre of these evolutionary models, are the fractional calculus based models. Fractional calculus based models have proved to be very effective modelling techniques in the asset pricing space as well as in other areas of science and engineering. In the asset pricing sphere, fractional calculus models provides for a somewhat unique framework, one that has evidently transformed conventional thinking in asset pricing theory and its general applications. Since fractional derivatives and integral operators are non-local by design, they provides for the best pool of tools for explaining trend and noise memory effects evidently observed in a number of real-time asset price returns.

This thesis therefore investigated the design and analysis of fractional Black-Scholes partial differential equations in pricing continuous dividend paying stock options under different market settings. A numerous hybrid of fractional Black-Scholes models were discussed, specifically falling within the following three categories, namely; time-

fractional Black-Scholes (tfBS) PDEs, space-fractional Black-Scholes (sfBS) PDEs and time-space-fractional Black-Scholes (tsfBS) PDEs as well as their corresponding robust numerical simulation methods. Compared to the classical Black-Scholes set-up, under the tfBS-PDEs, one replace (not analogously) the first order time derivative by its corresponding fractional derivative of order α where ($0 < \alpha \leq 1$) so as to generalise the order of rate of change unlike in the classical sense where the order is fixed at $\alpha = 1$. In case of sfBS-PDEs, the spatial derivatives are replaced (not analogously) by corresponding derivatives of fractional orders, the first order derivative replaced by α where ($0 < \alpha \leq 1$) and the second order derivative by β for ($1 < \beta \leq 2$). In the case of tsfBS-PDEs, one has a combination of the other two cases. In addition to the models designs, the thesis further discuss the design and analysis of several numerical methods for solving the designed fractional models.

In Chapter 2 we presented the formulation of a time-fractional Black-Scholes PDE for pricing standard European put options written on a dividend paying stock. Furthermore, we presented the design and analysis an implicit finite difference scheme to the resultant model. The numerical scheme therein was found to be unconditionally stable and convergent. Two numerical examples were presented suggesting that, the fractional framework is a very effective and robust approach for calculating European put options premiums.

In Chapter 3 a Crank Nicholson type scheme for solving a tfBS-PDE for pricing standard European options was proposed. To demonstrate the effectiveness of the method, two numerical examples were presented. Theoretical and numerical results therein suggests that the fractional approach is a very efficient tool for pricing stock options compared to its classical counterpart. Further conclusions from this chapter are that, the suggested numerical scheme herein provided high order convergent solutions to the tfBS-PDE. It is important to further highlight that, the scheme did not only provide convergent solutions, but also did reduce the computational time required to compute the solution.

To ease some mathematical complexity in solving and implementing fractional

Black-Scholes models, we proposed some transformation of the model in the previous chapters. For example, in Chapter 4 we proposed a heat equation transform of the tfBS-PDE proposed in Chapter 2. The transformation eased the computational efforts required to attain high order numerical results.

A hybrid of option problems are solved, ranging from European options, American to Barrier options. In Chapter 5 we proposed a robust front-fixing transformation method for pricing American put options under a time-fractional Black-Scholes setup. Using this approach, the early exercise boundaries of an American option problem are transformed into fixed boundaries allowing for the simultaneous computation of the option premiums as well as the corresponding optimal exercise boundaries.

The application of the approach to pricing exotic options was also investigate, in Chapter 6 we present a high order numerical method for pricing double barrier options under the time-fractional Black-Scholes setup. Results therein suggest that, the numerical method is unconditionally stable and converges with order $\mathcal{O}(h^4+k^2)$. Furthermore, to investigate the effects of fractional decays in both time and space directions, a time-space-fractional Black-Scholes (tsfBS) PDE and it's universal solution method is proposed. The results therein, suggest that, the approach is effective and does provide results which are consistent with actual financial market scenarios.

In conclusion therefore, overall, the obtained maturity payoff curves as well as the corresponding general solution profiles presented in this thesis work show that of the fractional Black-Scholes approach asymmetric performance effects depending on the value of α. The fractional approach discussed herein, has proven to be more robust and effective for when $1/2 \leq \alpha < 1$. as compared to when $0 < \alpha < 1/2$. These observations are however not strange, as, it is expected that, when $1/2 \leq \alpha < 1$, the underlying fractional stochastic processes involved in our models derivations become more persistent for when $1/2 \leq \alpha < 1$ characterised by positive correlations between increments. Therefore, it is expected for the approach to attain better performance compared to the case when $0 < \alpha < 1/2$ which represent the anti-persistent regime of the process.

Therefore, from the practical point of view, these results confirms the theoretical deductions presented in the during analysis of the models and method herein, as well as confirming the general consensus in literature that, stock markets dynamics are of a power law nature. Also empirical evidence suggest, in general, underlying stock return follows heavy-tailed distributions and as such, they are not independently distributed. Therefore, modelling such returns using the classical approach would greatly give rise to model risk. As evidently observed, the our approach performed effectively for when $1/2 \leq \alpha < 1$ as compared to when $0 < \alpha < 1/2$ in which case, the underlying process would be expected to cover less and less grounds than any ordinary Gaussian random process would do.

Another important observation to take note of is that, the Black-Scholes models proposed in classical setups are well known for producing option premium curves which are similar in shapes and as such, they may not fully reflect the real market anomalies, for examples, in markets with high an-anticipated news events. Whereas, such models when formulated in the fractional sense have the ability to produce option premium curves which are well sensitive to changes in almost all associated parameters, such as, volatility, dividends, interest rates, etc.

For **further research**, we intend to apply the fractional Black-Scholes models as well as their corresponding numerical methods to local and international real-time market data. Therefore, the calibration of the tfBS, sfBS, tsfBS PDEs and other corresponding hybrids fractional Black-Scholes models to real-time market data remain a subject of future research. Furthermore, the design and analysis of new robust higher order numerical solution methods, semi-analytic and analytic solutions methods for fractional Black-Scholes models also remain a subject of further research opportunities.

Bibliography

[1] V.V. Acharya and M. Richardson, Causes of the financial crisis, *Critical Review Foundation* **21** (2009) 195-210.

[2] J. Ahmad, M. Shakeel, Q.M.U. Hassan and S.T. Mohyud-Din, Analytic solution of Black-Scholes model using fractional variational iteration method, *International Journal of Modern Mathematical Sciences* **5** (2013) 133-142.

[3] C. Alvaro and D. del-Castillo-Neqrete, *Fractional diffusion models of option prices in markets with jumps.*, Birkeck University, School of Economics, Mathematics and Statistics (2006)

[4] A.E. Asma, K.J. Adem and M.T. Bachok, Homotopy pertubation method for fractional Black-Scholes European option pricing equations using Sumudu transform, *Chaos, Solitons and Fractals* **40** (2009) 1428-1448.

[5] A. Atangana and A. Secer, A note on fractional order derivatives and table of fractional derivatives of some special functions, *Abstract and Applied Analysis* **2** (2013) 1-8.

[6] E. Azmoodeh,Yu. Mishura, E. Valkeila, On hedging European options in geometric fractional Brownian motion market model, *Statistics Decisions* **27** (2009)129-144.

[7] R. Ballerster, C. Company and L. Jodar, An efficient method for option pricing with discrete dividend payment, *Computers and Mathematics with Applications* **56** (2008) 822-835.

[8] C. Bender, T. Sottinen T., and E. Valkeila, *Fractional Processes as Models in Stochastic Finance. In: Di Nunno G., Øksendal B. (eds).*, Advanced Mathematical Methods for Finance. Springer, Berlin, (2011).

[9] D.A. Benson, S.W. Wheatcraft and M.M. Meershaert, Application of a fractional advection-dispersion equation, *Water Resource* **35** (2000) 1403-1412.

[10] T.R. Bielecki, I. Cialenco and R. Rodriquez, No-arbitrage pricing for dividend-paying securities in discrete time markets with transaction costs, *Mathematical Finance* **25** (2015) 673-701.

[11] T. Bollersleva, M. Gibson and H. Zhoud, Dynamic estimation of volatility risk premia and investor risk aversion from option-implied and realized volatilities, *Journal of Econometrics* **160** (2011) 235-245.

[12] W. Bu, Y. Tang and J. Yang. Galerkin finite element method for two-dimensional Riez space fractional diffusion equations, *Computational Physics* **267** (2014) 26-38.

[13] P. Buchen and O. Konstandatos, A new approach to pricing double barrier options with arbitrary payoffs and exponential boundaries, *Applied Mathematical Finance* **6** (2009) 497-515.

[14] M. Broadie and P. Glasserman, A continuity correction for discrete barrier options, *Mathematical Finance* **4** (1997) 325-348.

[15] F. Black and M. Scholes, The pricing of options and corporate liabilities, *Political Economy* **81** (1973) 637-654.

[16] R. Caponetto, G. Dongola, L. Fortuna and I. Petras, *Fractional Order Systems: Modeling and Control Applications.*, World Scientific, New Jersey, USA (2010).

[17] M.Caputo, Linear models of dissipation whose Q is almost frequency independent, part II, *Geophysical Journal International* **13 (5)** (1967) 529-539.

[18] C. Canuto, M.Y. Hussaini, A. Quarteroni and T.A. Zang, Spectral methods: Fundamentals in Single Domains, *Springer-Verlag*, Berlin, Germany (2006).

[19] R. Cont and P. Tankov, *Financial Modelling With Jump Processes.*, Chapman and Hall/CRC financial mathematics series, Boca Raton, Florida (2004).

[20] R. Company, M.-A. Piqueras and L. Jodar, A front-fixing numerical method for a free boundary nonlinear diffusion logistic population model, *Computational and Applied Mathematics* **308** (2017) 473-481.

[21] R. Company, V. N. Egorova, and L. Jodar, Constructing positive reliable numerical solution for American call options: A new front-fixing approach, *Journal of Computational and Applied Mathematics* **291** (2016) 422-431.

[22] D. Colander, H. Fllmer, A. Haas, M. Goldberg, K. Juselius, A. Kirman, T. Lux, and B. Sloth, The Financial Crisis and the Systemic Failure of Academic Economics, *Department of Economics, University of Copenhagen*, (2009).

[23] C. Chang-Ming, L. Fawang and B. Kevin, Finite difference methods and a fourier analysis for the fractional reaction subdiffusion equation, *Applied Mathematics and Computation* **2** (2008) 754-769.

[24] W. Chen, C. Wu, and H. Li, A jump-diffusion model for option pricing under fuzzy environments, *Insurance: Mathematics and Economics* **44** (2009) 337-344.

[25] W. Chen, X. Xu and S. Zhu, Analytically pricing double barrier options on a time-fractional Black-Scholes equation, *Computers and Mathematics with Applications* **69** (2015) 1407-1419.

[26] N.J. Cutland, P. E. Kopp and W. Willinger, Stock price returns and the Joseph effect: A fractional version of the Black-Scholes model, *Proceedings of the Former Ascona Conferences on Stochastic Analysis, Random Fields and Applications, Progress in Probability* **36** (1995) 327-351.

[27] L. Decreusefond and A.S. Ustunel, Stochastic analysis of the fractional Brownian motion, *Potential Analysis* **10** (1999) 177-214.

[28] G. Deng, Pricing American continuous-installment options under stochastic volatility model, *Mathematical Analysis and Applications* **424** (2015) 802-823.

[29] E.H. Doha, A.H. Bhrawy and S.S. Ezz-Eldien, Effecient chebyshev spectral methods for solving multi-term fractional differential equations, *Applied Mathematical Models* **35** (2011) 5662-5672.

[30] C. Donny and W. Song, An upwind finite difference method for a nonlinear Black-Scholes equation governing European option valuation under transaction costs, *Applied Mathematics and Computation* **219** (2013) 8811-8828.

[31] D. Duy-Minh, N. Duy and S. Granville, Numerical schemes for pricing Asian options under state-dependent regime-switching jump-diffusion models, *Computers and Mathematics with Applications* **71** (2016) 443-458.

[32] A. Flavio and H. Stefano, Delta hedging in discrete time under stochastic interest rate, *Computational and Applied Mathematics* **259** (2014) 385-393.

[33] L. Feng and V. Linetsky, Pricing discretely monitored barrier options and defaultable bonds in levy process models: A fast Hilbert transform approach, *Mathematical Finance* **3** (2008) 337-384.

[34] L. Feng, V. Linetsky, J.L. Morales, and J. Nocedal, On the solution of complementarity problems arising in American option pricing, *Optimization Methods and Software* **26** (2011) 813-825.

[35] N.J. Ford, J.Y. Xiao, and Y.B. Yan, A finite element method for time fractional partial differential equations, *Fractional Calculus and Applied Analysis* **14**(2) (2011) 454-474.

[36] B. Gao, D. Ahn and S. Figlewski, Pricing discrete barrier options with an adaptive mesh model, *Quantitative Analysis in Financial Markets* **33** (2002) 296-313.

[37] F. Garzarelli, M. Cristelli, G. Pompa, A. Zaccaria and L. Pietronero, Memory effects in stock price dynamics:evidence of technical trading, *Scientific Reports* **4** (2014) 4487.

[38] P. Guasoni, No arbitrage under transaction costs with fractional Brownian motion and beyond. *Mathematical Finance* **16** (2006) 569-582.

[39] H. Han and X. Wu, A fast numerical method for the Black-Scholes equation of American options, *SIAM Journal on Numerical Analysis* **41** (2003) 2081-2095.

[40] S. Haq and M. Hussain, Selection of shape parameter in radial basis functions for solution of time-fractional Black?Scholes models, *Applied Mathematics and Computation* **335** (2018) 248-263.

[41] G. Huang, Q. Huang, H. Zhan, Evidence of one-dimensional scale-dependent fractional advection-dispersion, *Journal of Contemporary Hydrology.* **85** (2006) 53-71.

[42] J. Hull, *Options, Futures and other Derivatives.*, Pearson Prentice Hall Upper Saddle River, New Jersey (2009).

[43] L. Hsuan-Ku and C. Jui-Jane, A closed-form approximation for the fractional Black-Scholes model with transaction costs, *Computers and Mathematics with Applications* **65** (2013) 1719-1726.

[44] Y.L. Hsiao, S.Y. Shen, and A. M. L. Wang, Hybrids finite difference method for pricing tow-asset double barrier options, *Mathematical Problems in Engineering* **3** (2015) Article ID 692695.

[45] J. Jeon, J, Yoon. Kim, and C. Park, An analytic expansion method for the valuation of double-barrier options under as stochastic volatility model, *A Mathematical Analysis and Applications* **449** (2016) 207-227.

[46] G. Jumarie, Merton's model of optimal portfolio in a Black and Scholes market driven by a fractional Brownian motion with short-range dependence, *Insurance: Mathematics and Economics* **37** (2005) 585-598.

[47] G. Jumarie, Modified Reimann-Liouville derivative and fractional Taylor series for non-differentiable functions, further results, *Computers and Mathematics with Applications* **51** (2006) 1367-1376.

[48] G. Jumarie, Stock exchange fractional dynamics defined as fractional exponential growth driven by (usual) Gaussian white noise. Application to fractional Black-Scholes equations, *Insurance: Mathematics and Economics* **42** (2008) 271-287.

[49] G. Jumarie, Derivation and solutions of some fractional Black-Scholes equations in coarse-grained space and time. Application to Merton's optimal portfolio, *Computers and Mathematics with Applications* **59** (2010) 1142-1164.

[50] Y.J. Jiang and J.T. Ma, High-order finite element methods for time-fractional partial differential equations, *Computational Mathematics* **235** (2011) 3285-3290.

[51] S. Kumar, A. Yildrim, Y. Khan, H. Jafari, K. Syevand and L. Weis, Analytical solution of fractional Black-Scholes European option pricing equation by using Laplace Transform, *Journal of Fractional Calculus and Applications* **8** (2012) 1-9.

[52] Y.-K. Kwok and L. Wu, A front fixing method for the valuation of American options, *The Journal of Financial Engineering* **6** (1997) 83-97.

[53] Y.-K. Kwok, *Mathematical Models of Financial Derivatives*, Springer, Berlin (2008).

[54] H. Kleinert and J. Korbel, Option pricing beyond Black-Scholes based on double-fractional diffusion, *Physica A* **449** (2016) 200-214.

[55] D. Kristensen and A. Mele, Adding and subtracting black-scholes: A new approach to approximating derivative prices in continuous-time models, *Finance and Economics* **102** (2011) 390-415.

[56] D. Kristensen, Analytical solution of fractional Black-Scholes European option pricing equation by using Laplace transform, *Fractional Calculus and Application* **8** (2012) 1-9.

[57] L. Kristoufek and M. Vosvrda, Measuring capital market efficiency: long-term memory, fractal dimension and approximate entropy, *European Physical Journal* **B 87** (2014)157-162.

[58] H.G. Landua, *Heat Conduction in a Melting Solid.*, Quarterly of Applied Mathematics **8** (1950).

[59] S. Lahmiri, Long memory in international financial markets trends and short movements during the 2008 financial crisis based on variational mode decomposition and detrended fluctuation analysis, *Physica* **A 437** (2015) 130-138.

[60] H. Leland, Option pricing and replication with transaction costs, *Finance* **5** (1985).1283-1301.

[61] V.B. Luca, P. Graziella, R. Davide, A very efficient approach for pricing barrier options on an underlying described by the mixed fractional Brownian motion, *Chaos, Solitons and Fractals* **87** (2016) 240-248.

[62] C.P. Li and F.W. Liu. Spectral approximations to the fractional integral and derivative, *Fractional Calculus and Applied Analysis* **15** (2012) 383-406.

[63] J. Liang, J. Wang, W. Zhang, W. Qiu and F. Ren, Option pricing of a bi-fractional Black-Scholes model with the Hurst exponent H in $[1/2, 1]$, *Applied Mathematics Letters* **23** (2010) 859-863.

[64] B.B. Mandelbrot and J.W. van Ness, Fractional Brownian motions, fractional noises and applications, *SIAM Review* **10** (1968) 422-437.

[65] B.B. Mandelbrot and R. Cioczek-Georges, A class of micro pulses and anti-persistent fractional Brownian motions, *Stochastic Processes and Applications* **60** (1995) 1-18.

[66] B.B. Mandelbrot and R. Cioczek-Georges, Alternative micropulses and fractional Brownian motion, *Stochastic Processes and their Applications* **64** (1996) 143-152.

[67] B.B. Mandelbrot, *A Fractal Set is One for Which the Fractal (Hausdorff-Besicovitch) Dimension Strictly Exceeds the Topological Dimension.*, Fractals and Chaos, Springer-Verlag, Berlin (2004).

[68] J. Martin-Vaquero, A.Q.M. Khaliq and B. Kleefed, Stabilized explicit Runge-Kutta methods for multi-asset American options, *Computers and Mathematics with Applications* **67** (2014) 1293-1308.

[69] M.M. Meerschaert and C. Tadjeran, Finite difference methods for two-dimensional fractional dispersion equation, *Computational Physics* **211** (2006) 249-261.

[70] R.C. Merton, On the pricing of corporate debt: the risk structure of interest rates, *Finance* **29** (1974) 449-470.

[71] G.H. Miller and E.G. Puckett, A Neumann preconditioned iterative sub-structuring approach for computing solutions to Poisson's equation with prescribed jumps on an embedded boundary, *Computational Physics* **235** (2013) 683-700.

[72] A.M.G. Mohammad and R. Majtaba, European option pricing of fractional Black-Scholes model with new Lagrange multipliers, *Computational Methods for Differential Equations* **2** (2014) 1-10.

[73] C.A. Monje, Y. Chen, B. Vinagre, D. Xue, and V. Feliu, *Fractional-Order Systems and Controls: Fundamentals and Applications.*, Springer-Verlag, Berlin (2010).

[74] D.A. Murio, Implicit finite difference approximation for time fractional diffusion equations, *Computers and Mathematics with Applications* **56** (2008) 1138-1145.

[75] B.F. Nielsen, O. Skavhaug and A. Tveito, Penalty and front-fixing methods for the numerical solution of American option problems, *Computational Finance* **5** (2002) 69-97.

[76] T.J. Osler, Taylor's series generalized for fractional derivatives and applications, *SAIM-Jounal of Mathematical Analysis* **2** (1971) 37-47.

[77] E. Panas, Long memory and chaotic models of prices on the London metal exchange, *Resources Policy* **4** (2001) 485-490.

[78] I. Pollubny, *Fractional Differential Equations.*, Academic Press, Calif, USA (1999).

[79] I. Pollubny, Geometric and physical interpretation of fractional integration and fractional differentiation, *Fractional Calculus and Applied Analysis* **5 (4)** (2002) 367-386.

[80] U.S. Rana and A. Ahmad, Numerical solution of pricing of European option with stochastic volatility, *International Journal of Engineering* **24** (2011) 189-202.

[81] U.S. Rana and A. Ahmad, Numerical solution of European call option with dividends and variable volatility, *Applied Mathematics and Computation* **218** (2012) 6242-6250.

[82] L.C.G. Rogers, Arbitrage with fractional Brownian motion, *Mathematical Finance* **7** (1997) 95-105.

[83] J. Sabatier, O.P. Agrawal, J.A.T. Machado, *Advances in Fractional Calculus: Theoretical Developments and Applications in Physics and Engineering.*, Springer-Verlag, Dordrecht (2007).

[84] A. Sensoy and B. M Tabak, Time-varying long term memory in the European Union stock markets, *Physica A* **436** (2015) 147-158.

[85] Y. Shin Kim, J. Lee, S. Mittnik and J. Park, Quanto option pricing in the presence of fat tails and asymmetric dependence, *Economics* **187** (2015) 512-520.

[86] G.D. Smith, *Numerical Solution of Partial Differential Equations: Finite Difference Methods.*, The Clarendon Press, Oxford, UK (1985).

[87] Z. Song-Ping, B. Alexander and L. Xiaoping, A new exact solution for pricing European options in a two-state regime-switching economy, *Computers and Mathematics with Applications* **64** (2012) 2744-2755.

[88] L. Song, A space-time fractional derivative model for European option pricing with transaction costs in fractal market, *Chaos, Solitons and Fractals* **103** (2017) 123-130.

[89] S. Song and Y. Wang, Pricing double barrier options under a volatility regime-switching model with psychological barriers *Review of Derivatives Research* **2** (2017) 225-280.

[90] D.Y. Tangman, A. Gopaul, M. Bhuruth, A fast high-order finite difference algorithm for pricing American options, *Computational and Applied Mathematics* **222** (2008) 17-29.

[91] N.N. Taleb, *The black-swan: The Impact of the Highly Improbable.*, Random house, New York, USA (2007).

[92] E. Valkeila, On the approximation of geometric fractional Brownian motion. *Optimality and Risk-Modern Trends in Mathematical Finance* (2008) 251-266.

[93] H. Wang, K.X. Wang and T. Sircar, A direct $\mathcal{O}(N \log^2 N)$ finite difference method for fractional diffusion equations, *Computational Physics* **229** (2009) 8095-8104.

[94] Z. Wang and S. Vong, Compact difference schemes for the modified anomalous fractional sub-diffusion equation and the fractional diffusion-wave equation, *Computational Physics* **277** (2014) 1-15.

[95] Z. Wei-Gou, X. Wei-Lin and H. Chun-Xiong, Equity warrants pricing model under Fractional Brownian motion and an empirical study, *Expert Systems with Applications* **36** (2009) 3056-3065.

[96] F. Wen and Z. Liu, A copula-based correlation measure and its application in Chinese stock market, *International Journal of Information Technology and Decision Making* **4** (2009) 787-801.

[97] B.J. West and S. Picozzi, Fractional Langevin model of memory in financial time series, *Physical Review, Statistical, Nonlinear, and Soft Matter Physics* **3** (2002) Article ID 037106.

[98] P. Wilmott, *Derivatives: the Theory and Practice of Financial Engineering.*, West Sussex, England: John Wiley and Sons (1998).

[99] W. Wyss, The Fractional Black-Scholes equations, *Fractional Calculus Application and Analysis* **3** (2000) 51- 61.

[100] W. Xiao-Tian, Scaling and long-range dependence in option pricing I: pricing European option with transaction costs under the fractional Black-Scholes model, *Physica A* **389** (2010) 438-444.

[101] W. Xiao-Tian, M. Wu, Z. Zhou and W.S. Jing, Pricing European option with transaction costs under the fractional long memory stochastic volatility model, *Physica A* **391**(2012) 1469-1480.

[102] C. Xu and Y. Lin, Finite difference/spactral approximations for the time-fractional diffusion equation, *Computational Physics* **225** (2007) 1533-1552.

[103] H. Zhang, F. Liu, I. Turner and S. Chen, The numerical simulation of the tempered fractional Black-Scholes equation for European double barrier option, *Applied Mathematics and Computing* **3** (2006) 87-99.

[104] S. Zhu and W. Chen, A predictor-corrector scheme based on the ADI method for pricing American puts with stochastic volatility, *Computers and Mathematics with Applications* **62** (2011) 1-26.

[105] P. Zhuang and F. Liu, Implicit difference approximation for the time-fractional diffusion equation, *Applied Mathematics and Computing* **3** (2006) 87-99.